

AD A098799

AFFDL-TR-77-128

LEVEL

(2)

DTIC
SELECTED
MAY 11 1981
D
C

YC-14 INTERIOR NOISE MEASUREMENTS PROGRAM

BOEING COMMERCIAL AIRPLANE COMPANY
P. O. BOX 3707
SEATTLE, WASHINGTON 98124

390145

MARCH 1981

TECHNICAL REPORT AFFDL-TR-77-128
Final Report October 1975 - October 1977

Approved for public release; distribution unlimited.

NATIONAL AERONAUTICS AND SPACE ADMINISTRATION
LANGLEY RESEARCH CENTER
HAMPTON, VIRGINIA 23665

AIR FORCE FLIGHT DYNAMICS LABORATORY
AIR FORCE WRIGHT AERONAUTICAL LABORATORIES
AIR FORCE SYSTEMS COMMAND
WRIGHT-PATTERSON AIR FORCE BASE, OHIO 45433

DTIC
FILE COPY

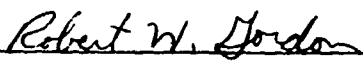
81 5 11 134

NOTICE

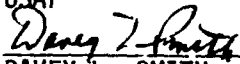
When Government drawings, specifications, or other data are used for any purpose other than in connection with a definitely related Government procurement operation, the United States Government thereby incurs no responsibility nor any obligation whatsoever; and the fact that the government may have formulated, furnished, or in any way supplied the said drawings, specifications, or other data, is not to be regarded by implication or otherwise as in any manner licensing the holder or any other person or corporation, or conveying any rights or permission to manufacture use, or sell any patented invention that may in any way be related thereto.

This report has been reviewed by the Office of Public Affairs (ASD/PA) and is releasable to the National Technical Information Service (NTIS). At NTIS, it will be available to the general public, including foreign nations.


This technical report has been reviewed and is approved for publication.


ROBERT W. GORDON
Project Engineer
USAF


JAMES A. SCHOENSTER
Technical Monitor
NASA/LaRC


DAVEY L. SMITH, Chief
Structural Integrity Branch
Structures and Dynamics Division

FOR THE COMMANDER


RALPH L. KUSTER, JR., Colonel, USAF
Chief, Structures and Dynamics Division

"If your address has changed, if you wish to be removed from our mailing list, or if the addressee is no longer employed by your organization please notify AFNAL/FIBED W-PAFB, OH 45433 to help us maintain a current mailing list".

Copies of this report should not be returned unless return is required by security considerations, contractual obligations, or notice on a specific document.

Unclassified

SECURITY CLASSIFICATION OF THIS PAGE (When Data Entered)

REPORT DOCUMENTATION PAGE		READ INSTRUCTIONS BEFORE COMPLETING FORM
1. REPORT NUMBER AFFDL/IR-77-128	2. GOVT ACCESSION NO AD-AC 98799	3. RECIPIENT'S CATALOG NUMBER
4. TITLE (and Subtitle) YC-14 INTERIOR NOISE MEASUREMENTS PROGRAM		5. TYPE OF REPORT & PERIOD COVERED October 1975 October 1977
7. AUTHOR(s) L. M. Butzel		6. PERFORMING ORG. REPORT NUMBER D748-10113-4
9. PERFORMING ORGANIZATION NAME AND ADDRESS The Boeing Company Seattle, Washington 98124		8. CONTRACT OR GRANT NUMBER(s) Change P00028, Phase I of USAF Contract F33657-72-C-0829
11. CONTROLLING OFFICE NAME AND ADDRESS Air Force Flight Dynamics Laboratory (AFFDL/FBE) Air Force Systems Command Wright-Patterson Air Force Base, Ohio 45433		10. PROGRAM ELEMENT, PROJECT, TASK AREA & WORK UNIT NUMBERS Project 24010127
14. MONITORING AGENCY NAME & ADDRESS (if different from Controlling Office)		12. REPORT DATE March 1981
		13. NUMBER OF PAGES 141
		15. SECURITY CLASS (of this report) Unclassified
		15a. DECLASSIFICATION/DOWNGRADING SCHEDULE
16. DISTRIBUTION STATEMENT (of this Report) Approved for Public Release; distribution unlimited		
17. DISTRIBUTION STATEMENT (of the abstract entered in Block 20, if different from Report)		
18. SUPPLEMENTARY NOTES		
19. KEY WORDS (Continue on reverse side if necessary and identify by block number) USB STOL Airplane Exterior fuselage noise YC-14 Airplane Upper surface blowing Analysis of cabin noise		
20. ABSTRACT (Continue on reverse side if necessary and identify by block number) A test and preliminary analysis program was conducted to develop a data base and initial understanding of the interior noise of a USB STOL airplane using the YC-14 as a test vehicle. A data base has been secured consisting of concurrent cabin noise, exterior fuselage fluctuating pressures; fuselage wall vibrations, and associated aerodynamic, propulsive, and mechanical performance values covering the normal operating envelope of the airplane. Results from preliminary analysis of data show orderly and intuitively reasonable trends. The resultant data base is judged capable of supporting further detailed analysis.		

Unclassified

SECURITY CLASSIFICATION OF THIS PAGE (When Data Entered)

FOREWORD

This report was prepared by the Boeing Company, Seattle, Washington, for the Structural Integrity Branch, Structural Mechanics Division, Air Force Flight Dynamics Laboratory (AFFDL), Wright-Patterson Air Force Base, Ohio. The effort documented herein was performed under Phase I of Modification P00028 to USAF Contract F33657-72-C-0829 and AFFDL Project Numbers, 14710127, 13670409, and 24010127, "YC-14 Interior Noise Measurements," during the period of October 1975 through February 1977. This effort is part of the Air Force Systems Command continuing program to establish methods of predicting and controlling the acoustic environment of military flight vehicles.

The effort described herein was jointly funded by AFFDL and NASA. The technical monitoring was accomplished by Messrs Davey Smith and Robert Gordon, AFFDL/FBE, and Mr. James Shoenster, NASA, Langley Research Center.

Staff direction or analysis and test planning was accomplished by Dr. Leo Butzel, with support provided by Mr. Keith Fluegel and Mr. James Reed. Mr. John Donaldson was instrumental in condensing Boeing Document D6-44350-1 into the present report. Contributions by the following Boeing personnel and organizations were essential to the work accomplished: Mr. Doug Lieberg, graphics; Mr. Hal Whidden, and Mr. Darryl Cruse, flight test engineers; Mr. Peter Krobath and Mr. Marion Lockleer, Acoustics Laboratory instrumentation and data processing; Mr. Richard Keller, flight test design and instrumentation; Mr. Gerry Mollen and Mr. Carl Doherty, dynamics test and data processing, and Mr. Wes Holmes, flight test data processing. Mr. John V. O'Keefe and Loyd D. Jacobs were the Boeing technical staff managers for this contract. Mr. Mark Sussman served as technical integrator of the overall effort on this contract.

Accession For	
NTIS GRA&I	<input checked="checked" type="checkbox"/>
DTIC TAB	<input type="checkbox"/>
Unannounced	<input type="checkbox"/>
Justification	
By	
Distribution/	
Availability Codes	
Avail and/or	
Dist	Special
A	

TABLE OF CONTENTS

	Page
I INTRODUCTION	1
II AIRPLANE CHARACTERISTICS	7
1. YC-14 Aircraft General Description (AMST)	7
2. Propulsion System	7
3. High-Lift Systems	10
4. USB Flaps and Vortex Generators	10
5. Fuselage Structure and Insulation	14
III DATA ACQUISITION SYSTEMS	19
1. Acoustic and Vibration Transducer Systems	19
a. Transducer Locations and Types	19
b. Acoustic Sensors	19
c. Vibration Sensors	31
2. Data Recording Systems	31
3. Basic YC-14 Data Acquisition Systems	31
IV TEST OPERATIONS	35
1. Test Conditions	35
a. Ground Test Conditions	35
b. Flight Test Conditions	37
V DATA REDUCTION SYSTEMS AND METHODS	45
1. Acoustics	45
a. OASPL Strip Charts	45
b. One-Third Octave Spectra	45
c. Acoustic Power Spectral Density	47
2. Dynamics Data Reduction	47
a. One-Third Octave Band Reductions	48
b. Vibration Power Spectral Density	48
VI RESULTS AND CONCLUSIONS	51
1. Synopsis	51
2. Principal Acoustic Test Results	51
3. Preliminary Fuselage Vibration Test Results	68
4. Concluding Remarks	74
APPENDIX REFERENCE ACOUSTIC ANALYSIS MATERIAL	83
REFERENCES	141

LIST OF FIGURES

Number		Page
1	YC-14 Maiden Flight, August 9, 1976	1
2	Cabin Noise OASPL Distribution	3
3	Summary of Exterior and Interior Noise Levels	4
4	No. 1 YC-14 Prototype Aircraft	8
5	Cutaway View of Airplane	9
6	YC-14 Flight Control Surfaces	11
7	USB Flap/Fuselage Geometry	12
8	YC-14 Low-Speed Configuration Summary	13
9	Typical YC-14 Fuselage Construction	15
10	YC-14 Fuselage Structure Diagrams	16
11	Acoustic/Thermal Insulation Blanket Construction (Prototype)	17
12	General Instrumentation Layout—Fuselage Accelerometers	20
13	General Instrumentation Layout—Microphones	21
14	Location of Microphone M51 on Flight Deck	24
15	View of Cabin Looking Forward From Station 750	25
16	View of Sidewall Microphones Looking Forward	26
17	View of Cabin Looking Aft From Station 530	27
18	Detail of Group of Five Accelerometers	28
19	Fuselage Microphone Installation	29
20	Schematic Block Diagram of Overall Acoustics and Dynamics Recording System	32
21	Block Diagram of Basic YC-14 Data System	34
22	YC-14/Sabre VI Configuration for Test Condition .002	38
23	Airplane Parameter Time Histories—Condition 7.01.001.013 (Takeoff, Flaps 20)	40
24	Airplane Parameter Time Histories—Condition 7.01.001.013.1 (Takeoff, Flaps 20)	40
25	Airplane Parameter Time Histories—Condition 7.01.001.018 (Go Around)	42
26	Airplane Parameter Time Histories—Condition 7.01.001.019 (Flap Cycle)	42
27	Airplane Parameter Time Histories—Condition 7.01.001.022 (Landing, Flaps 45)	43
28	Airplane Parameter Time Histories—Condition 7.01.001.022.1 (Landing, Flaps 30)	43
29	Airplane Parameter Time Histories—Condition 7.01.001.022.2 (Landing, Flaps 60)	44
30	Block Diagram—Broadband Data Reduction	46
31	Block Diagram—PSD Data Reduction	49
32	Summary of Exterior and Interior Noise Levels (Same as Figure 3)	52
33	Relation Between Interior Noise and Certain Airplane Parameters	53
34	Troop Compartment OASPL vs USB Flap Angle	56
35	Interior Noise vs Various Noise Measures	56

LIST OF FIGURES (Cont'd)

Number	Page
36	Correlation of Aft Troop Compartment (M60) Overall Noise With L_R Noise Measure 58
37	Variation in Exterior Fuselage Noise Spectra During Takeoff 59
38	Variation in Interior Noise Spectra (M60) During Takeoff 60
39	Exterior Fuselage Overall Noise Levels—Climbout and M 0.70 Cruise 61
40	Exterior Fuselage Noise Spectra—Climbout and M 0.70 Cruise 62
41	Aft Troop Compartment (M60) Noise Spectra—Climbout vs M 0.70 Cruise 64
42	Fuselage/Engine Spacing for YC-14 and 747 65
43	Proposed Fuselage Fluctuation Pressure Field Near M13 or M16 65
44	Effect of USB Flap Position on Exterior Fuselage OASPLs 66
45	Effect of USB Flap Position on Exterior Fuselage Noise Spectra 67
46	Effect of USB Flap Position on Interior Noise Spectra 69
47	Comparison of Estimated and Measured Interior Noise Levels 70
48	Overall Fuselage Vibration Levels vs L_R Noise Measure 71
49	Exterior Fuselage OASPL vs L_R Noise Measure 72
50	Cabin OASPL vs L_R Noise Measure 73
51	Skin Vibration/Exterior Sound at A56/M06 76
52	Skin Vibration/Exterior Sound at A57/M13 77
53	Skin Vibration/Exterior Sound at A60/M20 78
54	Comparative Behavior of Skin Vibration and Cabin Noise 79-81
A-1	Summary of Cabin Noise OASPL 86
A-2	Cabin Noise OASPL Distribution 86
A-3	Summary of Cabin Noise 88
A-4	Summary of Cabin Noise 88
A-5	Summary of Cabin Noise 89
A-6	Summary of Cabin Noise 89
A-7	Summary of Cabin Noise 90
A-8	Summary of Cabin Noise 90
A-9	Summary of Cabin Noise 91
A-10	Summary of Cabin Noise 91
A-11	Summary of Cabin Noise 92
A-12	Distribution of Dominant One-Third Octave Band (Ambient) Noise Levels Along Cabin Center Aisle 92
A-13	Summary of Exterior Fuselage Noise OASPL 96
A-14	Summary of External Fuselage Noise Activity 96
A-15	Summary of Exterior Noise 98
A-16	Summary of Exterior Noise 98
A-17	Summary of Exterior Noise 99
A-18	Summary of Exterior Noise 99
A-19	Summary of Exterior Noise 100
A-20	Summary of Exterior Noise 100
A-21	Summary of Exterior Noise 101

LIST OF FIGURES (Cont'd)

Number		Page
A-22	Summary of Exterior Noise	101
A-23	Summary of Cabin Noise OASPL vs Exterior Fuselage Noise OASPL . . .	104
A-24	Exterior Noise Level Time Histories, Condition 7.01 001.019 (Flap Cycle)	106
A-25	Airplane Parameter Time Histories, Condition 7.01 001.019 (Flap Cycle)	106
A-26	Effect of USB Flap Position on External Fuselage OASPLs	107
A-27	Cabin Noise Level Time Histories, Condition 7.01 001.019 (Flap Cycle)	107
A-28	Effect of USB Flap Position on Cabin OASPLs	108
A-29	One-Third Octave Spectra, M03, Flap Cycle	109
A-30	One-Third Octave Spectra, M05, Flap Cycle	109
A-31	One-Third Octave Spectra, M06, Flap Cycle	110
A-32	One-Third Octave Spectra, M14, Flap Cycle	110
A-33	One-Third Octave Spectra, M16, Flap Cycle	111
A-34	One-Third Octave Spectra, M12, Flap Cycle	111
A-35	One-Third Octave Spectra, M20, Flap Cycle	112
A-36	One-Third Octave Spectra, M13, Flap Cycle	112
A-37	One-Third Octave Spectra, M15, Flap Cycle	113
A-38	One-Third Octave Spectra, M51, Flap Cycle	113
A-39	One-Third Octave Spectra, M53, Flap Cycle	114
A-40	One-Third Octave Spectra, M57, Flap Cycle	114
A-41	One-Third Octave Spectra, M59, Flap Cycle	115
A-42	One-Third Octave Spectra, M60, Flap Cycle	115
A-43	One-Third Octave Spectra, M03, Takeoff	118
A-44	One-Third Octave Spectra, M05, Takeoff	118
A-45	One-Third Octave Spectra, M06, Takeoff	119
A-46	One-Third Octave Spectra, M14, Takeoff	119
A-47	One-Third Octave Spectra, M15, Takeoff	120
A-48	One-Third Octave Spectra, M12, Takeoff	120
A-49	One-Third Octave Spectra, M20, Takeoff	121
A-50	One-Third Octave Spectra, M13, Takeoff	121
A-51	One-Third Octave Spectra, M15, Takeoff	123
A-52	One-Third Octave Spectra, M51, Takeoff	123
A-53	One-Third Octave Spectra, M53, Takeoff	124
A-54	One-Third Octave Spectra, M57, Takeoff	124
A-55	One-Third Octave Spectra, M59, Takeoff	125
A-56	One-Third Octave Spectra, M60, Takeoff	125
A-57	Variation of External Fuselage OASPLs with Cruise Condition	126
A-58	Variation of Cabin OASPLs with Cruise Condition	126
A-59	One-Third Octave Spectra, M03, Cruise Type Conditions	127
A-60	One-Third Octave Spectra, M05, Cruise Type Conditions	127
A-61	One-Third Octave Spectra, M06, Cruise Type Conditions	128
A-62	One-Third Octave Spectra, M14, Cruise Type Conditions	128
A-63	One-Third Octave Spectra, M16, Cruise Type Conditions	129
A-64	One-Third Octave Spectra, M12, Cruise Type Conditions	129

LIST OF FIGURES (Cont'd)

Number		Page
A-65	One-Third Octave Spectra, M20, Cruise Type Conditions	130
A-66	One-Third Octave Spectra, M13, Cruise Type Conditions	130
A-67	One-Third Octave Spectra, M15, Cruise Type Conditions	131
A-68	One-Third Octave Spectra, M51, Cruise Type Conditions	131
A-69	One-Third Octave Spectra, M53, Cruise Type Conditions	132
A-70	One-Third Octave Spectra, M57, Cruise Type Conditions	132
A-71	One-Third Octave Spectra, M59, Cruise Type Conditions	133
A-72	One-Third Octave Spectra, M60, Cruise Type Conditions	133
A-73	Comparison of Measured and Estimated Interior Noise Climbout Levels . . .	136
A-74	Comparison of Measured and Estimated Interior Noise Cruise Levels	136
A-75	One-Third Octave Spectra, M8, Various Conditions	138
A-76	One-Third Octave Spectra, M10, Various Conditions	138
A-77	Comparison of Microphone M8 and M10 Behavior—Current Test Program vs Tulalip Test Program	139
A-78	Interior Noise, Cruise, M70	140
A-79	Interior Noise, Sabre to Starboard	140

LIST OF TABLES

Number		Page
I	Technical Objectives for YC-14 Interior Noise Measurements Program	5
II	Instrument Locations	22
III	Instrument Types	23
IV	Comparative Capabilities of Microphones	30
V	Recorder/Group Switch Position/Data Type Matrix	33
VI	Summary of Interior Noise Measurements Conditions	36
VII	YC-14 Engine Ground Runs	39
VIII	Summary of Airplane Parameters for Conditions Indicated in Figures 32 and 33	54
IX	Skin Accelerometer/Exterior Microphone Sets	75
X	Selected Condition Characteristics	75
A-I	One-Third Octave Analysis Log	84
A-II	Summary of Condition Numbers and Airplane Parameters for Conditions Indicated in Figures A-1 and A-2	87

LIST OF ABBREVIATIONS AND SYMBOLS

A (as in A50)	Accelerometer number
ACCL (ACCELS)	Accelerometer(s)
A/C	Air conditioning
AFFDL	Air Force Flight Dynamics Laboratory
ALT	Altitude
AMB	Ambient (idle) condition
AMST	Advanced Medium STOL Transport
APPR	Approach
A/P	Airplane
ARND	Around
B&K	Bruel & Kjaer (microphones)
BBN	Bolt, Beranek & Newman (accelerometers)
BL	Buttock line
BS, STA	Body station
CEI	Critical engine inoperative
\bar{C}	Centerline of symmetry
CLMB	Climb
COND, CON	Condition
CTR AISLE	Center aisle
dB	Decibel (re 200 pico-bar)
DEG	Degree (of angle)
DWN	Down

ELECT	Electronics
ENG (ENGs)	Engine(s)
EQUIP	Equipment
EXT	Exterior (fuselage microphones)
EXTEN	Extended
F	Frequency
FLPS	Flap (handle position)
F/S	Feet per second
FT	Feet
FTIR	Flight Test Instrumentation Request
FUS. FUSE	Fuselage
G	32.2 ft/sec^2 (or equivalent)
GR	General Radio (analyzer)
GS	Glide slope angle
HI-PW, HI-POW	High power
HR	Hour
Hz	Hertz
INSTR	Instrument (transducer)
INT	Interior (cabin)
IRIG	Interrange Instrument Group (time code system)
KFT	Thousands of feet
KNTS	Knots
LD	Landing

LE	Leading edge
LH	Left hand
$L_R, L_{MX}, L_{A/P}$	Noise measures based respectively on V_R, V_{MX} , and $V_{A/P}$
LI	Left
M	Mach number
M (as in M13)	Microphone number, test rack number
MED-PW	Medium power
MIC (MICs)	Microphone(s)
MIX	Mixed transducer group
MIN	Minutes
NAC	Nacelle
NASA	National Aeronautics and Space Administration
NO.	Number
NOM	Nominal
N_1	Fan speed
OASPL	Overall sound pressure level
P	Photocon (microphone)
PARAMs	Parameters
PICO-BAR	10^{-12} BAR
PRES	Pressure
PSD	Power spectral density
PSIL	Preferred speech interference level
PSI	Pound per square inch
Q	Dynamic pressure

REF	Reference
REVERB	Reverberation
RMS	Root mean square
RPM	Revolutions per minute
RT	Right
SEC	Second
SIM	Simulated (at altitude)
SPEED	True airplane speed
SPL	Sound pressure level
SPOIL	Spoilers
STA. BS	Body station
STBD	Starboard
STOL	Short Takeoff and Landing
TBL	Turbulent boundary layer
TO	Takeoff
USAF	U.S. Air Force
USB	Upper surface blowing
USBFA	Upper surface blown flap angle
V_A P	True airplane speed
V_{OR} , V_{OA} P, V_{OMX}	Reference velocities
V_{CEI}	Critical engine failure speed
V_E , V_c	Equivalent airspeed
VG (VGs)	Vortex generator(s)

V_{IND}	Indicated velocity
V_L	Limit speed (structural)
V_{LF}	Maximum flaps extended speed
$VMX, VMIX$	Mixed flow exhaust velocity
V_R	$(VMX - V_{A/P}) =$ Engine relative mixed exhaust jet velocity
WL	Water line
X-DUCER	Transducer
δ	Position or angle
δ FLAP	Flap angle
δ LE	Leading-edge flap angle
δ NOZ	USB nozzle door position
δ OB	Outboard flap angle
δ SP	Spoiler angle
δ USB, Δ USB	USB flap angle

SECTION I

INTRODUCTION

This report describes a program to develop a data base and initial understanding of the interior noise of a flightworthy USB STOL airplane using the YC-14 as a test vehicle. The prototype airplane, which flew for the first time in August 1976, (Figure 1) has recently completed operational evaluation by the USAF. One of the most complete sets of interior



Figure 1 YC-14 Maiden Flight, August 9, 1976

noise instrumentation, and a resultant data base for any new airplane, is included. A preliminary analysis of this data base is presented, based upon which the following trends have emerged. (Summarized in Figures 2 and 3.)

1. Spatially, the highest cabin and exterior fuselage noise levels occur aft of the engine nozzle exit plane, hence, where the exhaust flow approaches closest to the fuselage.
2. Extension of the USB flaps causes the aft exterior fuselage noise pattern to simply rotate down. Raising of the wing mounted vortex generators produces distinctive high-frequency noise. Within the cabin, modest noise increases are observed (overall about 5 dB) as the USB flaps are deployed, with low-frequency increases due to increasing flow turning over the flaps, and high-frequency increases due to the vortex generator.

Additionally, interior (and exterior) noise levels appear to generally correlate with engine mixed exhaust relative jet velocity, except at cruise, where levels are higher than would be anticipated based on relative jet velocity.

For the most part these trends, which are described in detail in Section VI-2 and the APPENDIX, are orderly and intuitively reasonable. They approximately agree with estimates made prior to the conduct of this test program. The data base acquired during this program provides a sound and generous source of information for further analysis, and for design refinement.

Prior to construction of the YC-14, very little experimental effort had been directed toward definition of cabin noise environment of a USB type aircraft. Estimates, those of References 1, 2 and 3 for example, had been formulated. These were strongly dependent upon static scale model test data defining USB external fuselage acoustic environment, and upon sidewall noise reduction methods developed for conventional (non-USB) jet aircraft. With construction of the YC-14, an opportunity was realized to experimentally define the cabin noise environment of a USB aircraft, to assess estimates developed for such an aircraft, and to pave the way for refined estimates based upon improved understanding of USB STOL airplane cabin noise behavior.

The present interior noise measurements program was undertaken in response to these opportunities. The program was conducted in conjunction with, and as an addition to, the USB Flap Loads program (Reference 4). Both programs were structured to concurrently

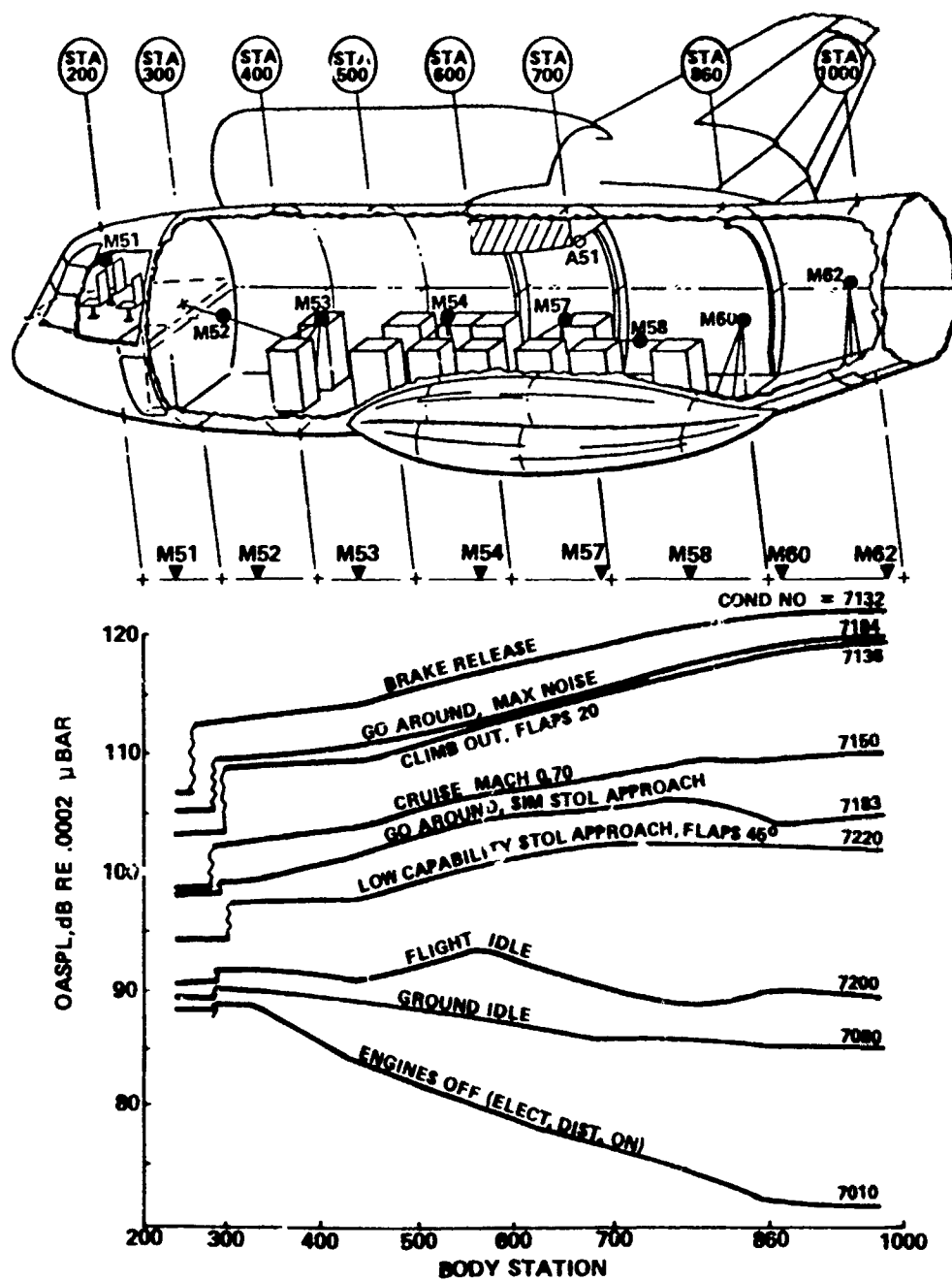


Figure 2 Cabin Noise OASPL Distribution

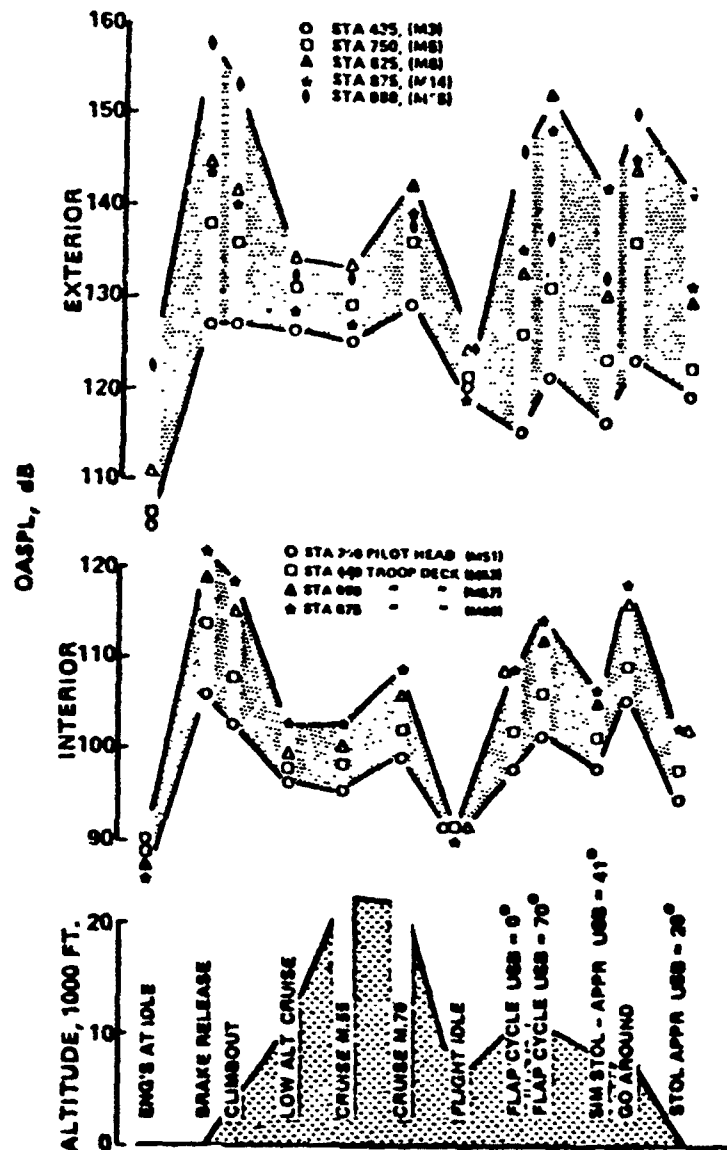


Figure 3 Summary of Exterior and Interior Noise Levels

utilize the No. 1 YC-14 prototype airplane, and to accomplish all measurements on a non-interference basis in conjunction with YC-14 development testing. Both programs were developed under provisions of the U. S. Air Force/National Aeronautics and Space Administration Memorandum of Understanding involving NASA participation in the AMST program. The Interior Noise Measurements program was sponsored jointly by Air Force Flight Dynamics Laboratory (AFFDL) and by NASA-Langley, and administered via the NASA AMST Experiments Office, NASA-Ames.

The current program has been successful in acquiring and preliminarily analyzing a data base responsive to technical objectives shown in Table I. Further, this data base is anticipated to be extensive enough, when supplemented with data acquired under the closely related P00023 Flap Loads Measurements program (Reference 4), to support detailed analysis leading to the successful accomplishment of these objectives.

Table I Technical Objectives for YC-14 Interior Noise Measurements Program

Number	Objective
1	Define general interior noise environment (for normal ground and flight operations) <ul style="list-style-type: none"> ● Includes identification of equipment noise conditions
2	Define general exterior fuselage fluctuating pressure environment (for normal ground and flight operations)
3	Understand relationship between interior and exterior noise <ul style="list-style-type: none"> ● includes assessment of general fuselage wall vibration ● Includes identification (with respect to externally originating fuselage excitation) of fuselage structure from which important radiation to the interior originates
4	Understand special USB propulsion system noise effects, such as those associated with USB flap/flow interaction or vortex generators <ul style="list-style-type: none"> ● Includes assessment of structure borne engine and flap vibration effects and jet exhaust coincidence effects
5	Understand effects of flight on exterior and interior fuselage noise
6	Assess applicability of current prediction methods to USB STOL type airplanes

SECTION II

AIRPLANE CHARACTERISTICS

The No. 1 YC-14 Prototype Aircraft, (Figure 4) provided the vehicle for the interior noise measurements test program. This section describes the general characteristics of the airplane, and its specific design features of interest together with some of its special capabilities as a test aircraft.

1. YC 14 AIRCRAFT GENERAL DESCRIPTION (AMST)

The YC-14 is a prototype advanced military medium STOL jet powered wide body cargo transport of unique design. This advanced design concept utilizes powered lift achieved by means of upper surface blowing (USB) flaps. Two (2) currently available CF6-50D turbofan engines are used to meet the propulsion-lift requirements.

A cutaway view of the YC-14 is shown in Figure 5. Principal characteristics are.

Wing Span, ft	120.0
Body Length, ft	121.4
Overall Length, ft	131.9
Tail Span, ft	54.9
Overall Height, ft	48.2
Engines—Number and Type	(2) GE CF6-50D
Engine Sea Level Static Thrust, lb	48,720
Fuel Capacity, Total, U.S. gal	9,659
Maximum Design Weight, Overload, lb	206,200

2. PROPULSION SYSTEM

The airplane propulsion installation consists of two high bypass (BPR=5) General Electric CF6-50D engines installed in a twin engine over-the-wing airplane configuration. The nacelle structure is basically a half-cylinder that is attached to and cantilevered from the wing front spar. The inner skin of the nacelle structure forms the fan duct outer wall.

The engine installation incorporates a long fan duct of mixed-flow design with a confluent D-shaped exhaust nozzle. The D-shaped nozzle exit is designed with a moderate aspect ratio of 3.2 (USB door closed) and an internal kickdown angle of 22° along the nacelle centerline.



Figure 4 No. 1 YC-14 Prototype Aircraft

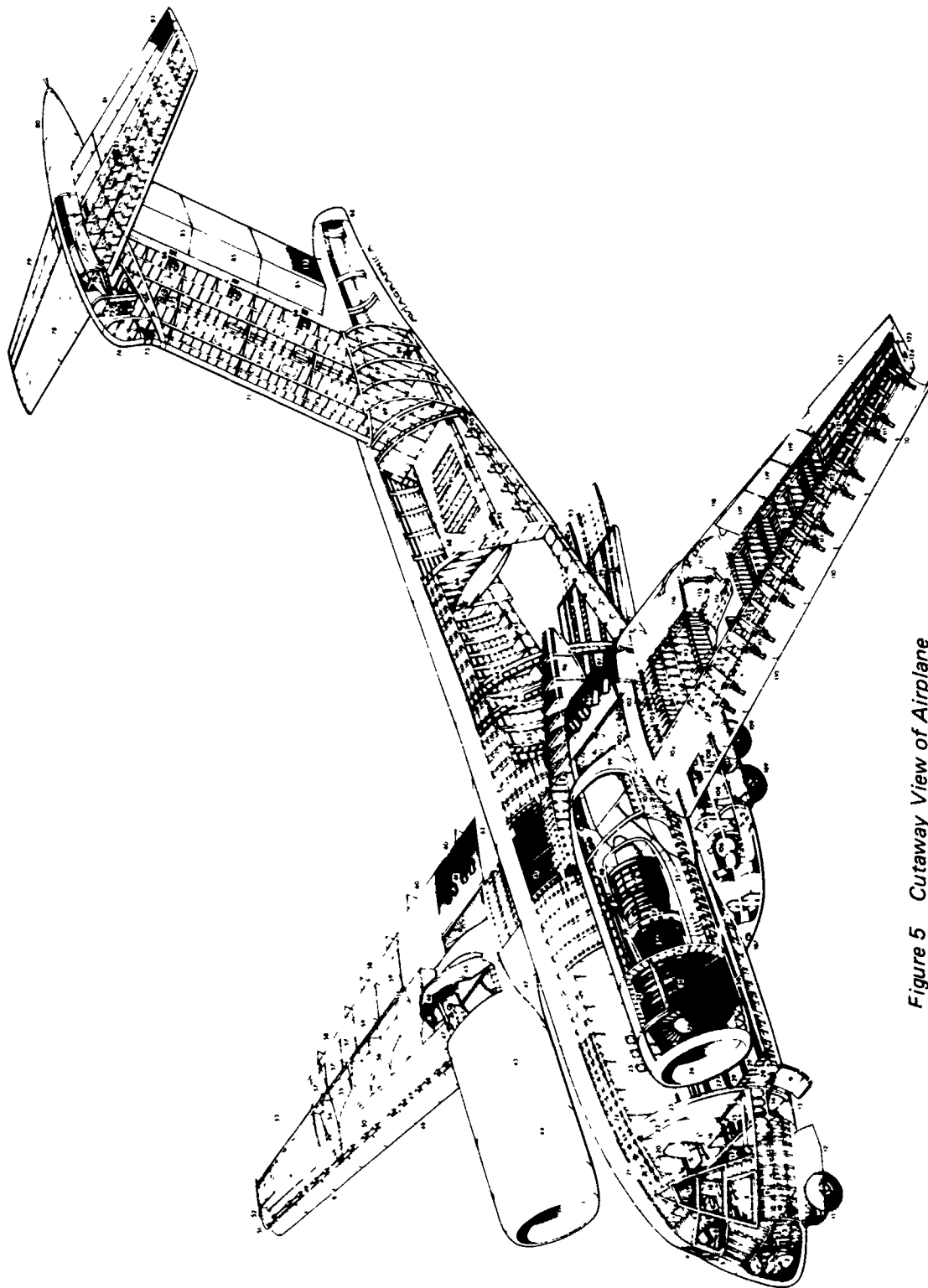


Figure 5 Cutaway View of Airplane

The mean exit plane of the D-nozzle is at Body Station (BS) 640. The lower side of the D-nozzle is flush with the top wing surface, at Water Line (WL) 270. The nozzle width and height are 112 in. by 35 in. The inboard lip of the nozzle is 106 in. to the side of the vertical plane through the centerline of the fuselage, and is canted away from the fuselage 22° .

Nozzle geometry is varied with a two-position, triangular-shaped door located on the outboard side of the mixed flow nozzle. This upper surface blowing (USB) nozzle door is full open (approximately 35°) during low-speed operation, allowing the exhaust gas flow to spread outboard and over the extended inboard (USB) flap to promote powered lift. The door is closed during cruise.

The airplane flight inlet is a fixed geometry inlet design with a fairly large contraction ratio (34%) and essentially zero diffusion. Peripheral acoustic treatment is used to reduce aircraft noise levels.

The mean plane of the engine inlet is at BS 294 and has a diameter of 92 in. The centerline of the inlet is at WL 270, BL 161.

3. HIGH-LIFT SYSTEMS

The YC-14 high-lift system consists of leading- and trailing-edge flap systems, and wing spoilers (Figure 6). Lift may also be increased by thrust vector control using the USB flaps. These are described in Paragraph 4.

4. USB FLAPS AND VORTEX GENERATORS

The USB flaps are the inboard trailing-edge flaps of the YC-14 airplane. These flaps are used as thrust vectoring devices during STOL and assault operations. Figure 7 indicates the location of the USB flaps relative to the fuselage sidewall for various USB flaps angles between 0° (fully retracted) and 70° (fully deployed). Note, however, that except during powered lift and STOL landings the USB flaps are at 0° . For the two indicated landing operations the USB flap position is dynamically varied between 0° and 70° , as instructed by the Electronic Flight Control System (EFCS). Control of the USB flaps is through the EFCS from signals derived from flap drive unit position transmitters, speed control parameters, and engine-out system inputs.

Vortex generators, consisting of four plates on the wing trailing edge aft of each nozzle, (Figure 4 and 7) assist in turning the exhaust gas flow for powered lift modes.

An overall summary of the scheduling of the various high lift and USB installation components is given in Figure 8.

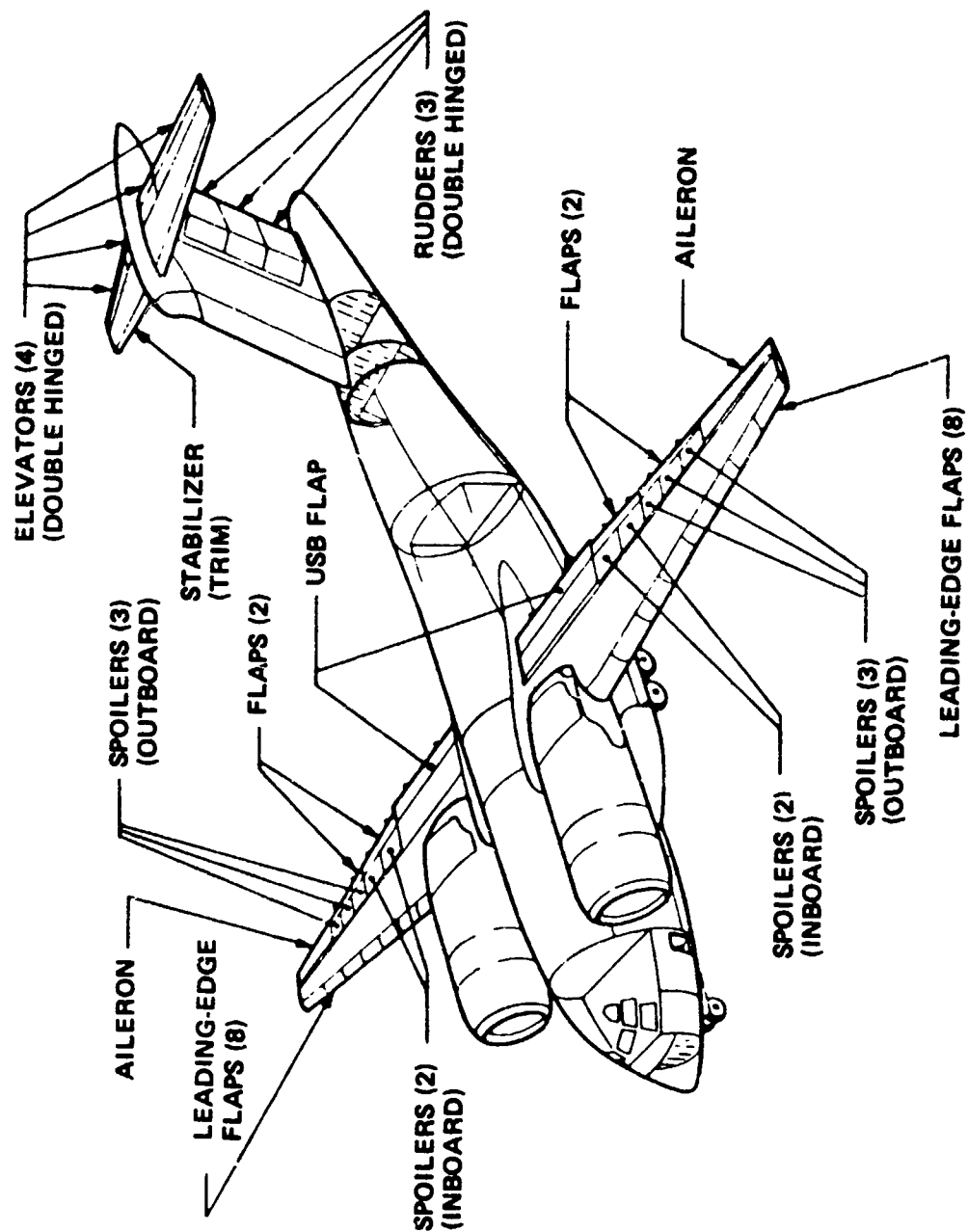
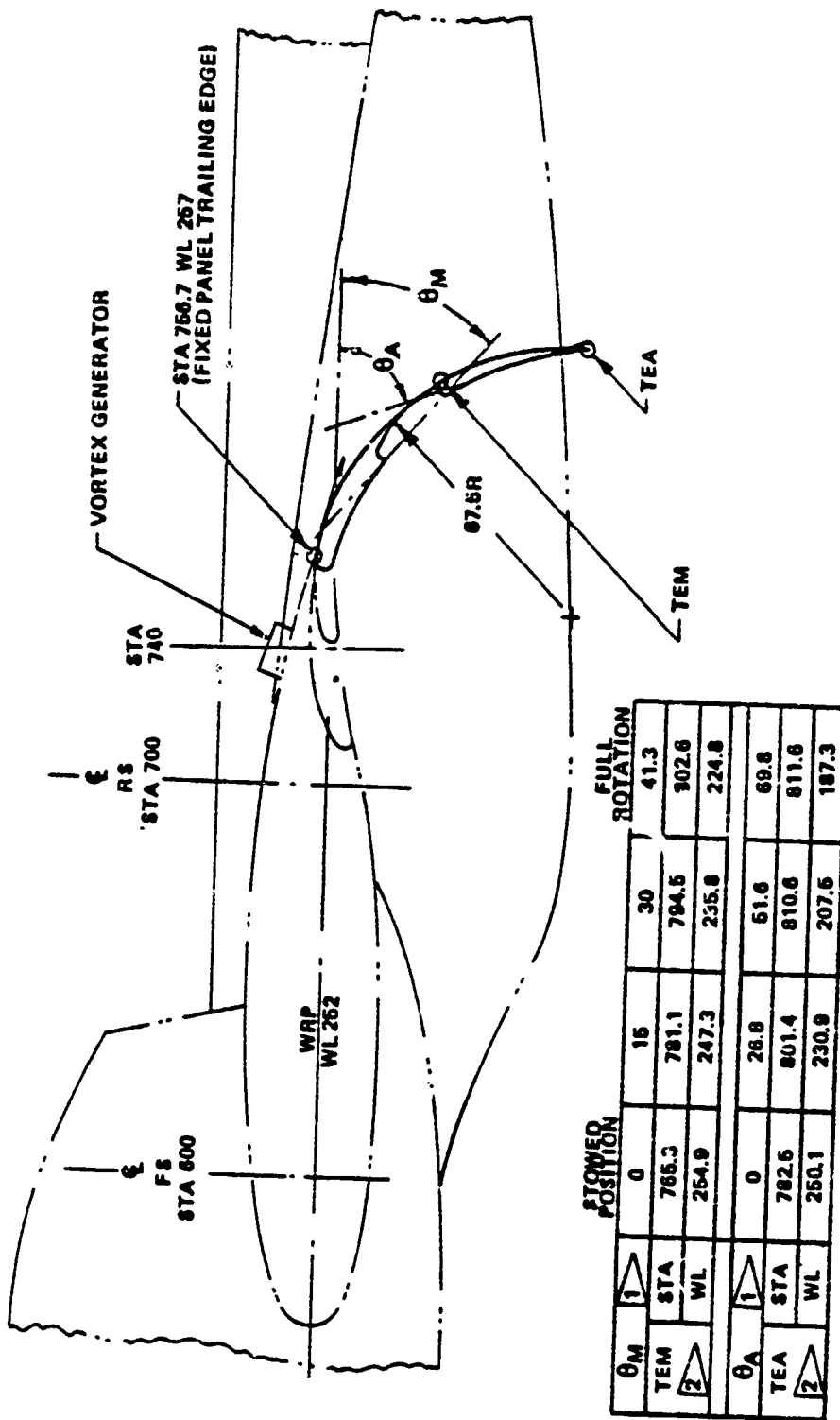


Figure 6 YC-14 Flight Control Surfaces



- 1 THE BROKEN LINES THRU MAIN FLAP (AFT FLAP) DEFINING θ_M (θ_A) COINCIDE WITH THE WRP IN THE STOWED POSITION. HENCE θ_M (θ_A) DEFINES ANGLE OF ROTATION FROM ITS STOWED POSITION.
- 2 TEM INDICATES THE LOCATION OF THE TRAILING EDGE/MAIN FLAP AND TEA INDICATES THE APPROXIMATE LOCATION OF THE TRAILING EDGE/AFT FLAP.

USB FLAP GEOMETRY

Figure 7 USB Flap/Fuselage Geometry

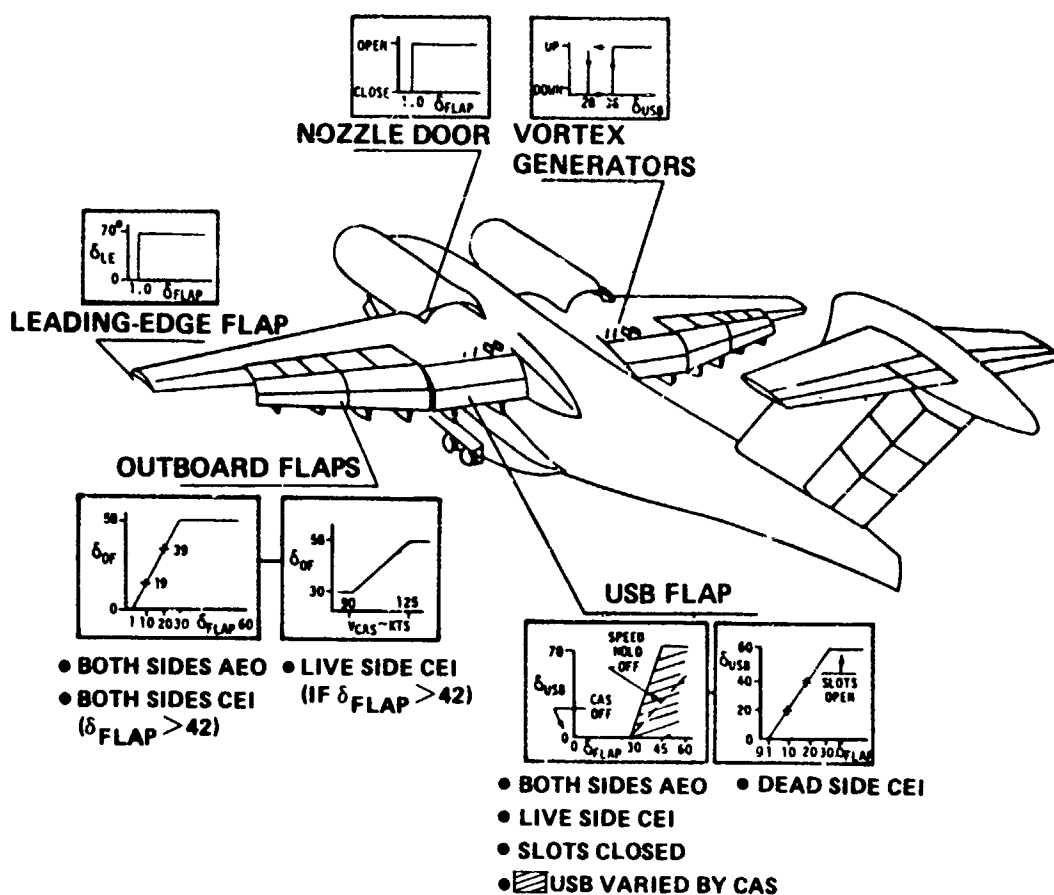


Figure 8 YC-14 Low-Speed Configuration Summary

5. FUSELAGE STRUCTURE AND INSULATION

The fuselage of the YC-14 is of a frame/stringer/skin type construction and is illustrated in Figure 9. Note that the frames are shear tied to the skin throughout virtually the entire fuselage.

Figure 10(a) summarizes skin panel construction and gages, and general location of heavy frames that are typically of wrought construction. Intermediate frames are on 10-in. centers forward of station 400, 20-in. centers to station 860, gradually spreading to 30-in. centers aft of the end of the main cargo ramp door area. Stringers are spaced nominally 8 in. apart between station 400 and 860, becoming more closely spaced aft of station 860. Forward of station 400, sidewall structure begins to approach stringerless construction. Note that the wing/body fairing (Figure 10(a)), is installed over existing skin structure. This fairing is constructed of fiberglass honeycomb.

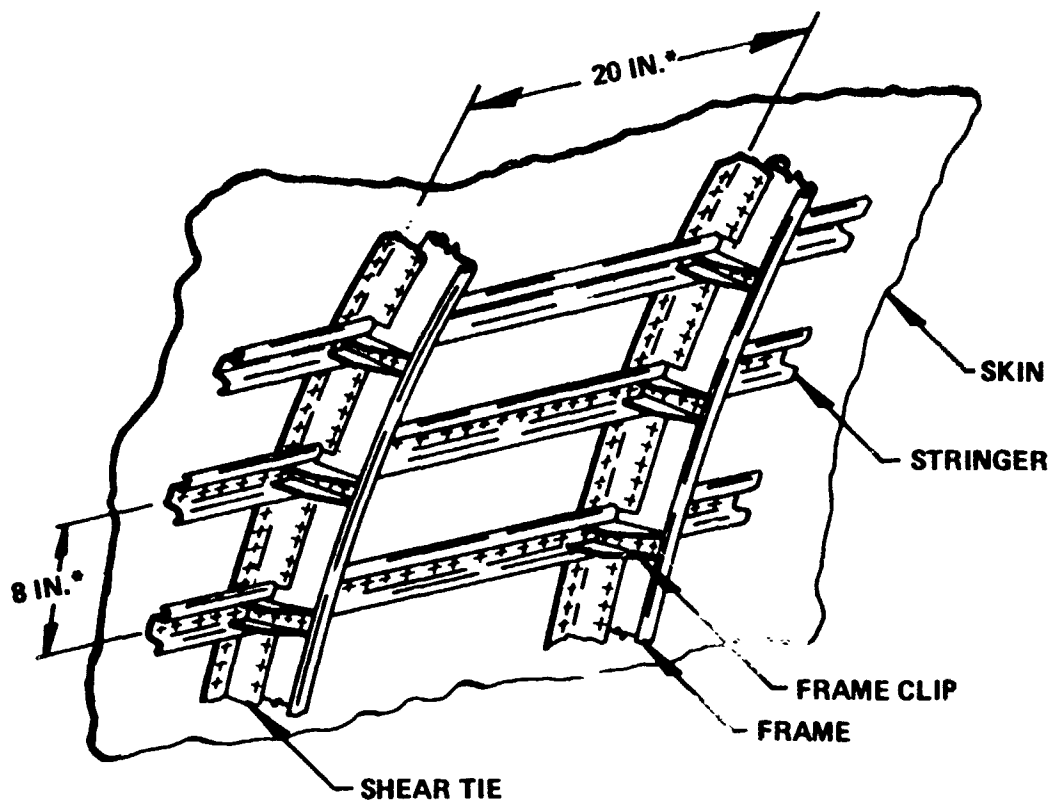
The interior of the YC-14 fuselage is lined with fiberglass or fiberglass/lead vinyl blankets, providing both acoustic and thermal insulation. Distribution and construction of the blankets is indicated in Figures 10(b) and 11.

Note that trim panels in addition to fiberglass blankets are utilized on the sidewalls and aft bulkhead wall of the flight deck. This trim is of a 3/8-in. thick, 1/4 in. cell size, 1.5 lb/ft³ core/fiberglass faced honeycomb structure weighing approximately 0.6 lb/ft².

The following areas of the flight and cargo deck are not insulated:

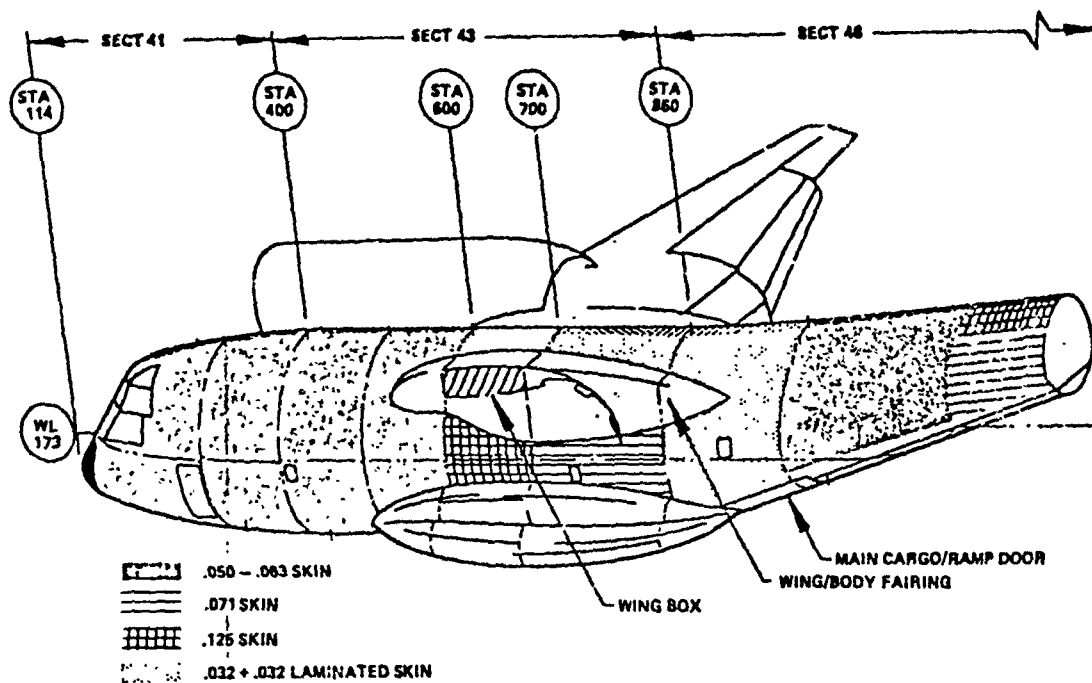
- Wing box section penetrating the cargo compartment (this section of the wing box is, however, constructed to be a reserve fuel tank and was kept filled during cabin noise testing)
- Cargo ramp door
- Cargo deck floor
- Fuselage walls aft of station 1250

The flight deck floor is covered with a commercial airplane type carpeting and pad.

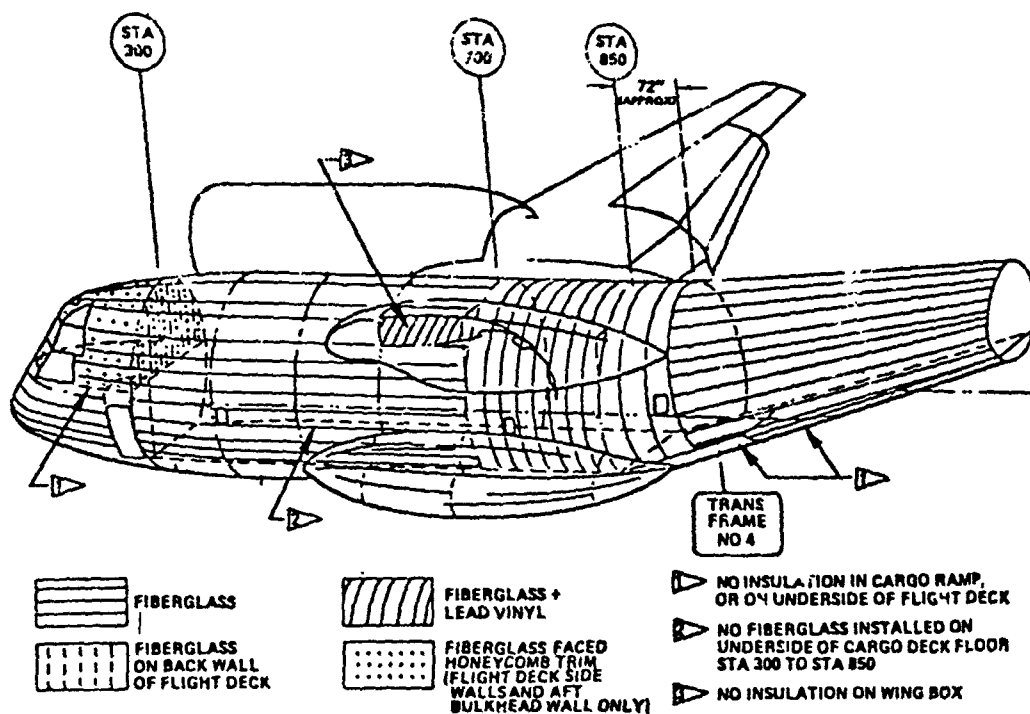


* STA 400 TO 860

Figure 9 Typical YC-14 Fuselage Construction



(a) SKIN PANEL DIAGRAM FOR YC-14



(b) FUSELAGE ACOUSTIC/THERMAL INSULATION DISTRIBUTION (PROTOTYPE)

Figure 10 YC-14 Fuselage Structure Diagrams

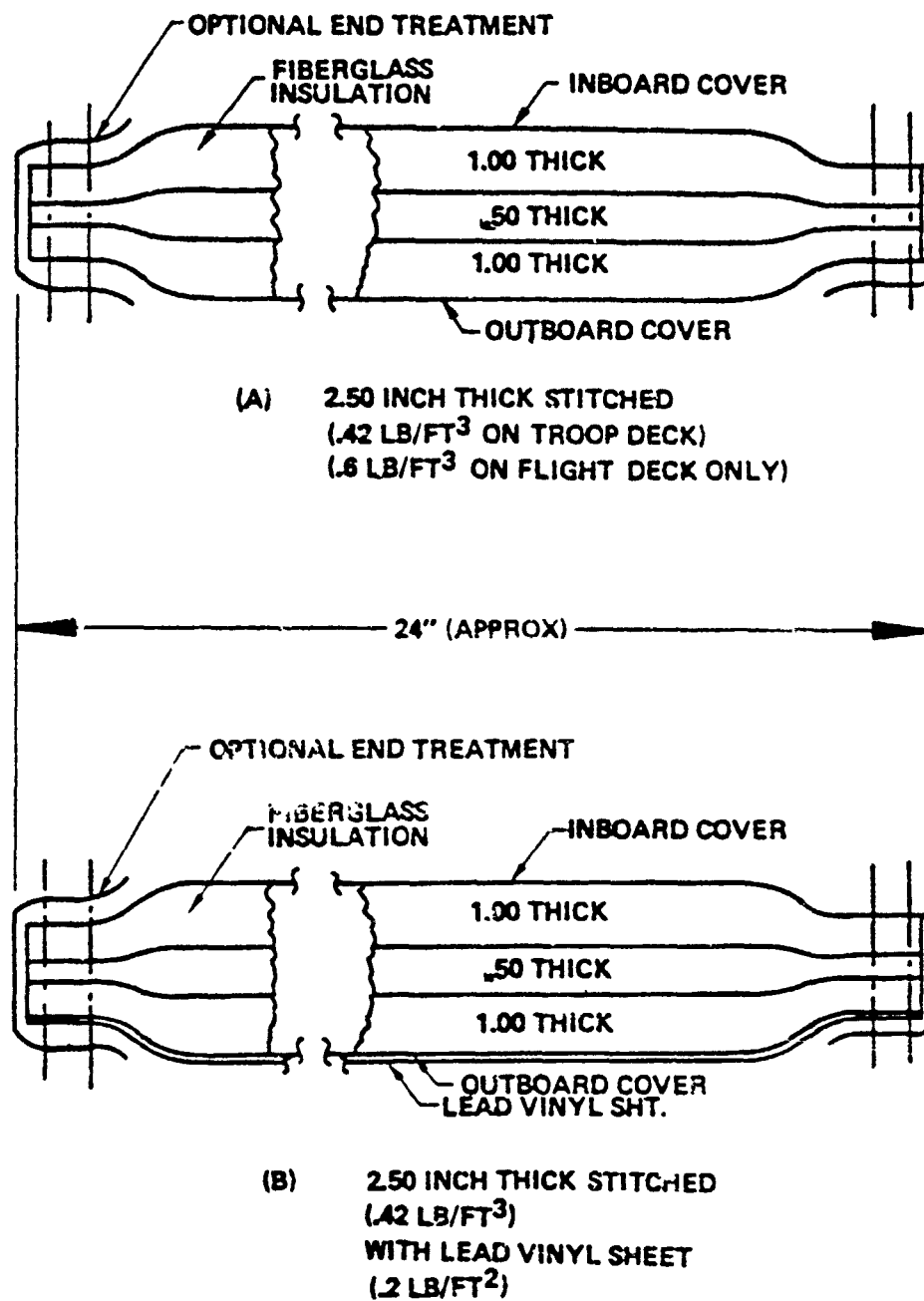


Figure 11 Acoustic/Thermal Insulation Blanket Construction (Prototype)

SECTION III

DATA ACQUISITION SYSTEMS

This section describes data systems explicitly installed on or existing systems utilized on the YC-14 for accomplishing interior noise measurements. Paragraph III-1 covers acoustic and vibration sensors, and Paragraph III-2 the corresponding recording systems. A brief description of the basic YC-14 data acquisition system is presented in Paragraph III-3.

1. ACOUSTIC AND VIBRATION TRANSDUCER SYSTEMS

a. Transducer Locations and Types

Transducers installed specifically to accomplish interior noise measurements included 14 flush mounted exterior (body) microphones, 10 cabin microphones, and 13 accelerometers attached to various points of the fuselage interior. The locations, required ranges, and accuracies of these transducers are indicated in Figures 12 and 13 and in Tables II and III. Typical installations are shown in Figures 14 through 19.

Flush mounted exterior body microphones were provided under and shared by the USB Flap Loads program (Reference 4) for which extensive instrumentation, including additional flush mounted body microphones, flush mounted wing and USB flap microphones, internal engine microphones, flap accelerometers, wing static pressure sensors, and wing and body temperature sensors, were also provided.

b. Acoustic Sensors

As noted in Table III, flush mounted exterior body microphones were either Photocon 524s or B&K 4136s. The Photocons were utilized at locations in the direct vicinity of large amplitude exhaust jet/USB flap interaction pressure fluctuations, and where levels in excess of 145 dB were anticipated. The less rugged but more sensitive B&K 4136s were employed in areas of lower amplitude pressure fluctuations, primarily for sensitivity to anticipated lower dB signal levels.

Comparative capabilities of the three types of microphones are summarized in Table IV.

The Bruel and Kjaer Model 4136 microphone used for exterior fuselage is a small microphone that has a 1/4-in.-diameter diaphragm. The Bruel and Kjaer Model 4134 used for cabin interior noise is similar with a 1/2-in.-diameter diaphragm. The microphone sensing element is a condenser using an A.C. power supply and a cathode follower. The 4136 microphone sensing element was flush mounted to the exterior pressure field and electrically isolated (Figure 19).

NOTE:
 → INDICATES POSITIVE
 RESPONSE AXIS

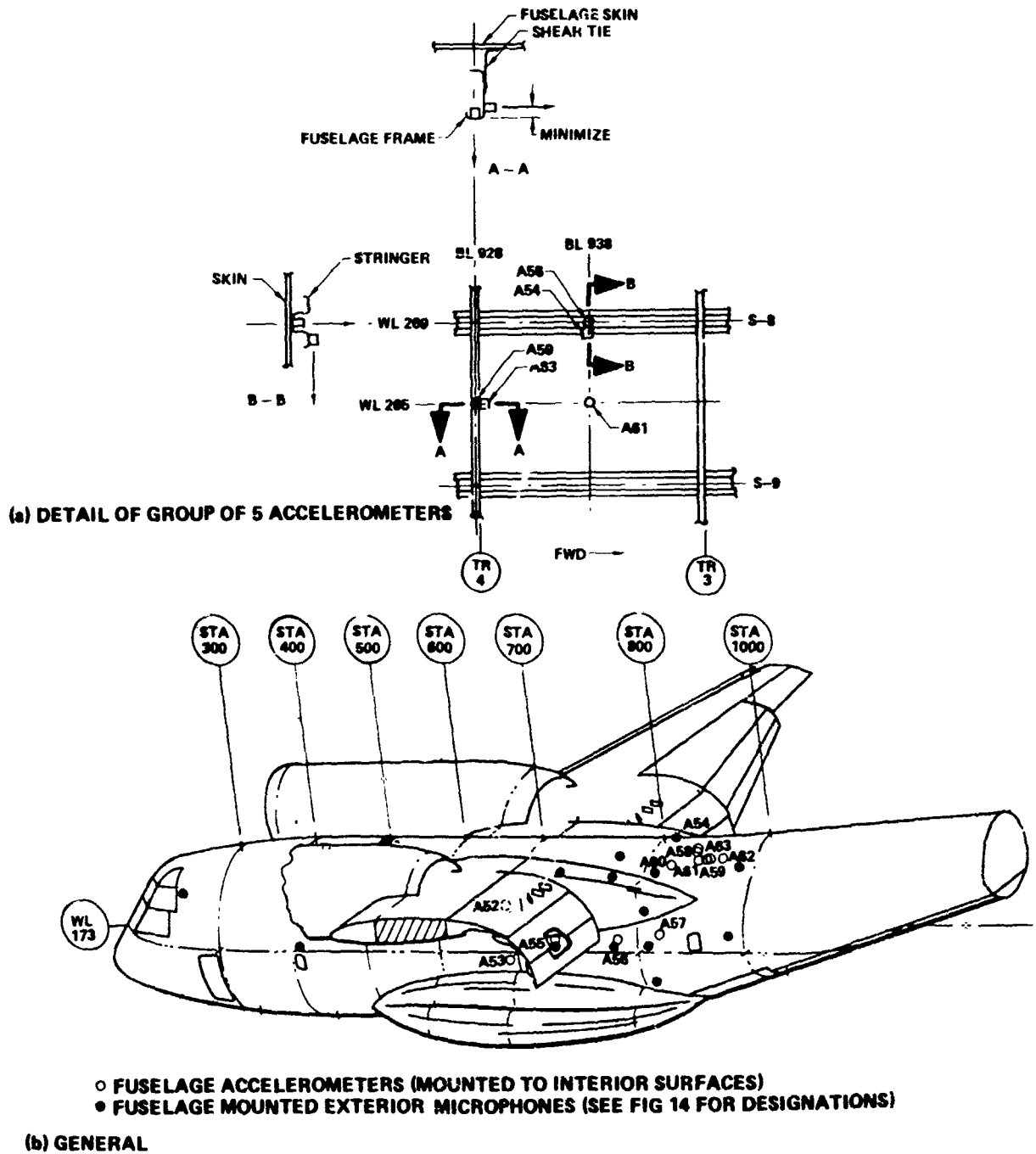
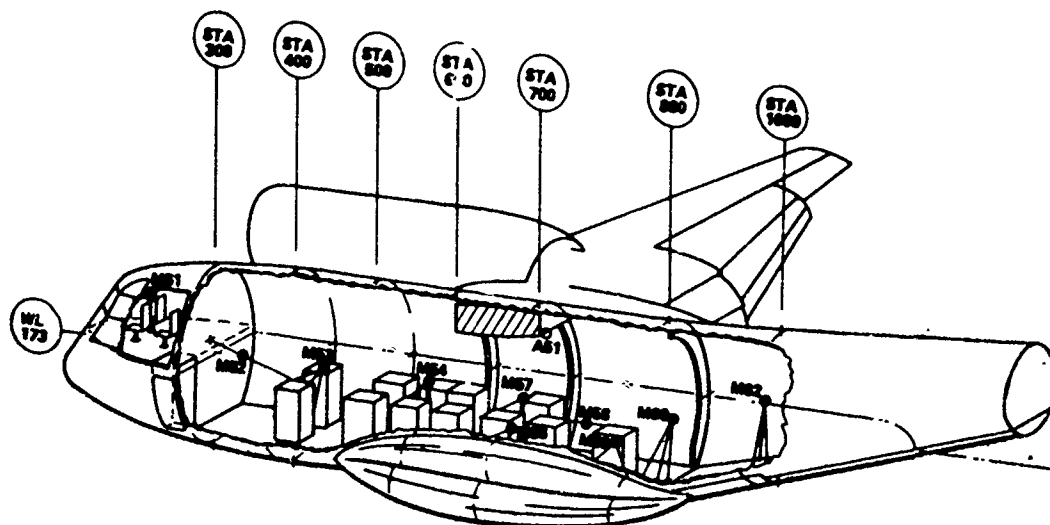
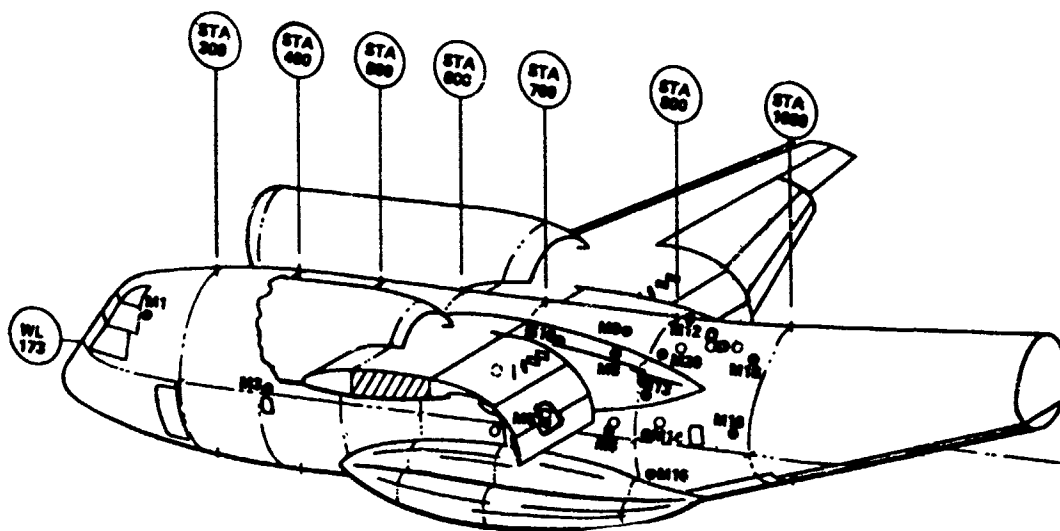


Figure 12 General Instrumentation Layout—Fuselage Accelerometers



(a) CABIN MICROPHONES



● FLUSH MOUNTED EXTERIOR MICS
○ FUSELAGE ACCELEROMETERS (SEE FIG 12 FOR DESIGNATIONS)
(b) FLUSH MOUNTED FUSELAGE MICROPHONES

Figure 13 General Instrumentation Layout—Microphones

Table III Instrumentation Types

CABIN MICROPHONES (INTERIOR)	FUSELAGE MICROPHONES (EXTERIOR)	FUSELAGE ACCELEROMETERS	NOTE	TYPE	RESPONSE RANGE		ACCURACY
					FREQUENCY	LEVEL	
M51 (1460) M52 (1461) M55 (1462) M54 (1463)	M1 (1381) M3 (1383)		1	B&K 4134	20-5000 Hz	60 140 dB	± 2 dB
M56 (1465)			2	B&K 4138 Except as noted	20 5000 Hz	70-160 dB	± 2 dB
M57 (1464)		A51 (1472) A52 (1473) A53 (1475)	3	Photocon 524	20-5000 Hz	120 170 dB	± 2 dB
	M5 (1385) M10 (1390)	A55 (1477)	4	BBN Type 501 except as noted	10-3000 Hz	0.02-100 Gs	± 10%
M58 (1466)			5	Vibra- metrics	10-3000 Hz	0.02-100 Gs	± 10%
M59 (1468)	M6 (1386) M8 (1388) M9 (1389)	A55 (1478)	6	Accelerometer Attached to Small Aluminum Block			
M60 (1469)	M12 (1392) M20 (1400) M13 (1393) M14 (1394) M15 (1395)	A57 (1479) A60 (1480)					
		A54 (1476) A58 (1474) A61 (1481) A59 (1470) A63 (1484)					
M62 (1471)	M16 (1396) M18 (1398)	A62 (1482)					



Figure 14 Location of Microphone M51 on Flight Deck



Figure 15 View of Cabin Looking Forward from Station 750



Figure 16 View of Sidewall Microphones Looking Forward



Figure 17 View of Cabin Looking Aft from Station 530

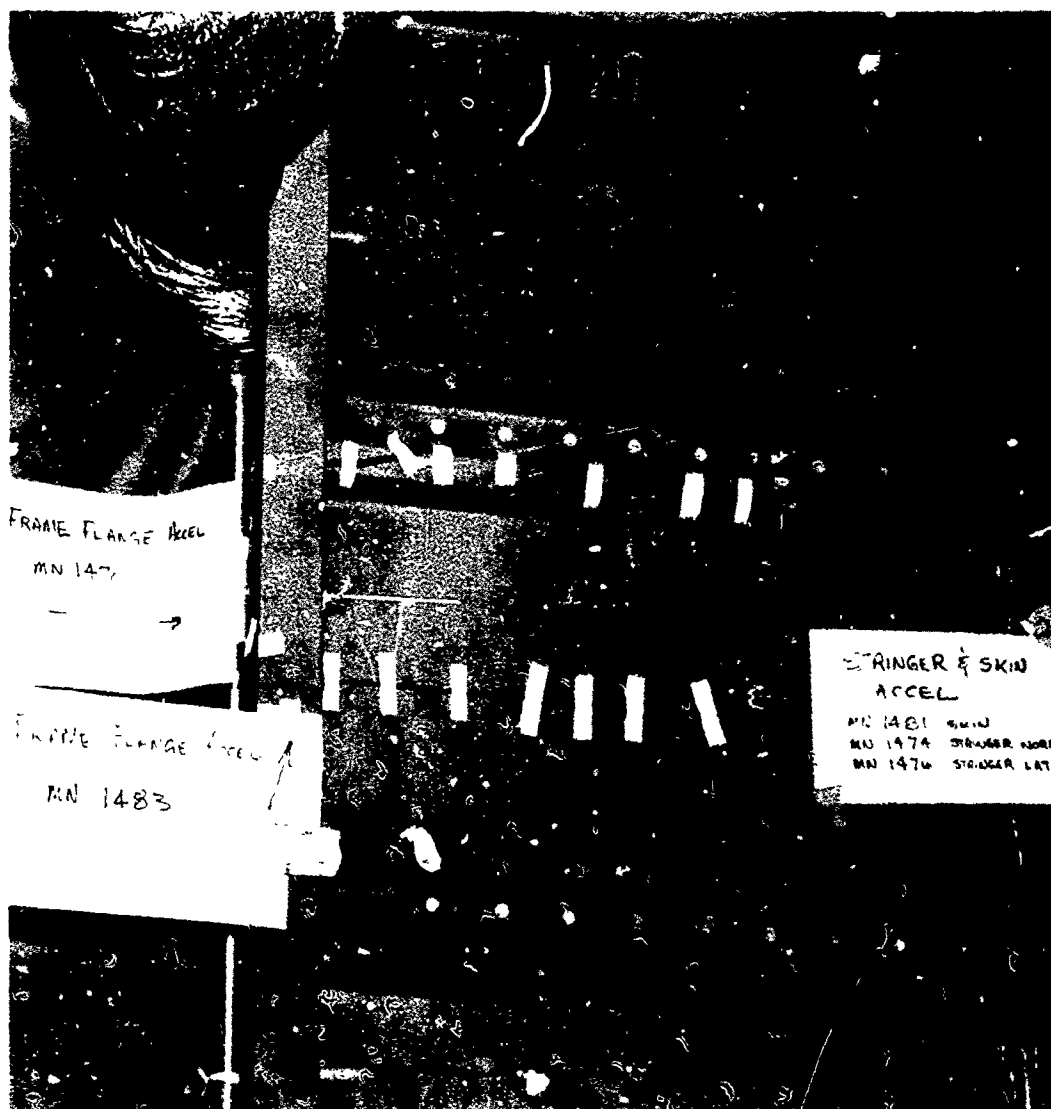
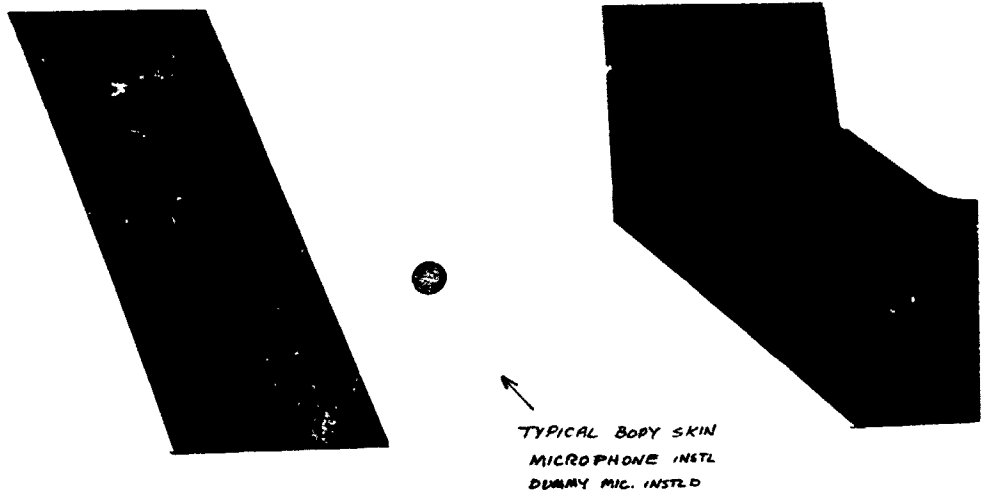


Figure 18 Detail of Group of Five Accelerometers




(a) INTERIOR VIEW




(b) EXTERIOR VIEW

Figure 19 Fuselage Microphone Installation

Table IV Comparative Capabilities of Microphones

	 Correlation limitations	Temperature limitations	Useable range	Moisture resistance	Large amplitude pressure fluctuation capability	Vibration limitation (RMS)
Photocon 524	OK for $f > 10$ Hz	$< 200^{\circ}\text{F}$ (AC signal only)	120 to 170 dB	Very good	Excellent	< 50 Gs
B&K 4136	OK for $f > 80$ Hz	$< 125^{\circ}\text{F}$	70 to 160 dB	Poor	Poor	< 10 Gs
B&K 4134	OK for $f > 40$ Hz	$< 125^{\circ}\text{F}$	60 to 140 dB	Poor	Poor	< 10 Gs

 Correlation capability is possible between any of the microphone types (or accelerometers) for the frequency ranges shown subject to data recording commonality

The Photocon Research Systems Model 524 microphone has a flush diaphragm that is 1/2-in. in diameter. The microphone is a condenser type that is electrically coupled with a very-high-frequency carrier. The microphone sensing element is flush mounted to the skin and electrically isolated from ground structure, as in Figure 19

c. Vibration Sensors

The accelerometers used to monitor the fuselage sidewall vibration were miniature (approximately 1.8 g) integrated types such as the BBN501 or the Vibra-Metrics M1001A. These accelerometers have a built-in electronic preamplifier on a rugged micro circuit chip that eliminates the need for a line driver and coaxial cable, while maintaining light weight and small size.

2. DATA RECORDING SYSTEMS

A block diagram of the overall acoustics and dynamics recording system is shown in Figure 20. The acoustics portion of this system recorded data for this contract effort as well as for the NASA USB Flap Loads program (Reference 4). The dynamics portion recorded data for these same two contract efforts and also for the basic YC-14 airplane project.

Microphone data were recorded at 30 in./sec. while acceleration data were recorded at 7-1/2 in./sec. Usable frequency range for the microphone data was 20 Hz to 10,000 Hz, while the range for the acceleration data was 7 Hz to 2500 Hz.

The number of transducers required for the test exceeded the number of record tracks available on the four magnetic tape recorders. To alleviate this problem, the transducers were divided into groups of 12 for acoustics and groups of 13 for dynamics. The transducer groups were labeled A, B, and C and were coupled to the magnetic tape recorders through switching networks as shown in block diagram of Table V. Each tape recorder recorded only one switch position at any given time and each tape recorder was independent of the other. However, each transducer group/switch position was dedicated to a particular tape recorder.

3. BASIC YC-14 DATA ACQUISITION SYSTEMS

Data defining airplane operating status during interior noise measurements test conditions were obtained from the extensive basic YC-14 instrumentation system.

Instrumentation installed on the No. 1 YC-14 prototype for recording of approximately 950 total channels of information on magnetic tape included approximately 535 channels of high-speed pulse code modulated (HSPCM) information, 320 channels of electronic flight control system (EFCS) serial digital and bit-by-bit data, and 100 channels of wideband FM information during the developmental flight period. Approximately 35 channels of data were also recordable on an onboard oscillograph, and approximately 37 channels were to be telemetered.

Figure 21 is a block diagram of the basic airplane HSPCM data system.

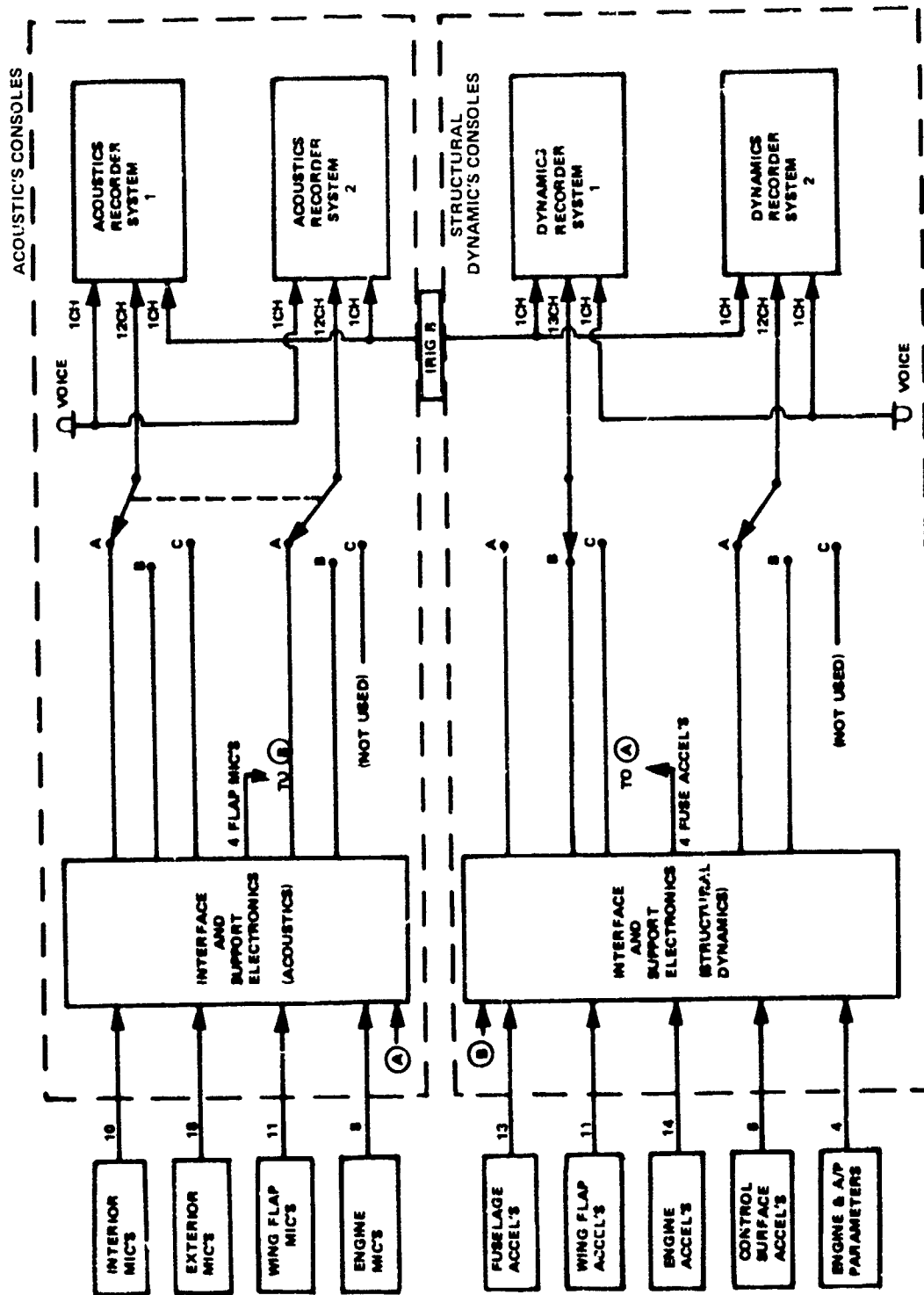


Figure 20 Schematic Block Diagram of Overall Acoustics and Dynamics Recording System

Table V Recorder/Group Switch Position/Data Type Matrix

	GROUP SWITCH POSITION		
	A	B	C
Acoustics recorder No. 1	(Interior noise and flap loads) ● 12 exterior microphones	(Flap loads) ● 4 exterior microphones ● 8 engine microphones	(Interior noise) ● 3 exterior microphones ● 5 interior microphones ● 4 fuselage accelerometers
Acoustics recorder No. 2	(Interior noise) ● 2 exterior microphones ● 10 interior microphones	(Flap loads) ● 1 exterior microphones ● 11 wing flap microphones	Not used
Dynamics recorder No. 1	(YC-14 project) ● 9 engine accelerometers ● 4 engine parameters	(Interior noise) ● 13 fuselage accelerometers	(Flap loads and YC-14 project) ● 4 flap accelerometers (NASA) ● 3 YC-14 flap accelerometers ● 6 equipment accelerometers
Dynamics recorder No. 2	(YC-14 project) ● 5 engine accelerometers ● 6 control actuator accelerometers ● 2 engine parameters	(Flap loads) ● 9 flap accelerometers ● 4 flap microphones	Not used

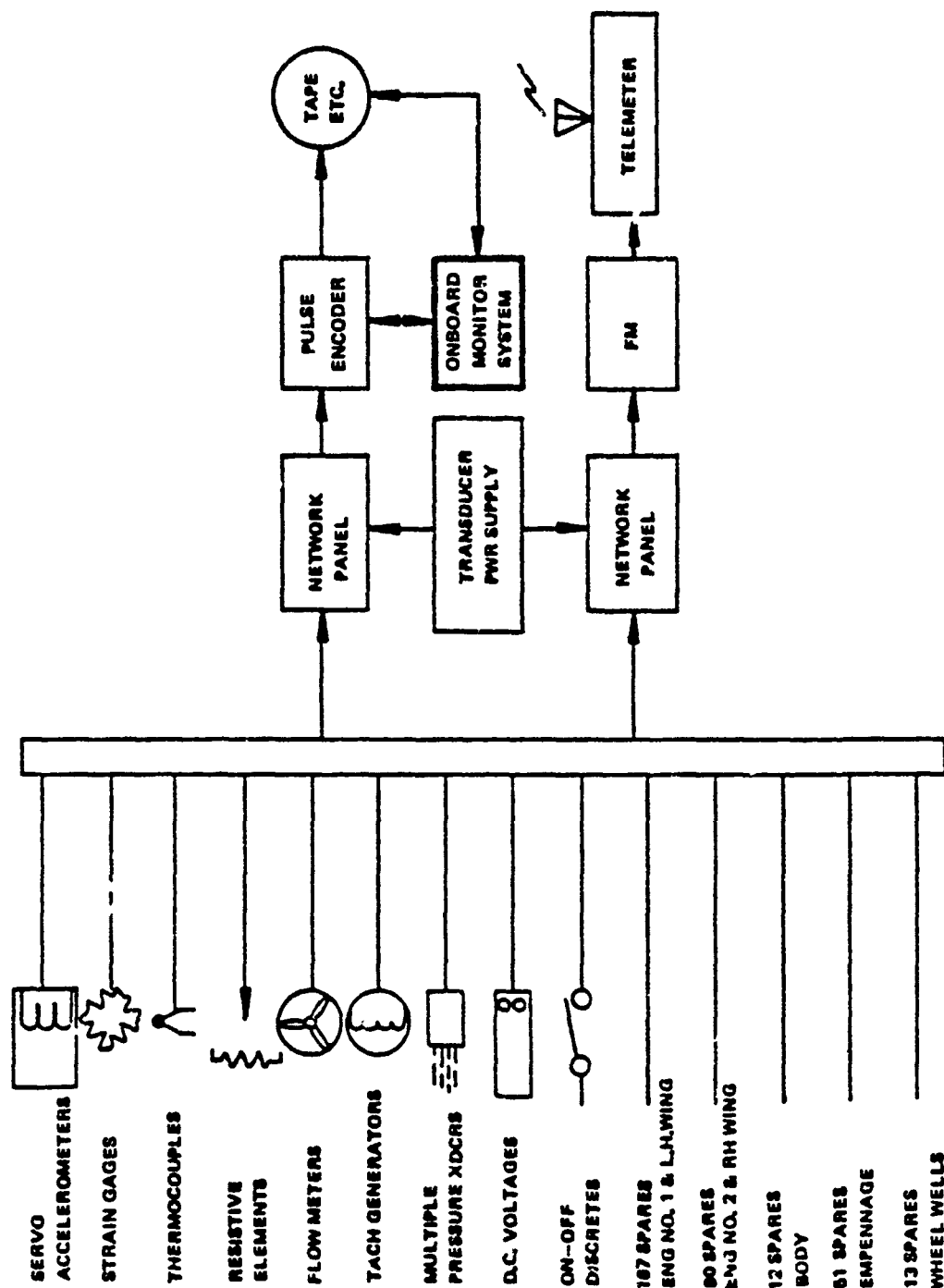


Figure 21 Block Diagram of Basic YC-14 Data System

SECTION IV

TEST OPERATIONS

This section describes test conditions and data acquisition procedures used during interior noise measurements data acquisition efforts.

1. TEST CONDITION

Table VI summarizes test conditions during which acquisition of interior noise measurement data was attempted.

The reader should keep in mind that in most cases interior noise measurement data were acquired concurrently at test conditions defined by basic YC-14 airplane test program requirements. Occasionally this would result in noise data acquisition at conditions slightly less than ideal: i.e., cruise data at 22,000 ft rather than 35,000 ft. Whenever possible, data would be acquired at a later time corresponding to a more suitable test configuration. In a few cases, as in that cited, because of lack of test time or higher priority airplane requirements, this was not possible. Such occurrences are pointed out in the following discussions.

Interior noise measurements data acquired during test flight 20-3 were done so remotely. Because this flight involved flutter testing, no acoustics or dynamics operators were present on the airplane. Data acquisition was controlled by the co-pilot via a remote tape recorder start/stop switch located to the right of his seat. Amplifier gains were set once prior to take-off and remained the same for all conditions during the flight. On occasion, resultant recorded data quality was unacceptable: i.e., levels too low or too high for the preset equipment to handle faithfully. Dynamics data were particularly subject to this difficulty.

a. Ground Test Conditions (7.01.001.001 through 7.01.001.012)

For condition .001 (dead airplane ambient), external electric power was provided to the airplane to operate acoustics and structural dynamics consoles and sensors, and required airplane internal systems. Airplane internal systems included most of the electrical distribution and control systems located on the front wall of the troop compartment, just under the aft floor of the flight deck. YC-14 engines were off during this condition.

For conditions .002 and .003 (Sabre VI to port and to starboard) only YC-14 systems per condition .001 were on within the airplane. Again, the YC-14 engines were off. Significant external noise was generated by the engine of the Sabre VI, a pure turbojet, which was run at $N_1 = 7220$ RPM (90% of takeoff N_1) with the Sabre VI parked in close proximity to the YC-14. During condition .002, the Sabre VI was to the port side of the YC-14 (the side on

Table VI Summary of Interior Noise Measurements Conditions

NASA/AFDL CONDITION NUMBER	CONDITION TIME (NOMINAL) HR : MIN : SEC	FLIGHT TEST NO. , DATE	CONDITION DESCRIPTION	NOMINAL TEST CONDITION PARAMETERS				DATA ACQUISITION ACTIVITY						
				ALT FT	SPEED F/S	N ₁ RPM	VMA F/S	USA DEG	EXT + INT MIC'S + ENG ACCEL'S	EXT MIC'S + FLAP MIC'S	EXT MIC'S + ENG MIC'S	EXT + INT MIC'S + FUS ACCEL'S	INTERIOR MICROPHONES	EXTERIOR MICROPHONES
7 01 001 001	18 52 29	19-1, 10/8/76	Dead airplane ambient	0	0	0	0	0	•	•	•	•	•	•
7 01 001 002	18 45 12	19-1, 10/8/76	Sabrejet to port, ground	0	0	0	0	0	•	•	•	•	•	•
7 01 001 003	18 45 12	19-1, 10/8/76	Sabrejet to port, ground	0	0	0	0	0	•	•	•	•	•	•
7 01 001 004	19 03 45	19-1, 10/8/76	Sabrejet to stbd, ground	0	0	0	0	0	•	•	•	•	•	•
7 01 001 005	Not Done	Not Done	Cabin reverberation	Not Done	Not Done	Not Done	Not Done	Not Done	•	•	•	•	•	•
7 01 001 006	18 08 55	19-1, 10/8/76	Port YC eng, idle, ground	0	0	820	220	0	•	•	•	•	•	•
7 01 001 007	14 12 58	19-1, 10/8/76	Port YC eng, hi-pw, ground	0	0	3150	890	0	•	•	•	•	•	•
7 01 001 008	14 12 58	19-1, 10/8/76	Port YC eng, hi-pw, ground	0	0	3150	590	0	•	•	•	•	•	•
7 01 001 009	14 16 41	19-1, 10/8/76	Port YC eng, med-pw, ground	0	0	2750	760	0	•	•	•	•	•	•
7 01 001 010	14 20 31	19-1, 10/8/76	Both YC eng's, idle, ground	0	0	810	220	0	•	•	•	•	•	•
7 01 001 011	14 24 50	19-1, 10/8/76	Both YC eng's, hi-pw, ground	0	0	3100	880	0	•	•	•	•	•	•
7 01 001 012	14 24 50	19-1, 10/8/76	Both YC eng's, hi-pw, ground	0	0	3100	880	0	•	•	•	•	•	•
7 01 001 013	16 04 00	19-3, 10/14/76	Both, idle, 0 PSI diff, ground	0	0	820	220	0	•	•	•	•	•	•
7 01 001 014	16 08 14	19-3, 10/14/76	Both, hi-pw, 4 PSI diff, ground	0	0	3100	880	0	•	•	•	•	•	•
7 01 001 015	14 29 09	19-1, 10/8/76	Stbd YC eng, hi-pw, ground	0	0	2740	760	0	•	•	•	•	•	•
7 01 001 016	14 35 50	19-1, 10/8/76	Stbd YC eng, med-pw, ground	0	0	3150	880	0	•	•	•	•	•	•
7 01 001 017	14 38 27	19-1, 10/8/76	Continuous takeoff, flaps 20	0	0	2770	760	0	•	•	•	•	•	•
7 01 001 018	11 42 18	19-3, 10/14/76	Continuous takeoff, flaps 20	0 to 6500	0 to 350	3800	1100	0	•	•	•	•	•	•
7 01 001 019	11 56 25	19-3, 10/14/76	Low alt cruise	0 to 1500	0 to 300	3700	1050	0	•	•	•	•	•	•
7 01 001 020	16 44 11	20-3, 10/29/76	Cruise, M 70	10600	490	2450	790	0	•	•	•	•	•	•
7 01 001 021	16 42 03	20-3, 10/29/76	Cruise, M 65	22400	720	3240	1140	0	•	•	•	•	•	•
7 01 001 022	16 39 50	20-3, 10/29/76	Cruise, M 55	22100	670	3160	1090	0	•	•	•	•	•	•
7 01 001 023	17 42 50	20-3, 10/29/76	No around	8000-10000	520	2690	910	0	•	•	•	•	•	•
7 01 001 024	12 51 10	19-3, 10/14/76	0° to 70° flap cycle	11000	210	2950	850	0	•	•	•	•	•	•
7 01 001 025	12 54 10	19-3, 10/14/76	0° to 70° flap cycle	10000	210	2950	930	0	•	•	•	•	•	•
7 01 001 026	15 39 42	19-3, 10/14/76	Flight idle, A/C and pres on	6700	300	1380	450	0	•	•	•	•	•	•
7 01 001 027	15 41 12	19-3, 10/14/76	Flight idle, A/C and pres off	5600	290	1380	440	0	•	•	•	•	•	•
7 01 001 028	18 41 51	19-1, 10/8/76	Continuous landing, flaps 45	2000-0	200-130	2300-300	600-220	0	•	•	•	•	•	•
7 01 001 029	15 55 00	19-3, 10/14/76	Continuous landing, flaps 30	2000-0	180	2100	500	0	•	•	•	•	•	•
7 01 001 030	17 56 00	20-3, 10/29/76	Continuous landing, flaps 60	2000-0	180	2100	600	0	•	•	•	•	•	•

which essentially all flush mounted fuselage microphones and fuselage accelerometers were installed), and to the starboard side during condition .003. Figure 22 provides dimensional data on the position of the Sabre VI relative to the YC-14. During both conditions, .002 and .003, at least 1 min of stabilized (Sabre VI operation at $N_1 = 7220$ RPM) microphone and accelerometer data was obtained. Weather conditions were clear and windless.

Condition .002.1 was a repeat of .002 with the internal exception that the recorders were set up for configuration C rather than configuration A data acquisition.

Condition .004 (cabin reverberation calibration) was not accomplished.

Conditions .005 through .012 were static ground runs with either port engine only, the starboard engine only, or both engines operating, per Table VII.

At least 1 min of stabilized engine operation was recorded at each of these conditions.

All of these conditions were accomplished during clear, dry 55°F to 65°F weather with a crosswind of less than 10 mph.

b. Flight Test Conditions (7.01.001.013 through 7.01.001.22.2)

Conditions .013 and .013.1 were essentially identical full power takeoffs ($N_1 = 3800$ RPM), with flap handle set to FLAPS 20; i.e., outboard flaps at 40°, USB flaps at 0°. Note that this is essentially identical to the non-STOL FLAPS 30 landing, except outboard flaps are at 58° rather than 40°. For these two conditions, data acquisition was begun at brake release and continued for at least 1 minute into climbout. Weather conditions for both takeoffs were clear and dry. Airplane behavior for the two conditions is shown in Figures 23 and 24.

For conditions .014, .015, .016, and .017, the airplane was configured for level flight cruise operation, i.e., flaps fully retracted and gear up. Altitude/speed combinations included:

- 10,600 ft @ 490 ft/sec (250 knots) (condition 7.01.001.014)
- 22,400 ft @ 720 ft/sec (Mach 0.70) (condition 7.01.001.015)
- 22,100 ft @ 620 ft/sec (Mach 0.65) (condition 7.01.001.016)
- 22,200 ft @ 570 ft/sec (Mach 0.55) (condition 7.01.001.017)

The normal pressurization system was in operation during these runs. Runs were accomplished in clear air. At least 1 minute of stabilized data was obtained for each. As noted in Section IV-1, data for conditions .015, .016, and .017 were acquired remotely, resulting in questionable dynamics data.

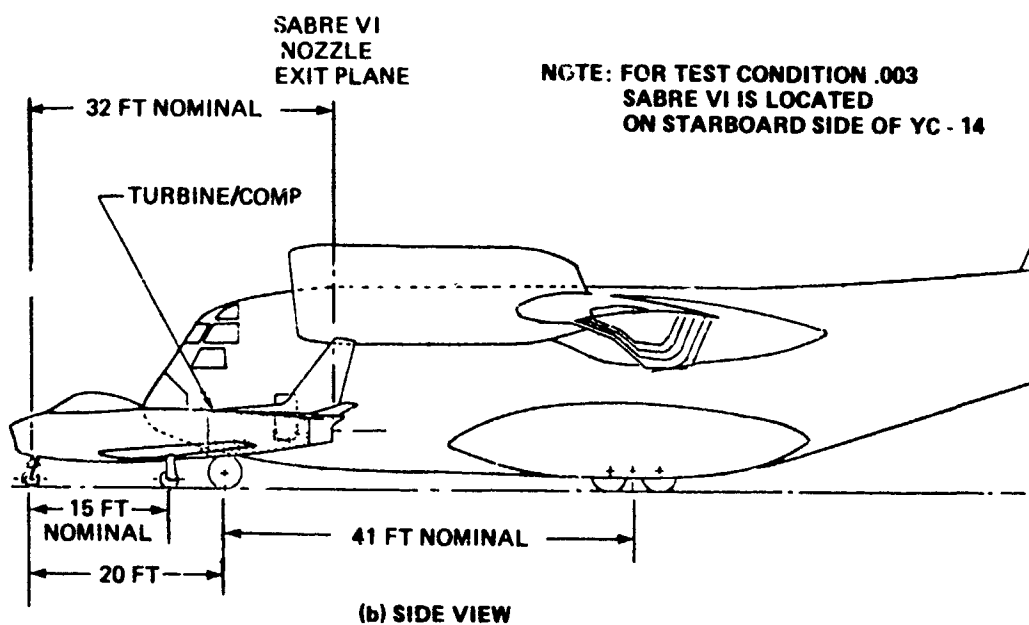
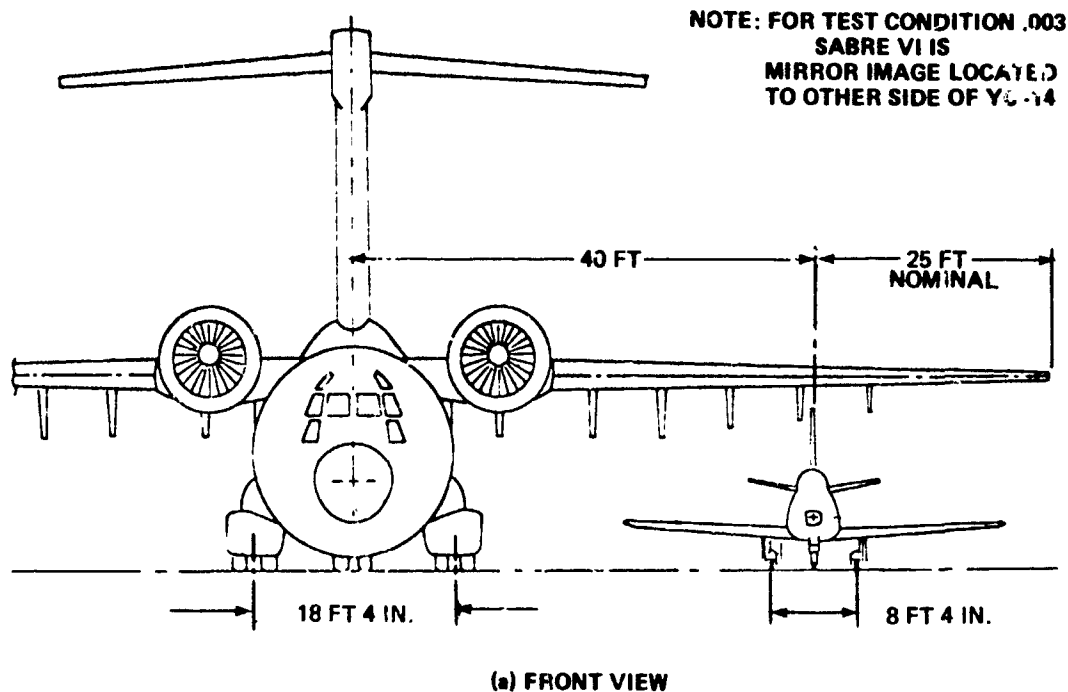
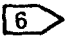



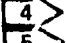
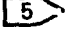



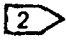
Figure 22 YC-14/Sabre VI Configuration for Test Condition .002


Table VII YC-14 Engine Ground Runs

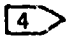
Condition	Note	Engine on	Power level	N ₁ 
7.01.001.005		Port	Idle	820
7.01.001.00		Port	High	3,150
7.01.001.006.1		Port	High	3,150
7.01.001.007		Port	Medium	2,750
7.01.001.008		Both	Idle	810
7.01.001.009		Both	High	3,100
7.01.001.009.1		Both	High	3,100
7.01.001.009.2		Both	Idle	820
7.01.001.009.3		Both	High	3,100
7.01.001.010		Both	Medium	2,740
7.01.001.011		Starboard	High	3,150
7.01.001.012		Starboard	Medium	2,740


Notes:

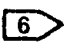
 Two of the three (A and C) engine hydraulic systems, all engine fuel pumps, and the cabin air conditioning (A/C) system were off for this run

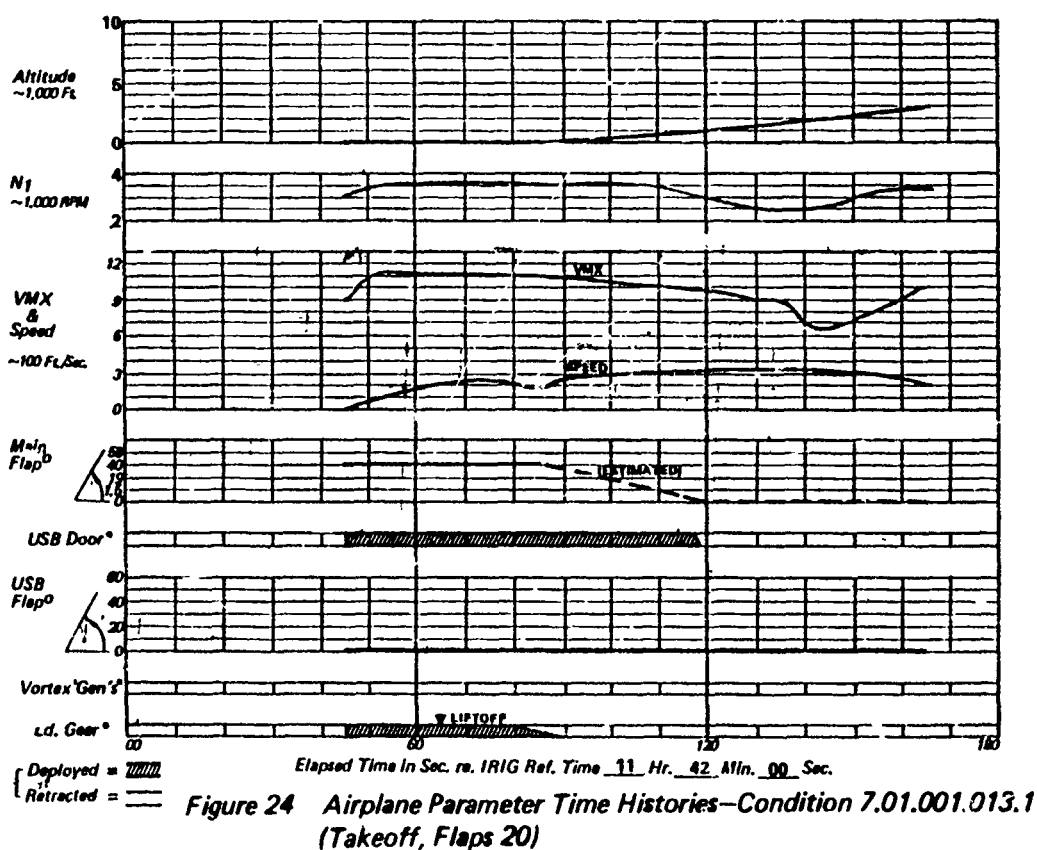
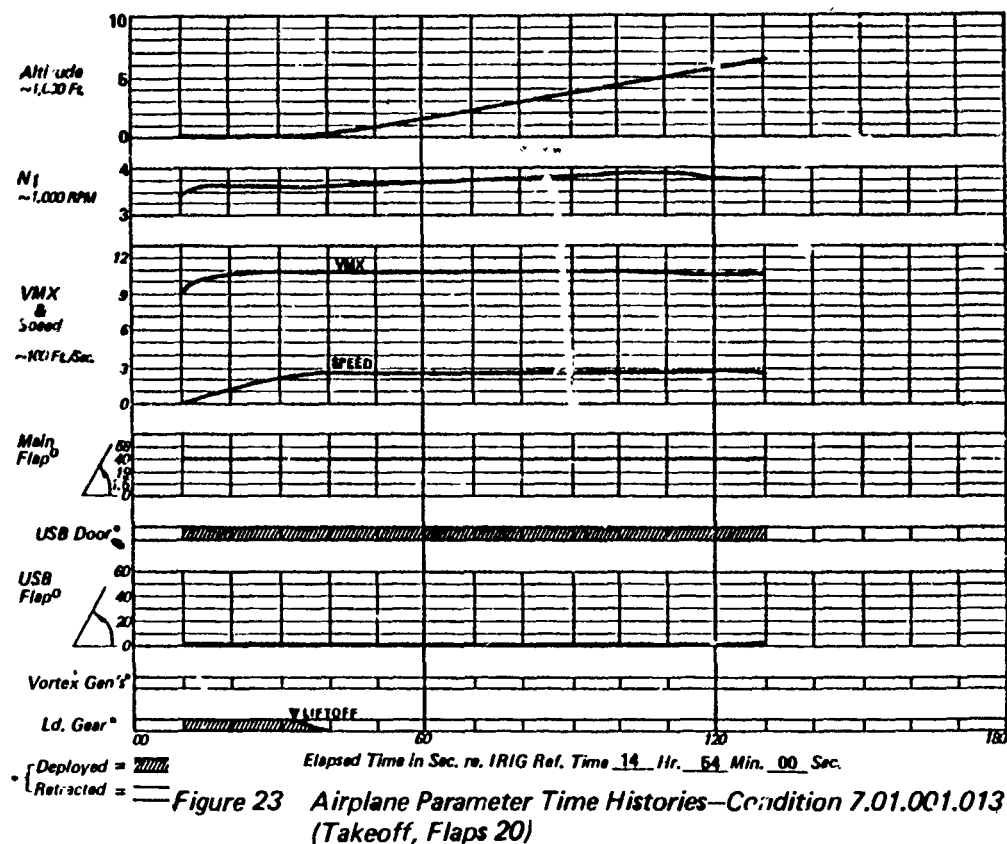
 This run was a repeat of run .006, except that configuration C data rather than configuration A data were acquired

 Same as Item 2, except with respect to run .009

 Repeat of run .005, except normal hydraulics, fuel pumps, and air conditioning systems were on

 For this run, the cabin was pressurized to 4 psi above external atmosphere pressure (to approximately 18.7 psi). This was accomplished via the airplane's pressurization system operated in the MANUAL mode

 For port engine, except during conditions .011 and .012



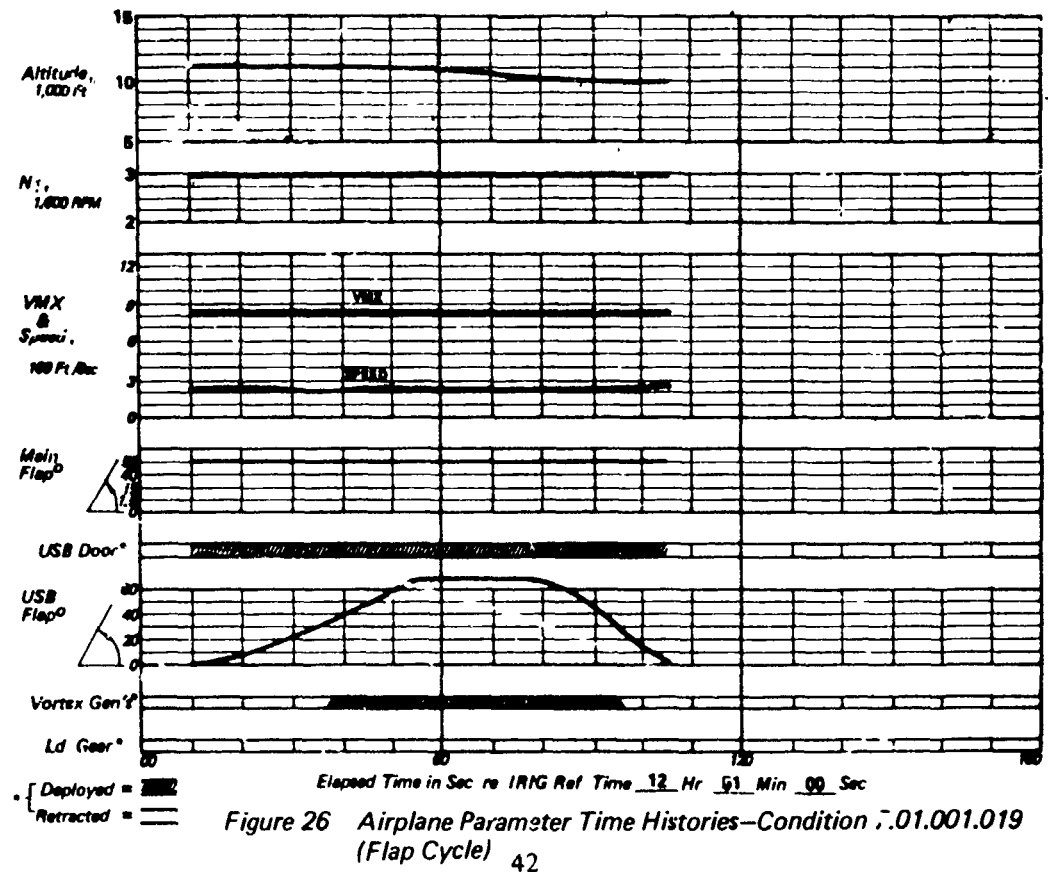
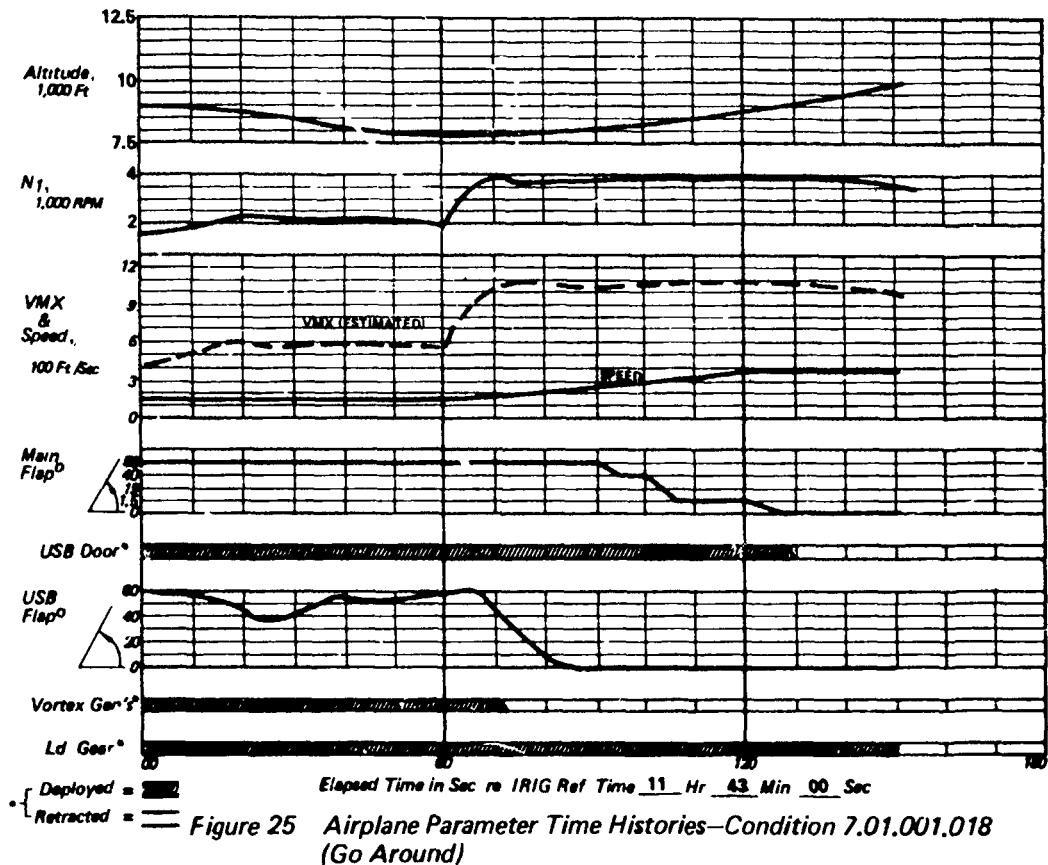
The anticipated normal YC-14 cruise altitude is 35,000 ft. Acquisition of interior noise data was requested at this altitude, but because of more urgent basic YC-14 flight test requirements, this request could not be met. External fuselage data, however, were obtained at 40,000 ft at M 0.76, M 0.60, and M 0.55 for the Flap Loads program (Reference 4). However, no cabin noise data or fuselage wall vibration data were obtained.

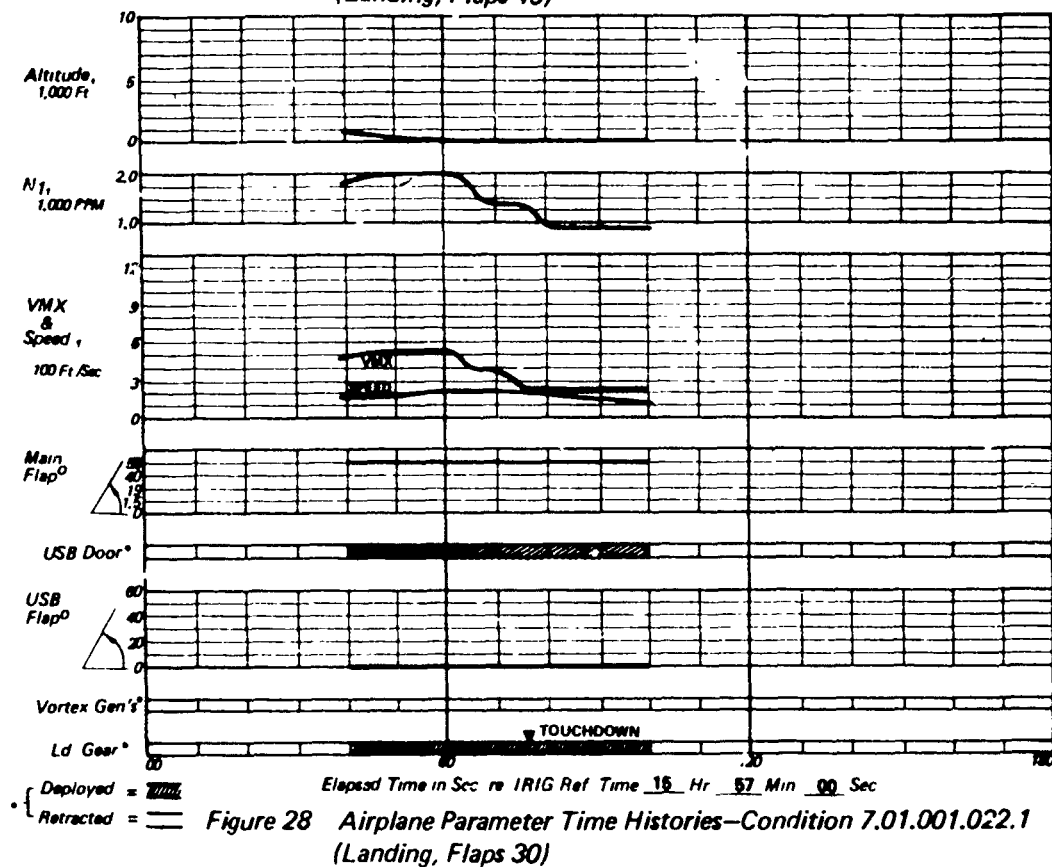
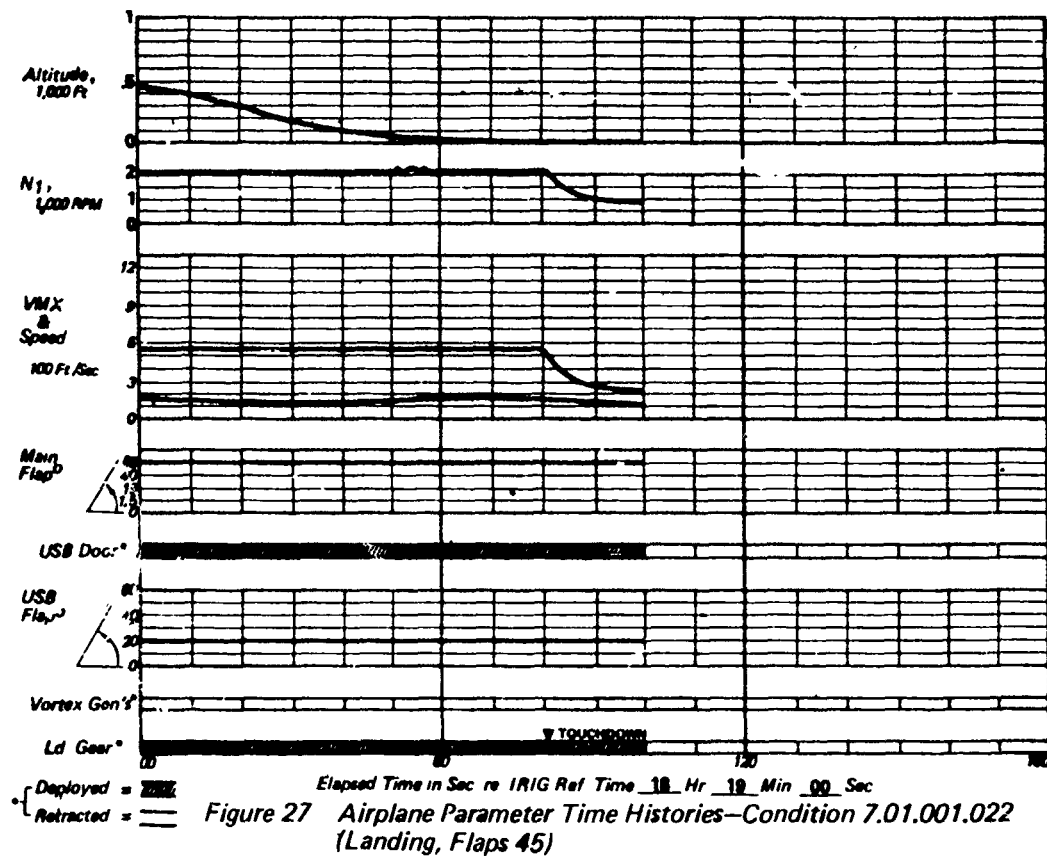
For condition .018 the airplane was put through a go-around maneuver with gear down and flap handle at FLAPS 60. The airplane was put into a 6° glide slope, 100-knot approach configuration using the EFCS. In this configuration, the USB flaps and engine power level modulated around nominal values of $USB = 40^\circ$, $N_1 = 2200$ RPM. After approximately 30 seconds in this mode, the throttles were advanced rapidly to takeoff power and the plane reestablished a go-around climb attitude at 150 to 200 knots. Note that during the change from the 6° glide slope to climbout, the USB flaps retract fully. This condition was conducted in clear air at 8,000 ft altitude. Data were remotely acquired continuously from the initiation of the 6° glide slope set up to about 30 seconds into the stabilized go-around climb. Airplane behavior for this condition is shown in Figure 25.

For conditions .019 and .019.1, the airplane was put through two essentially identical manual USB flap cycle runs. For each, airplane speed was maintained very nearly constant at 210 ft/sec and engine N_1 (hence power) at 2950 RPM throughout. Outboard flaps were held at 58° (flap detent at FLAPS 60). The EFCS was "modified" to allow manual positioning of the USB flaps. These flaps were then held first at 0° for approximately 20 seconds, then slowly "cranked down" to 70° in about 20 seconds, held at 70° for 30 seconds, and finally "cranked" back to 0° in approximately 20 seconds. In order to maintain constant speed, the airplane was put progressively more into a descent attitude as the USB flaps were lowered, resulting in about 1000 ft loss of altitude during a flap cycle. Data were acquired continuously throughout each flap cycle. Airplane behavior for condition .019 is shown in Figure 26. Behavior during condition .019.1 was essentially the same.

Conditions .020 and .021 were flight idle runs. During condition .020, all normal systems were on, while during condition .021 the cabin air conditioning and pressurization systems were shut down. Approximately 1 minute of stabilized data was acquired during each condition.

Conditions .022, .022.1 and .022.2 were continuous landings at FLAPS 45, FLAPS 30, and FLAPS 60 settings, respectively. For condition .022 the USB flaps were at 20° , for condition .022.1 at 0° , and for condition .022.2 the USB flaps modulated about 20° . All landings were on 3° glide slopes or less at speeds well above (20 to 50 ft/sec above) anticipated STOL speed. Hence, none of these landings represents a strict STOL landing. Data were acquired from at least 500 ft altitude to touchdown and on through a portion, if not all, of the runway deceleration. Airplane behavior for these conditions is shown in Figures 27, 28, and 29.





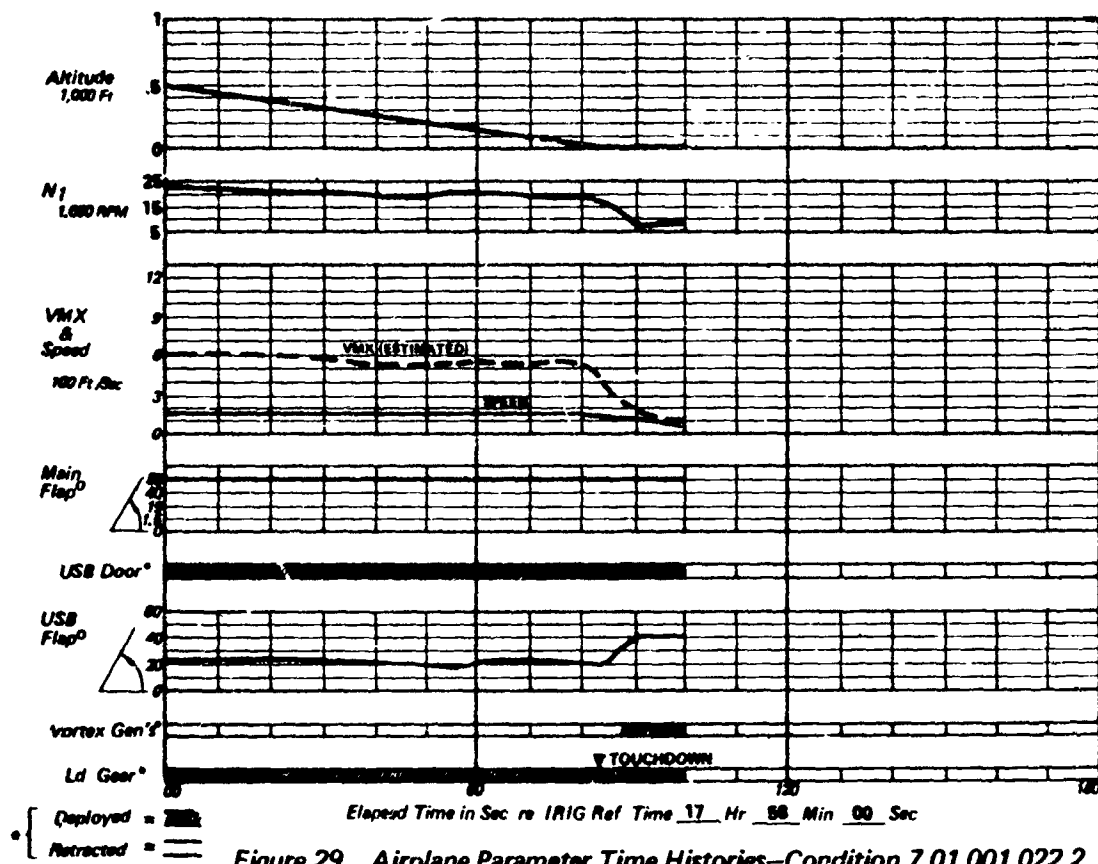


Figure 29 Airplane Parameter Time Histories—Condition 7.01.001.022.2 (Landing, Flaps 60)

SECTION V

DATA REDUCTION SYSTEMS AND METHODS

Data reduction systems and methods used on microphone data, on accelerometer data, and on YC-14 HSPCM data are discussed in this section. A thorough summary of the nature and extent of the data acquired is presented in Section 7 of Reference 5.

1. ACOUSTICS

Three types of reductions were performed on acoustic (microphone) data.

- Overall sound pressure level (OASPL) strip chart time history reductions
- One-third octave band reductions
- Power spectral density reductions

a. OASPL Strip Charts

Strip chart reductions were generated for many interior and exterior microphones for transient type conditions (such as takeoff, flap cycle, go-around, and landings). This type of reduction was, in conjunction with the basic YC-14 operating parameter time history charts, very useful for identifying flight and flap position effects, etc. Based on strip chart behavior, time slices for follow-on one-third octave (and power spectral density reductions) were identified.

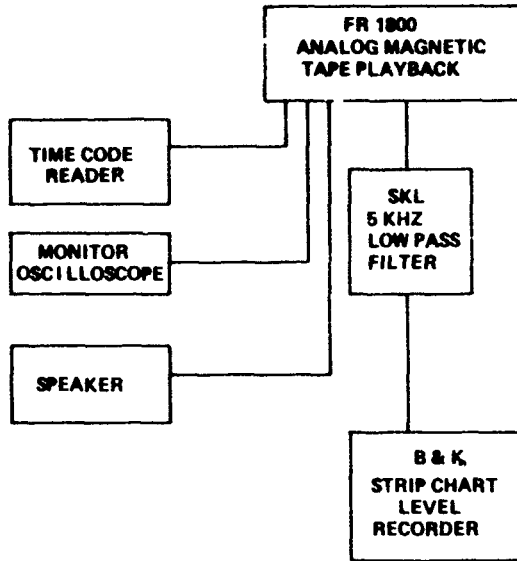
Figure 30(a) shows the set-up for generation of strip charts.

b. One-Third Octave Spectra

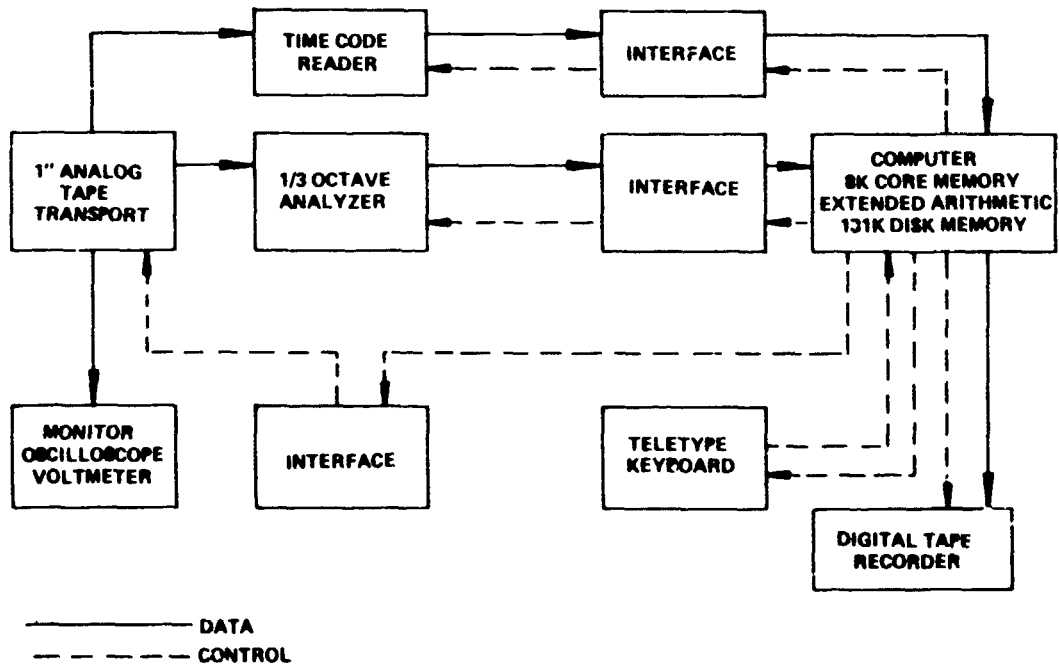
The largest portion of the acoustic data reduction effort was dedicated to generation of one-third octave band spectra. Such spectra were generated for essentially every operating interior and exterior fuselage microphone. Some one-third octave band spectra were also generated for fuselage wall accelerometers.

Figure 30(b) is a block diagram of the one-third octave band data reduction (DIANA) system.

Previously recorded data tapes are reproduced on the analog magnetic tape recorder and fed to the system input. The analyzer breaks the overall signal down into a one-third octave band spectrum from 25 Hz to 10 KHz, and converts each one-third octave level into SPL dB in a digital form. This value is transferred to the digital tape recorder through the computer. The digital tape generated is used in the CDC-6600 computer for follow-on computations.



(a) STRIP CHART DATA REDUCTION SYSTEM



(b) ONE-THIRD OCTAVE DATA REDUCTION SYSTEM

Figure 30 Block Diagrams—Broadband Data Reduction

A general purpose CDC-6600 interactive data bank/editing/plotting program was developed for manipulating the one-third octave spectra generated by the acoustic laboratory DIANA system. All one-third octave microphone and accelerometer spectra for all conditions for both the interior noise measurements program and the concurrent flap loads measurements program (Reference 4) generated on the DIANA system (about 3000 spectra in all) were directly and equally referenceable through this program. One-third octave band spectra plots containing up to any eight of these 3000 spectra could be placed on the same graph.

Spectra produced by the DIANA system covered the 27 bands from 25 Hz through 10 KHz. However, in order to conserve computer storage space, the three highest frequency band levels were dropped upon transfer to the CDC-6600. Hence, plotted spectra show values only up through the 5 KHz band.

c. Acoustic Power Spectral Density

Acoustic power spectral density (PSD) spectra were generated using a general purpose digital processor, known as ADP-1, utilizing a hard-wired, fast Fourier transform (FFT) system. The central element of the ADP-1 system is a Prime 300 computer that services and controls all peripheral equipment. This equipment includes the FFT analyzer, operator terminals, and output digital magnetic tape drives using a time-shared virtual memo γ in conjunction with high-speed disc storage [Figure 31(a)].

The FFT analyzer mode (number of averages, transform size, and frequency range, etc.) is set under program control in response to operator inputs. Acoustic data read from analog magnetic tape are then fed into a signal conditioner for amplitude scaling, anti-aliasing filtering, and digitizing. The digitized time series then undergoes a high-speed finite Fourier series analysis in the FFT analyzer. The analyzer, in combination with the signal conditioner, graphics terminal, high-speed disc memory, and high-speed graphics plotter printer, produces calibrated and scaled PSD plots. These plots are four to a page with appropriate condition and instrument identification printed on each one.

FFT mode parameters were set to perform an effective 1.8 Hz constant bandwidth spectral analysis covering the frequency range from 10 Hz to 1000 Hz.

2. DYNAMICS DATA REDUCTION

Two types of reductions were performed on dynamics data:

- One-third octave band reductions
- Power spectral density reductions

a. One-Third Octave Band Reductions

All one-third octave reductions, of which only a limited number were performed, were done on the acoustic DIANA system described in Paragraph V-1-b.

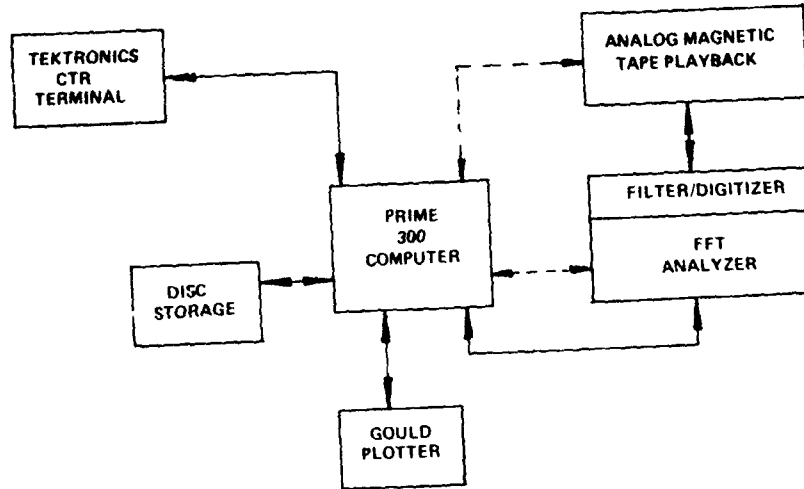
b. Vibration Power Spectral Density

The Dynamics group uses a Fourier analyzer system to process high-frequency vibration data. The heart of the system is the HP2100S minicomputer. A typical data reduction flow chart is given in Figure 31(b).

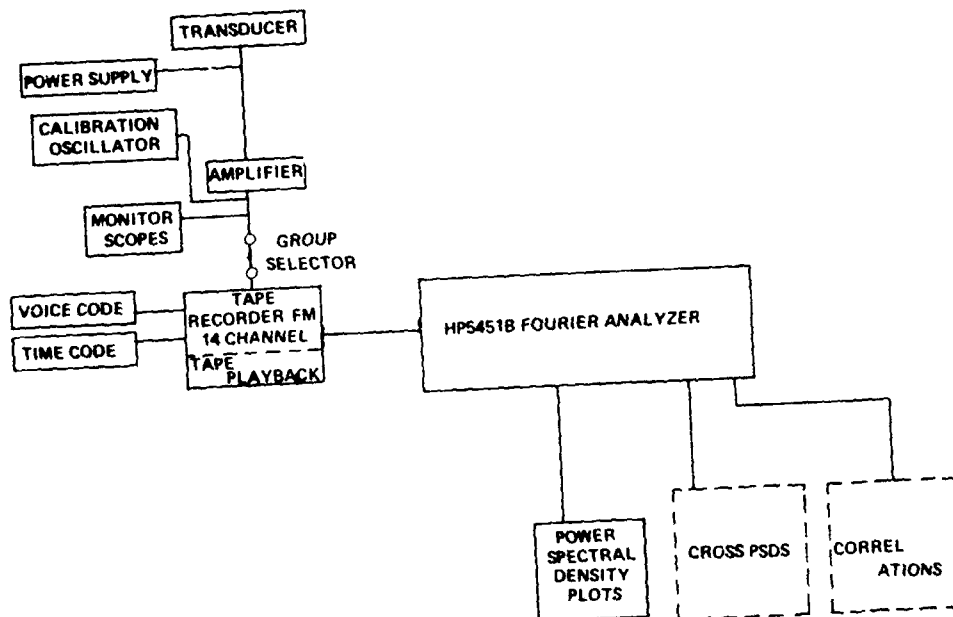
Analog signals from the tape recorder are put through anti-aliasing filters and then digitized through a 12-bit ADC at a minimum rate of four times the maximum frequency of interest. The data is then Fourier-transformed by FFT techniques and complex-conjugate multiplied to generate the power spectral density.

The analyzer is a completely calibrated system with all displays and data outputs accompanied by a scale factor relating them to physical units.

Analyzer control parameters were set to perform a 2 Hz constant bandwidth spectral analysis covering the frequency range from 10 Hz to 1,000 Hz.



(a) ACOUSTIC SYSTEM



(b) DYNAMIC SYSTEM

Figure 31 Block Diagrams--PSD Data Reduction

SECTION VI

RESULTS AND CONCLUSIONS

1. SYNOPSIS

Full-scale ground and flight test measurements have been successfully accomplished to describe the cabin noise environment of an upper-surface-blown propulsive lift transport. These tests complete current efforts to establish a full-scale data base for future analysis.

Based upon preliminary analysis, the following trends have emerged:

- Spatially, the highest noise levels on the exterior fuselage and in the cabin occur aft of the engine nozzle exit plane where the exhaust flow approaches closest to the fuselage.
- Extension of the USB flaps causes the aft exterior fuselage noise pattern to simply rotate downward. Raising the wing-mounted vortex generators produces distinctive high-frequency noise. Within the cabin, noise levels increase modestly (overall about 5 dB) with USB flap angle. Low-frequency increases are apparently due to turning of the flow over the flaps, and high-frequency increases are due to the vortex generators.
- Interior and exterior noise levels appear to correlate very well with engine mixed exhaust relative jet velocity, except at cruise where levels are higher than would be anticipated based on relative jet velocity.

For the most part, trends observed in the data are orderly and intuitively very reasonable. The data base acquired during this AFFDL/NASA sponsored test program should provide a sound and valuable source for further detailed analysis to establish the cabin noise behavior of a USB STOL transport.

2. PRINCIPAL ACOUSTIC TEST RESULTS

Detailed data underlying figures and comments presented in this section can be found in the Appendix.

Figures 32 and 33 summarize overall cabin and exterior fuselage surface noise levels experienced during this test program. Airplane status for indicated flight conditions is summarized in Table VIII. Note

- o Similarity in the condition-to-condition variation of exterior and interior overall noise level patterns, suggesting that interior noise is predominantly controlled by exterior fuselage surface noise.

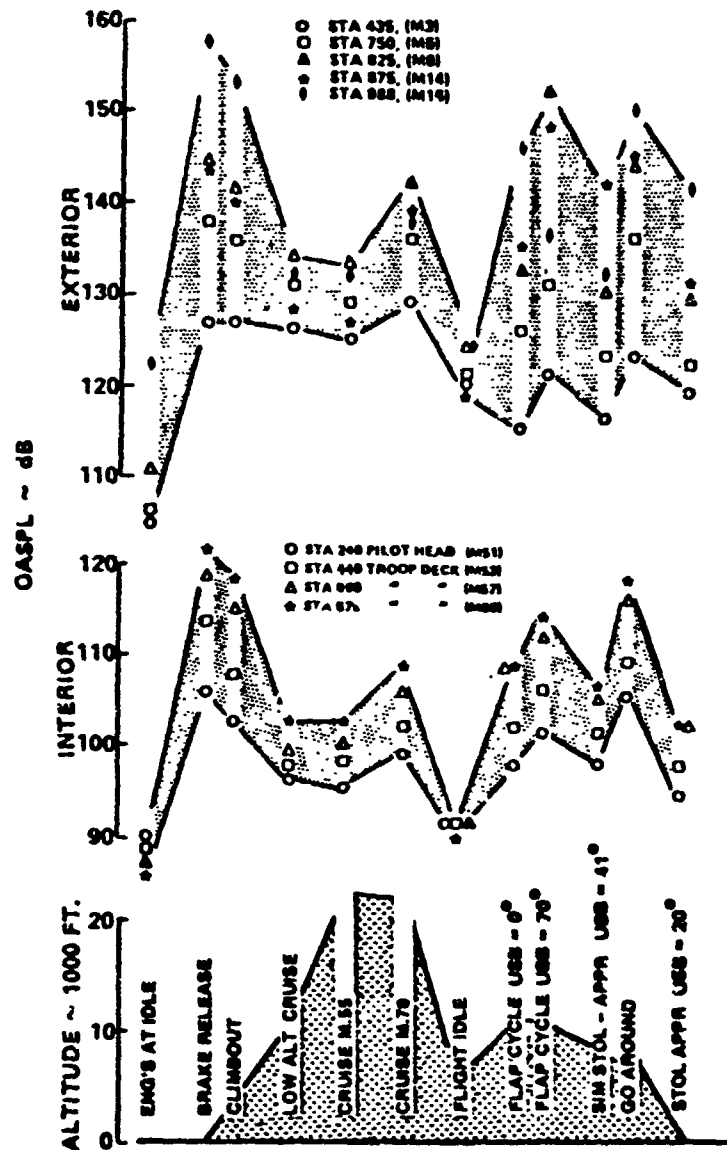


Figure 32 Summary of Exterior and Interior Noise Levels (Same as Figure 3)

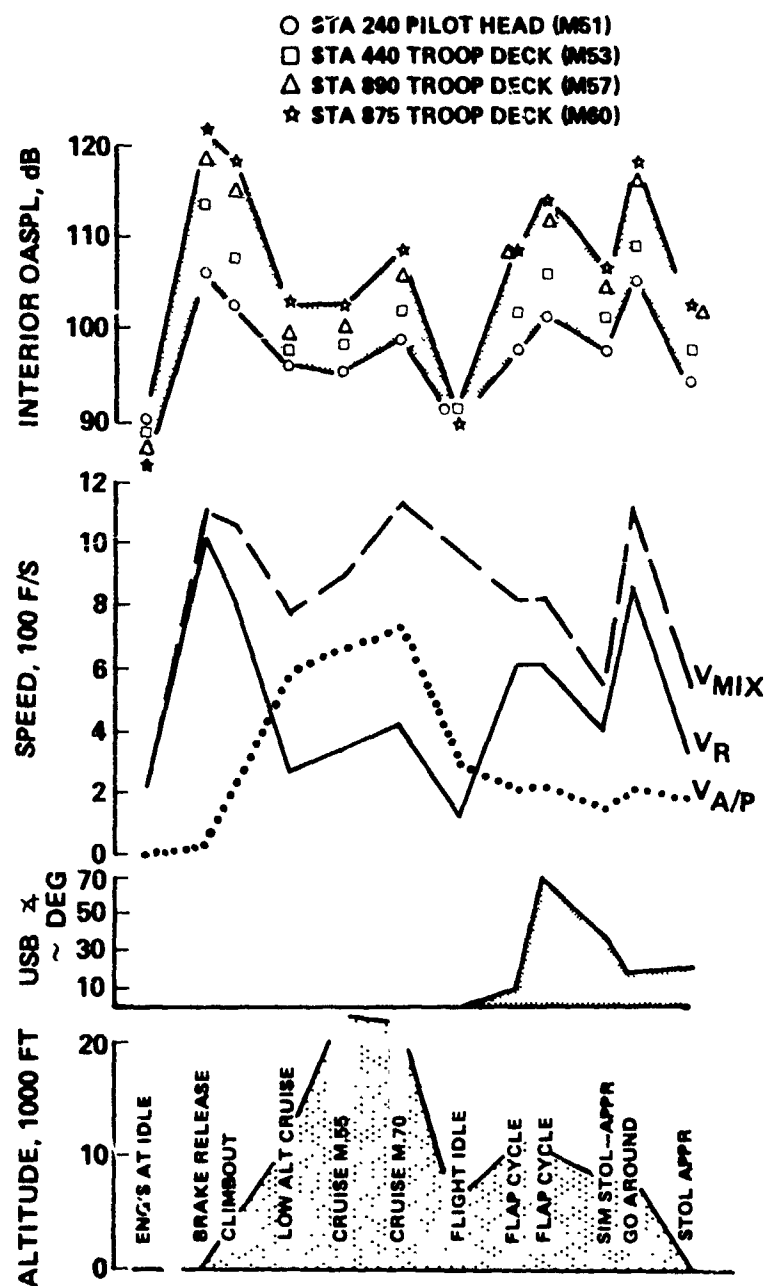


Figure 33 Relation between Interior Noise and Certain Airplane Parameters

Table VIII Summary of Airplane Parameters for Conditions Indicated in Figures 32 and 33

CONDITION DESCRIPTION	AIRPLANE PARAMETERS				
	ALT, FT	V _{A/P} , F/S	N ₁ RPM	VMIX, F/S	δ USB DEG
Ground idle	0	0	810	220	0
Brake release	0	40	3,540	1,050	0
Climbout, flaps '20'	100	220	3,710	1,100	0
Low altitude cruise	11,570	490	2,440	790	0
Cruise, Mach 0.55	22,170	570	2,690	910	0
Cruise, Mach 0.70	22,370	725	3,240	1,140	0
Flight idle	6,670	300	1,380	450	0
Flap cycle	11,050	215	2,950	830	8
Flap cycle	10,700	215	2,950	830	70
Go-around, STOL portion (6° glide slope)	8,300	170	2,200	560	41
Go-around, climb portion	7,700	215	3,670	1,100	18
STOL approach	800	180	2,200	560	20

- Increase in interior and exterior levels from front to back of the airplane (except at idle conditions), suggesting that forward cabin noise is controlled by aft fuselage exterior noise entering through the aft portion of the fuselage
- Relationship of the condition-to-condition noise levels with mixed exhaust relative (and to a lesser extent absolute) jet velocity patterns.
- Modest increase in overall noise levels occurring with extension of the USB flaps (flap cycle, STOL approach, and go-around conditions).

Note that overall levels at ground and flight idle are about the same, and vary only slightly along the length of the troop compartment. Levels at these two conditions are largely set by electrical, hydraulic, and air conditioning systems.

Within the main troop compartment, noise levels increase about 0.08 dB per degree of USB flap extension (Figure 34). For the flight deck, the rate is less about 0.04 dB per degree. These values are based on data acquired during the USB flap cycle test condition during which engine power—hence V_{MX} —and airplane speed were held nearly fixed.

The correlation between noise and relative jet exhaust velocity suggested in Figure 33 is reasonably impressive. An even more impressive correlation, particularly with respect to aft troop compartment noise, can be established with a noise measure L_R defined as:

$$L_R = 20 \text{LOG} \left[\frac{1/2 \rho V_R^2}{1/2 \rho_0 V_{0R}^2} \right] + 0.08 \Delta \text{USB}$$

This is shown in Figure 35. Noise measurements based on absolute jet velocity and airplane velocity,

$$L_{MX} = 20 \text{LOG} \left[\frac{1/2 \rho V_{MX}^2}{1/2 \rho_0 V_{0MX}^2} \right] + 0.08 \Delta \text{USB}$$

$$L_{A/P} = 20 \text{LOG} \left[\frac{1/2 \rho V_{A/P}^2}{1/2 \rho_0 V_{0A/P}^2} \right] + 0.08 \Delta \text{USB}$$

are also shown. The denominator of L_R is chosen so that its value is the same as the OASPL at M60 at brake release, the denominator of L_{MX} is chosen in the same way, and the denominator of $L_{A/P}$ is chosen so that its value is the same as the OASPL at M60 at Mach 0.70 cruise.

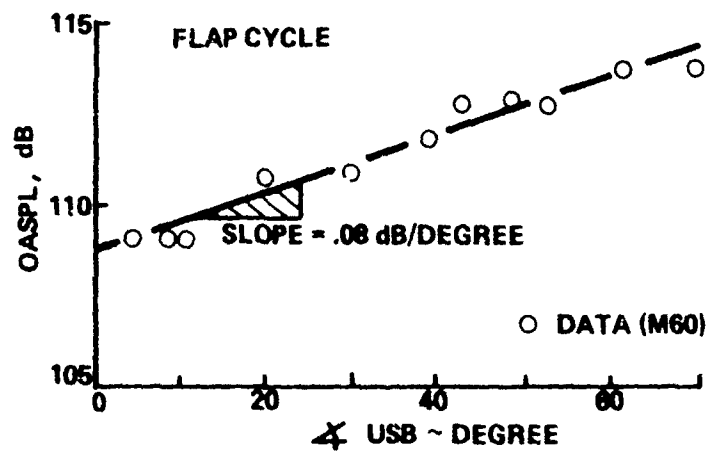


Figure 34 Troop Compartment OASPL vs USB Flap Angle

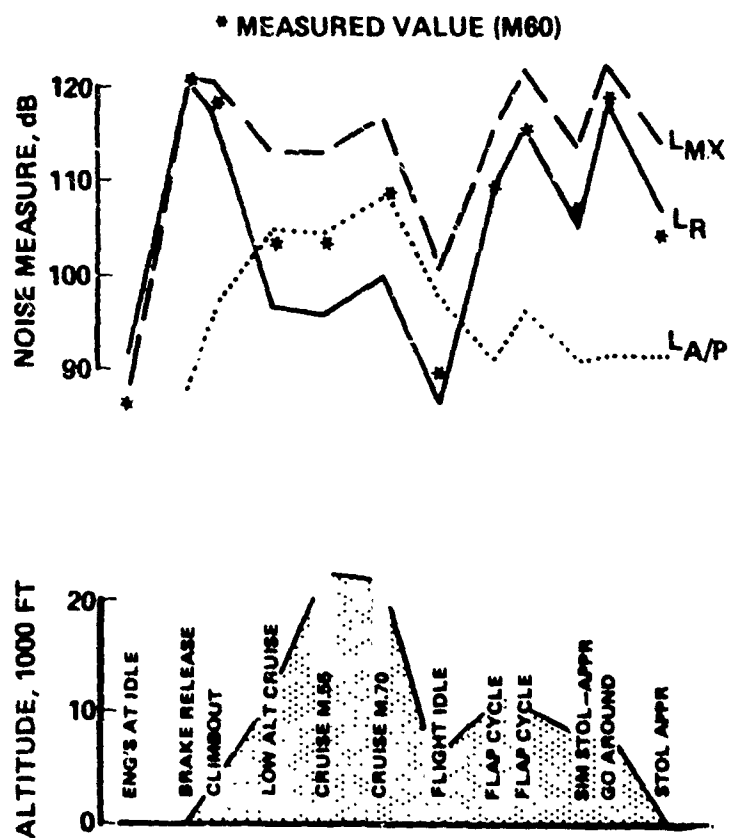


Figure 35 Interior Noise re Various Noise Measurements

Of the three noise measurements, L_R appears to be the most successful. Hence, Figure 36 shows the overall noise at M60 plotted against L_R for most of the ground and flight conditions performed during the test program. This figure and Figure 35 indicate cruise noise levels higher than would be anticipated based on relative jet velocity.

Note that for the three cruise conditions shown in Figure 35, relative changes in all three noise measures are about the same as the relative change in overall noise at M60. Hence, variations in overall noise with changes in cruise condition provide little insight into whether cruise noise is engine-noise controlled or boundary-layer-noise controlled. L_{MX} and L_R typically correlate with engine noise and $L_{A/P}$ with boundary layer noise, suggesting that (with the possible exception of cruise) cabin noise appears to be engine-noise dominated.

Based on the previous discussion overall levels go down as relative jet velocity decreases. The manner in which this effect is accounted for on a spectral basis is indicated in Figures 37 and 38 for exterior and interior noise. These spectra were obtained during a takeoff, during which engine power (hence, mixed jet velocity) was maintained steady, while airplane speed increased from essentially zero to 135 knots (230 ft/sec).

The exterior spectra (Figure 37) are for three exterior fuselage points aft of the engine nozzle exit plane. Of these points, M13 is (with USB flaps retracted) believed to be on the line of closest approach of exhaust flow stream. M14 is below this line and M20 is above it. At all three points, sizeable low-frequency reductions are observed. The sizeable higher frequency reduction at M13 (observed at M16 as well) is speculated to be an engine exhaust flow effect.

The interior spectra (Figure 38) are for an aft troop compartment point, M60. Here a more or less uniform (across the frequency spectrum) modest reduction of 2 dB to 3 dB is observed with increasing airplane speed.

Another feature shown in Figure 32 is the much greater range of exterior noise levels observed during takeoff/approach operations (20 dB to 30 dB) than during cruise operations (10 dB to 15 dB). This range is detailed in Figure 39. Levels at fuselage points M13 and M16 (and to a lesser degree M8 and M10) are significantly higher than levels at other fuselage points at climbout, but this behavior disappears at cruise.

Exterior fuselage noise spectra for climbout and cruise are shown in Figure 40, indicating that the special behavior of M13 and M16 is a low-frequency phenomenon. Overall, spectra for cruise contain noticeably less low-frequency energy, but slightly more high-frequency energy, than corresponding climbout spectra.

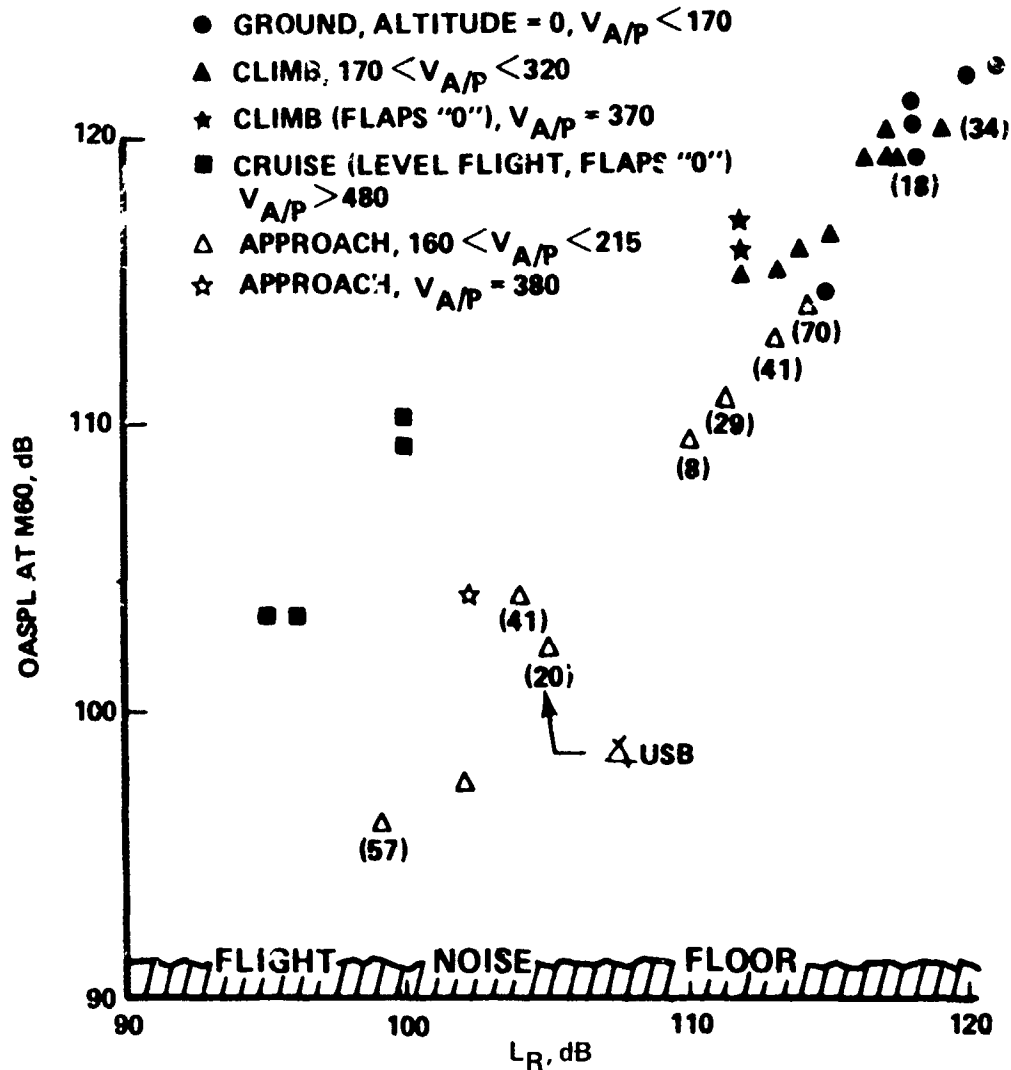


Figure 35 Correlation of Aft Troop Compartment (M60) Overall Noise with L_R Noise Measure

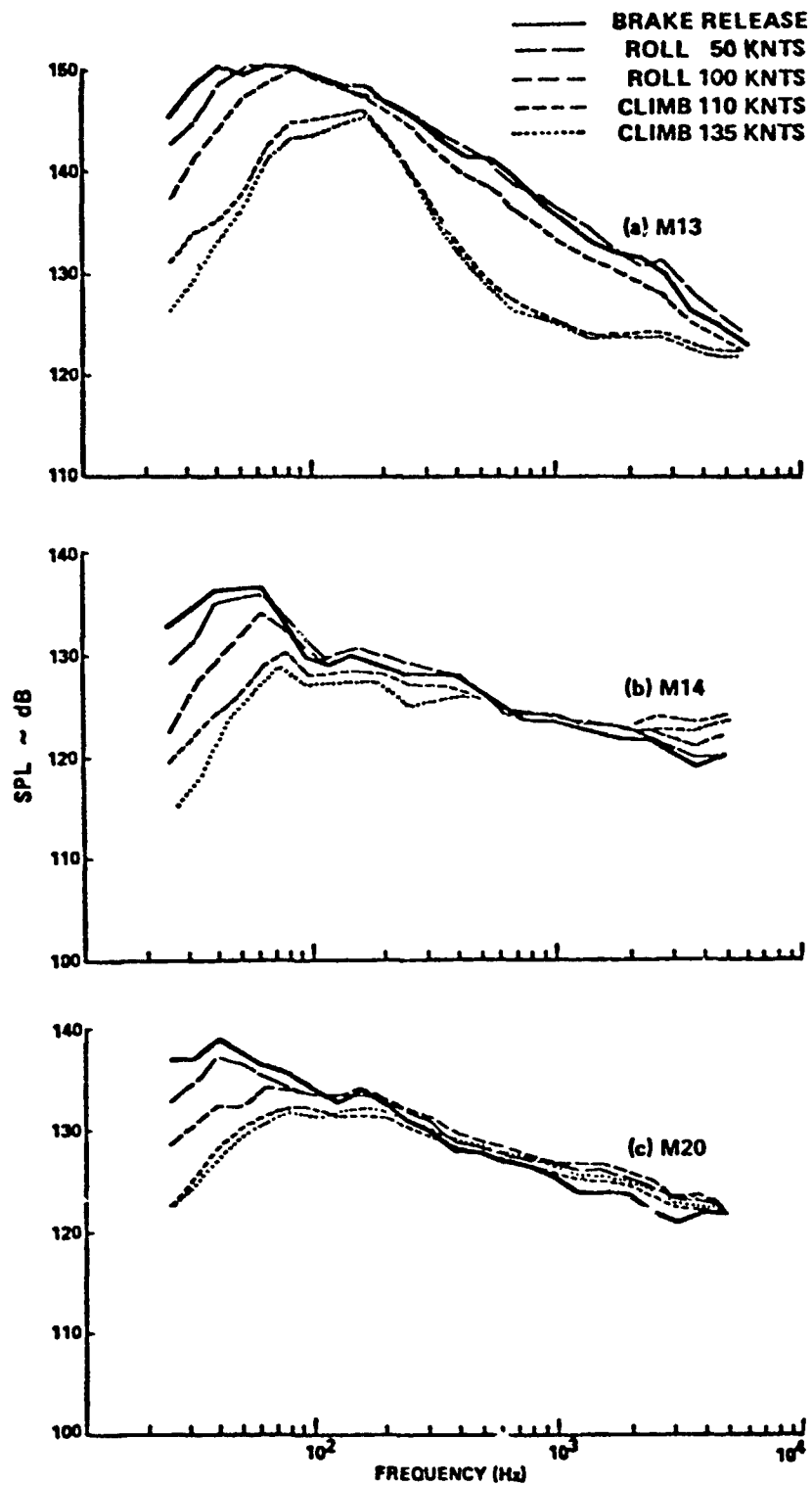


Figure 37 Variation in Exterior Fuselage Noise Spectra During Takeoff

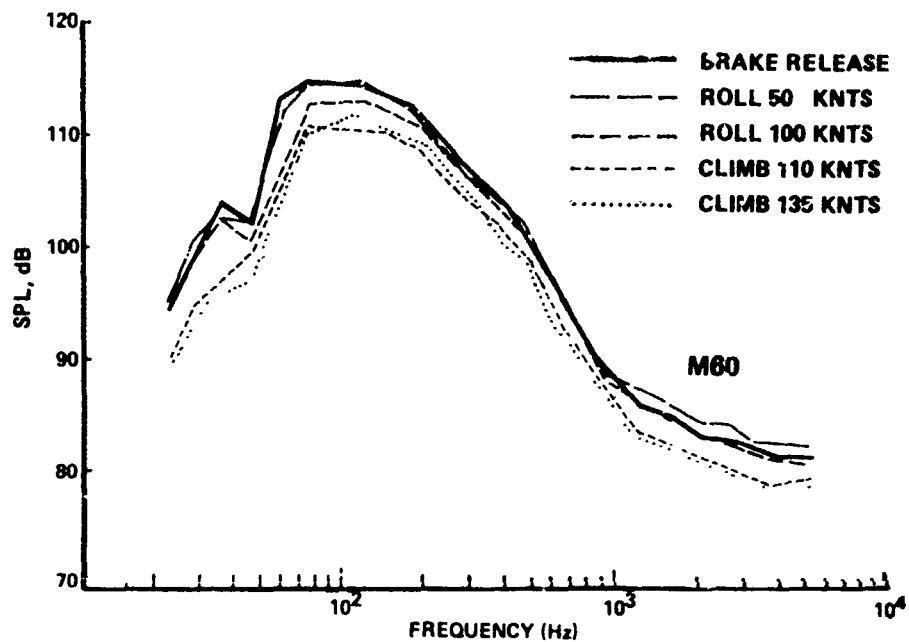
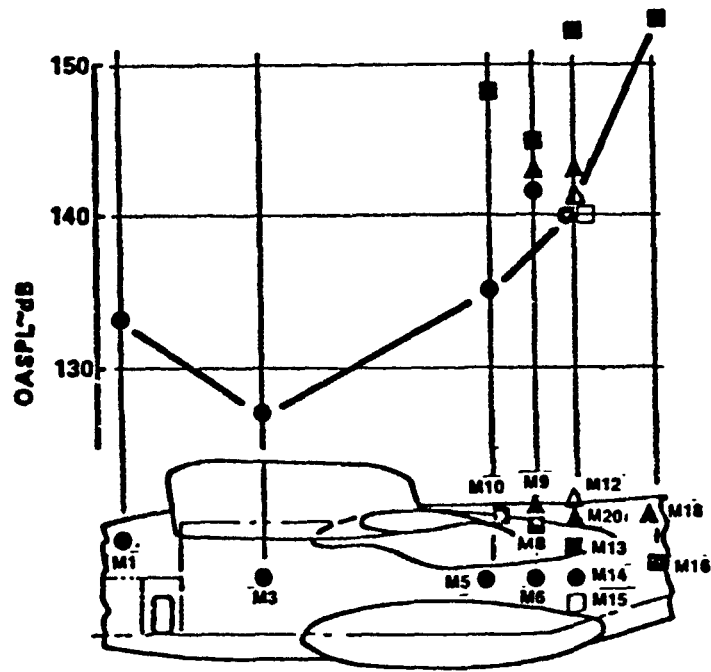
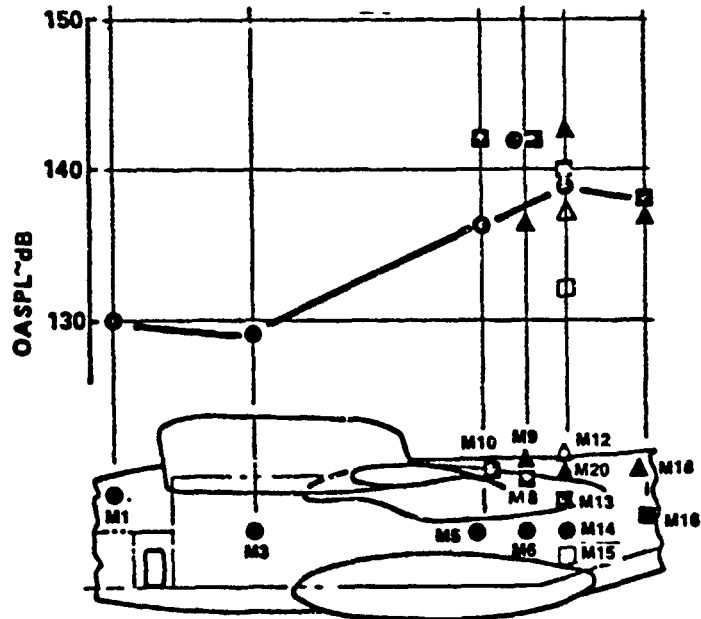


Figure 38 Variation in Interior Noise Spectra (M60) During Takeoff

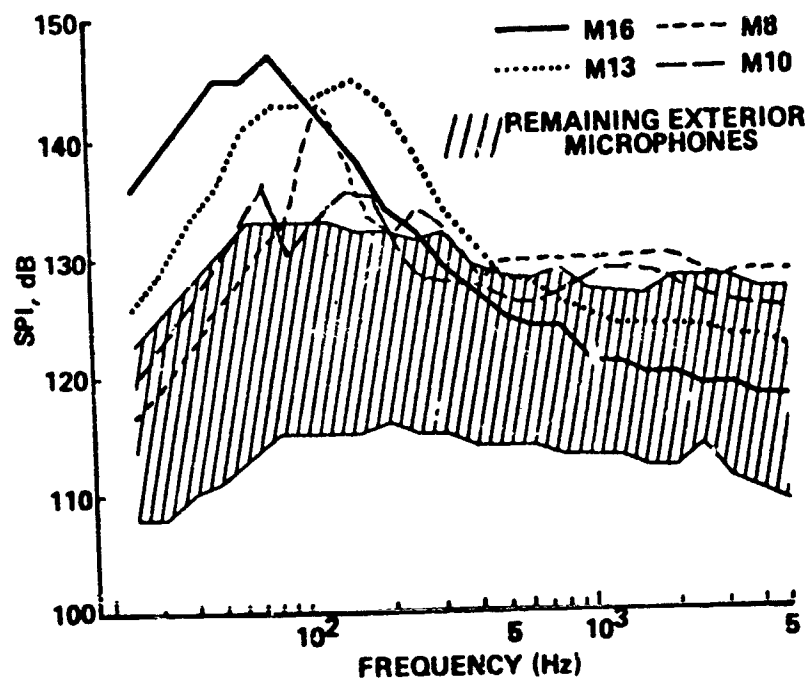


(a) CLIMBOUT

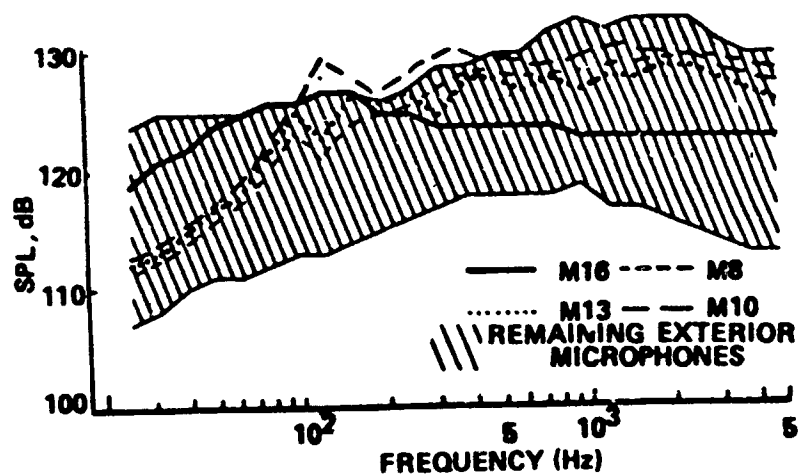


(b) M.70 CRUISE

Figure 39 Exterior Fuselage Overall Noise Levels—Climbout and M 0.70 Cruise



(a) CLIMBOUT



(b) CRUISE; M.70

Figure 40 Exterior Fuselage Noise Spectra—Climbout and M 0.70 Cruise

The same general characteristics carry over to interior noise (Figure 41). A closer examination suggests, however, that the extensive changes in exterior noise at M13 and M16 are at best only weakly reflected in interior noise changes.

An added note in Figure 41 is the distinctive peak at 40 Hz in the cruise spectra, but not in the climbout spectra. Such behavior is not suggested by the exterior spectra. Computations suggest the peak might be due to low-order room modes. Why these modes are so much more active at cruise than at climbout remains to be determined.

The prime factor likely responsible for the distinct field levels observed during climbout (but not cruise) at exterior points M13 and M16 is the nearby engine nozzle. This nozzle is about 3 ft away from the YC-14 sidewall, as compared to about 25 ft for a Boeing 747 jet (Figure 42). Fuselage areas closest to the flow (this area contains points M13 and M16 with USB flaps retracted) experience fluctuating pressure levels that change very rapidly with fuselage position, and with airplane velocity, $V_{A/P}$.

General behavior of the fluctuating pressure levels on these areas is suggested in Figure 43. Here "s" is the circumferential distance along the fuselage surface from M13 or M16, which are essentially on the line of closest approach of the flow field to the fuselage. The effect of decreasing engine/fuselage spacing is based on observations from YC-14 development model tests, and not from the current test program. The unequal sensitivity to $V_{A/P}$ is felt to be due to increased effect of engine exhaust flow spreading on fuselage points with progressively smaller "s" values. Such reductions in exhaust flow spreading, which as was noted previously occur with increasing $V_{A/P}$, produce larger percentage increases in exhaust flow stream/fuselage spacing. Thus, the larger the reduction in fluctuating pressure level, the smaller the "s" value.

As might be anticipated from Figure 43, and the high flow-turning capability of the USB system of the YC-14, exterior fuselage levels do change strongly as the USB flaps are deployed. Such overall levels are shown in Figure 44. The curves suggest that the fluctuating pressure field simply rotates down the fuselage, pivoting about the USB flap rotation axis as the flaps are deployed. This behavior seems very logical considering the nearby location of the engines and the effective flow-turning capability of this USB system.

Figure 45 shows the effect of USB flap position on exterior fuselage noise spectra at three aft fuselage points (M15, M16, and M20) and one forward fuselage point (M03). The behavior at M15 is suggestive of the approach of a noise source with (spatially) invariant frequency spectra. Behavior at M16 is suggestive of departure of the same invariant source, except that the invariance breaks down with deployment of the VGs (vortex generators). The sudden increase in the spectra at M20 also correlates with VG deployment. Note that if increases observed at M20 were subtracted from the spectra at M16, the M16 spectra would be nearly the reverse of those at M15. Extension of USB flaps appears to increase only low-frequency noise on the forward fuselage. Effects associated with VG deployment do not show up.

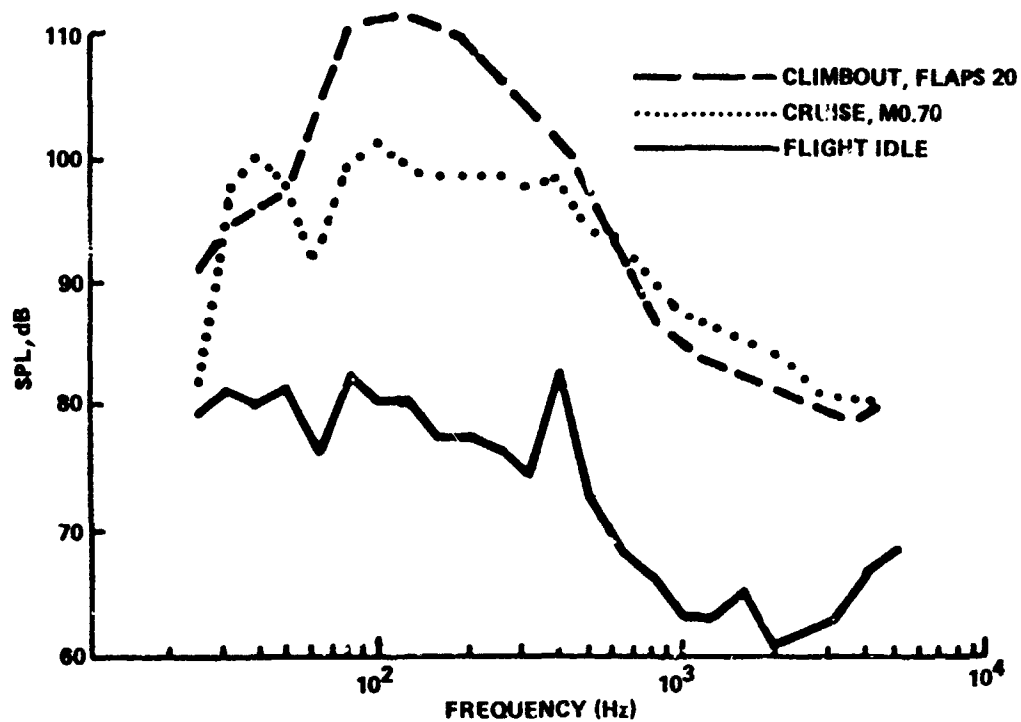


Figure 41 Aft Troop Compartment (M60) Noise Spectra Climbout vs M.70 Cruise

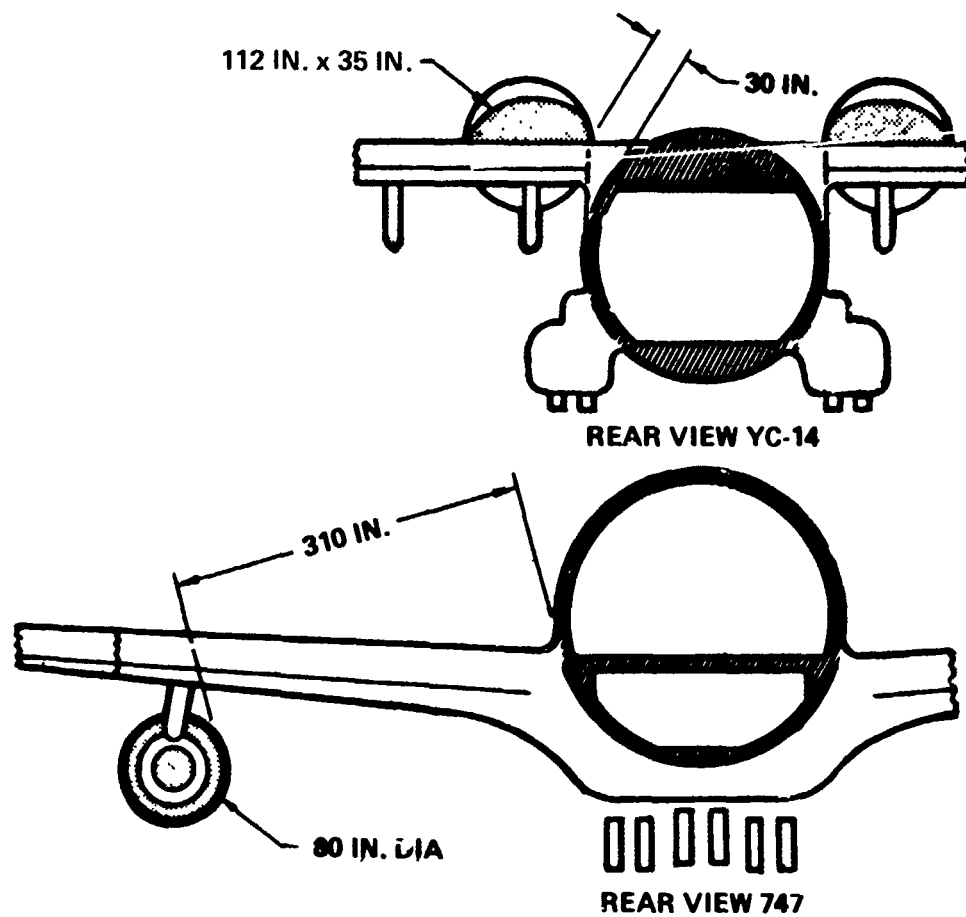


Figure 42 Fuselage/Engine Spacing for YC-14 and 747

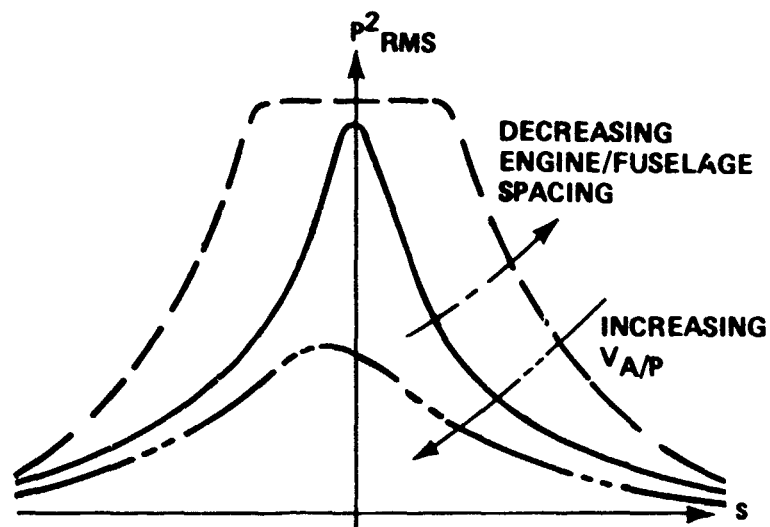
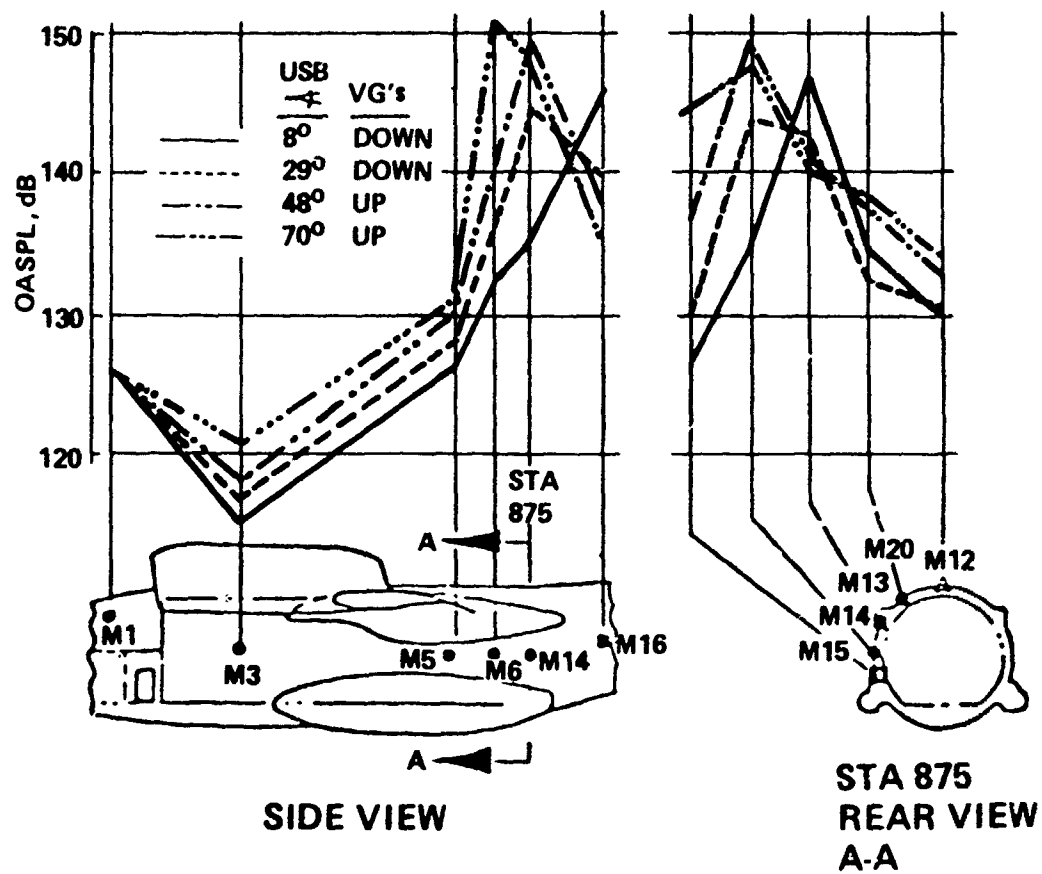


Figure 43 Proposed Fuselage Fluctuation Pressure Field Near M13 or M16



NOTE: FOR ALL INDICATED CONDITIONS

$N_1 = 2950 \text{ RPM}$

$VMIX = 830 \text{ F/S}$

$V_{A/P} = 210 \text{ F/S}$

ALT = 11000 FT

Figure 44 Effect of USB Flap Position on Exterior Fuselage OASPLs

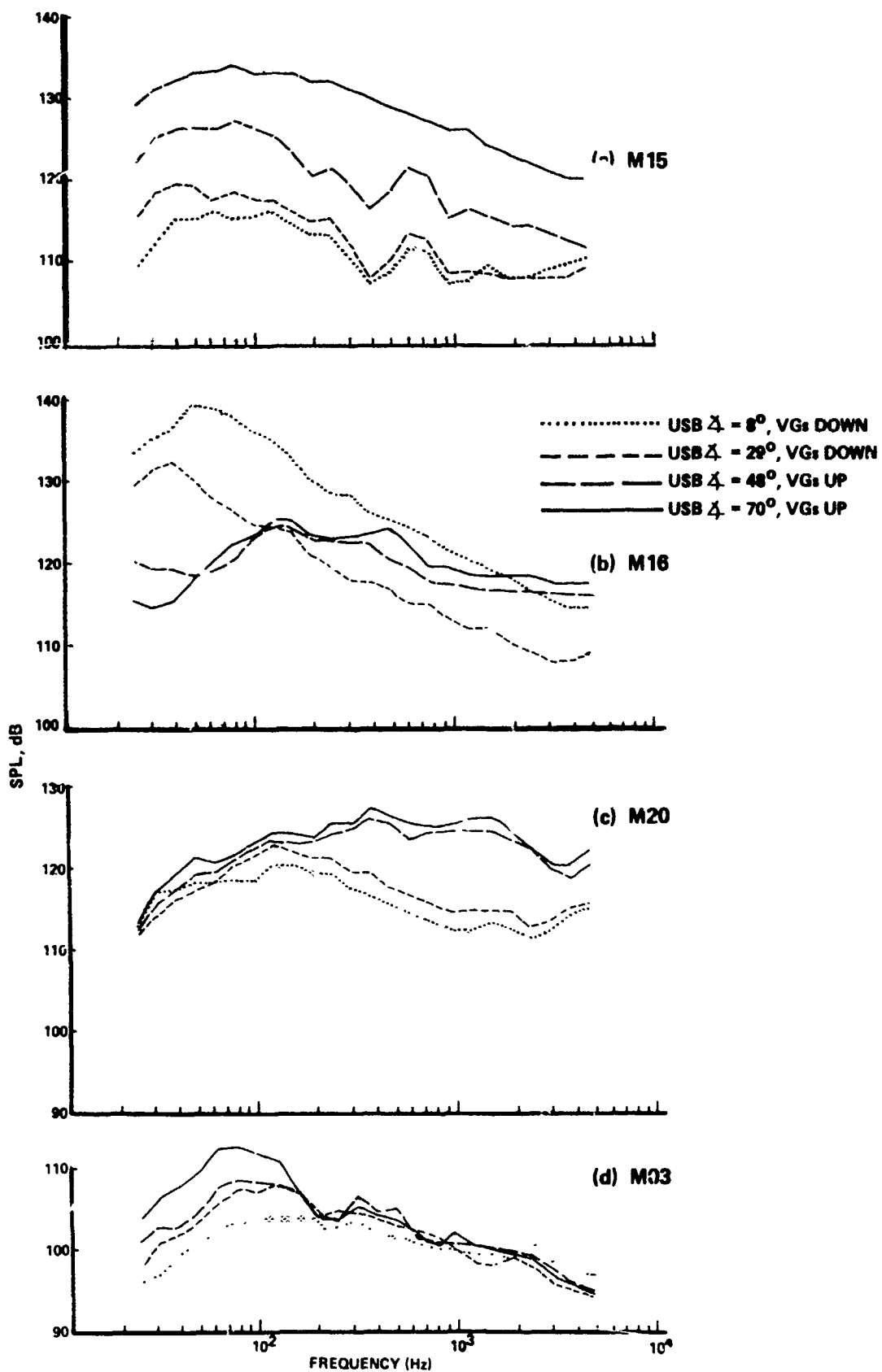


Figure 45 Effect of USB Flap Position on Exterior Fuselage Noise Spectra

The effect of USB flap position on interior noise spectra of an aft troop compartment point (M60) and a forward troop compartment point (M53) is shown in Figure 46. The apparent VG effect is noticeable at M60 but weak at M53. Otherwise, spectra throughout the troop compartment increase smoothly over the indicated frequency band (25 Hz to 5000 Hz) as the USB flaps are deployed.

The data trends explored so far are for the most part orderly and intuitively reasonable. Additionally, observed levels are reasonably in line with Boeing estimates (Reference 1) developed prior to the present test program. For example, comparisons between estimated and measured levels in the aft troop compartment for climbout and cruise are shown in Figure 47. Estimates made by AFFDL and NASA (References 2 and 3) are shown for completeness. Above about 500 Hz for climbout and 250 Hz for cruise, measurements are above (Boeing) estimates. This is postulated to be due to the lack of insulation in the cargo ramp doors and/or ambient noise effects, both of which were not considered in the (Boeing) estimates. Further assessment of prediction methods for YC-14 interior noise appears feasible and highly desirable.

3. PRELIMINARY FUSELAGE VIBRATION TEST RESULTS

Only a very brief analysis of fuselage vibration data has been attempted

- Within the brief analysis period allotted under this test program, higher initial return with regard to understanding interior noise was projected by concentrating on acoustic data, at the expense of vibration data.
- Examination of acoustic data was highly rewarding, leading to an even less than initially anticipated fuselage vibration data analysis effort.

Figure 48 shows overall acceleration levels for all fuselage accelerometers measuring normal wall motion. Conditions included cover nearly all those corresponding to zero or small USB flap angles for which one-third octave band and/or narrow band (PSD) accelerometer data reductions were accomplished. Considerable additional data remain available for reduction. Figures 49 and 50 show corresponding overall levels for neighboring interior and exterior microphones. In comparing this accelerometer and microphone data, note that acoustic overall levels are based on true one-third octave band levels including the 25 Hz through 5000 Hz bands. Acceleration overalls are based on scaled one-third octave levels covering the 25 Hz through 2500 Hz bands. Scaled levels were obtained by reducing true levels (with crossover at the 100 Hz band) at the rate of 6 dB per octave. This scaling scheme has been found in the past to provide a good basis for comparing at least interior fuselage noise and fuselage wall vibration. This scaling scheme has been applied to all one-third octave band acceleration data shown in this section.

The use of the noise measure L_R as the common (independent variable) plotting parameter is based upon its past success as a correlator of aft cabin (M60) overall noise, except at cruise conditions. However, in its present application it appears--in part likely due to the limited number of conditions considered--to be a much less effective correlator.

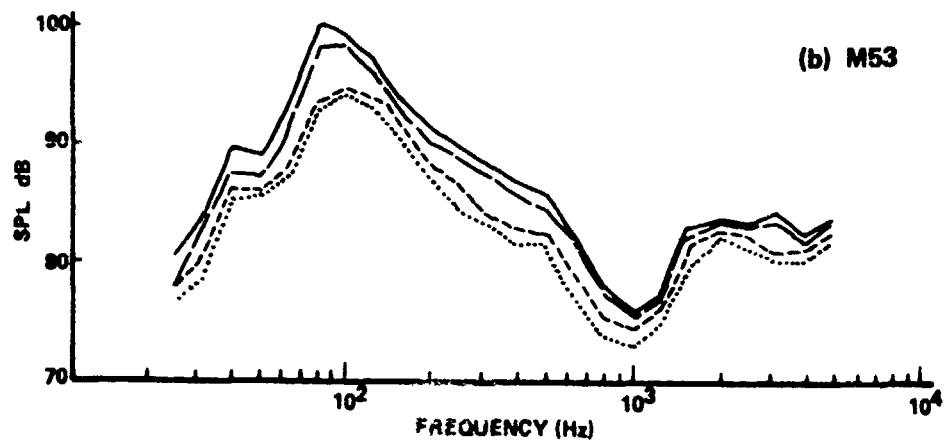
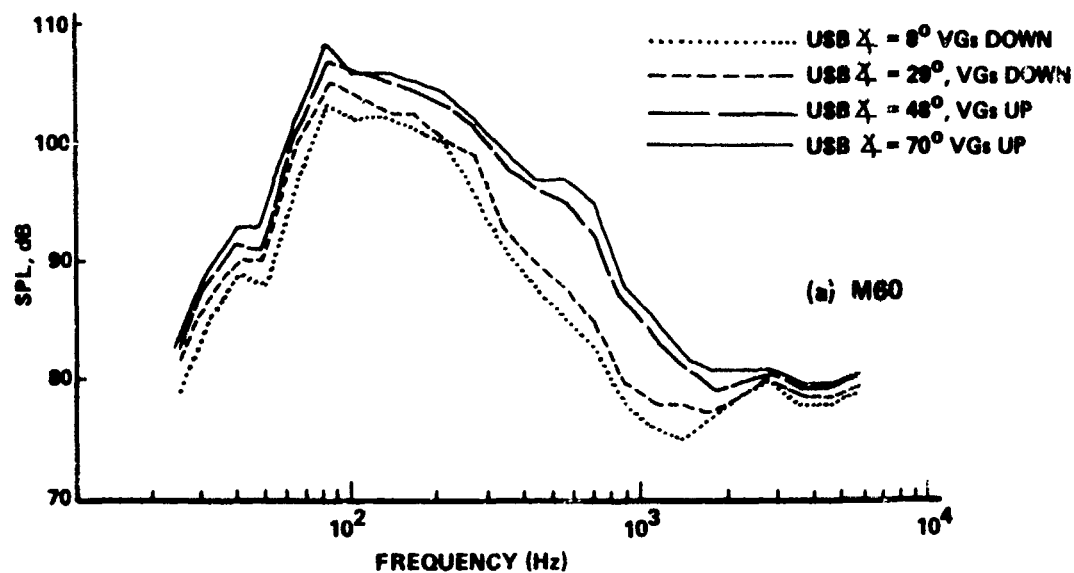
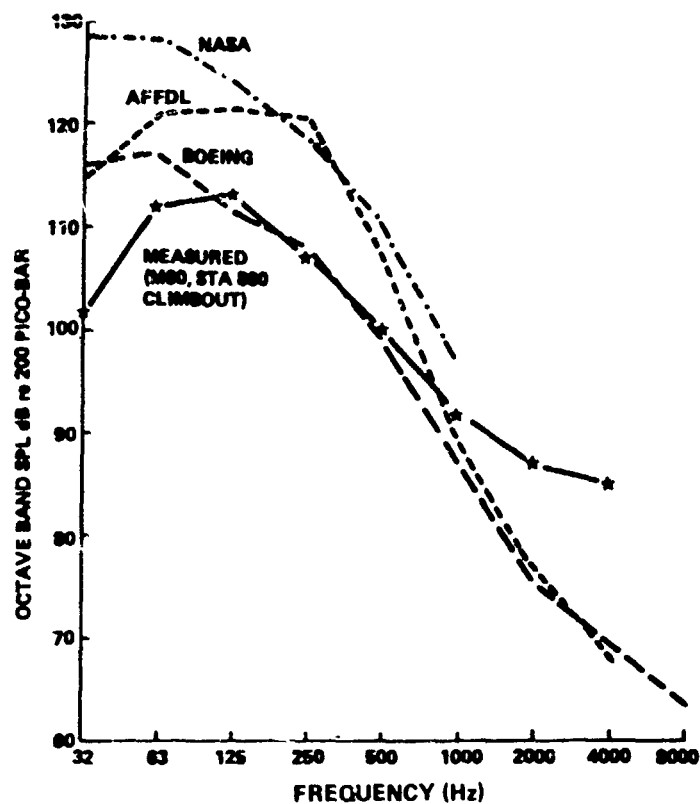
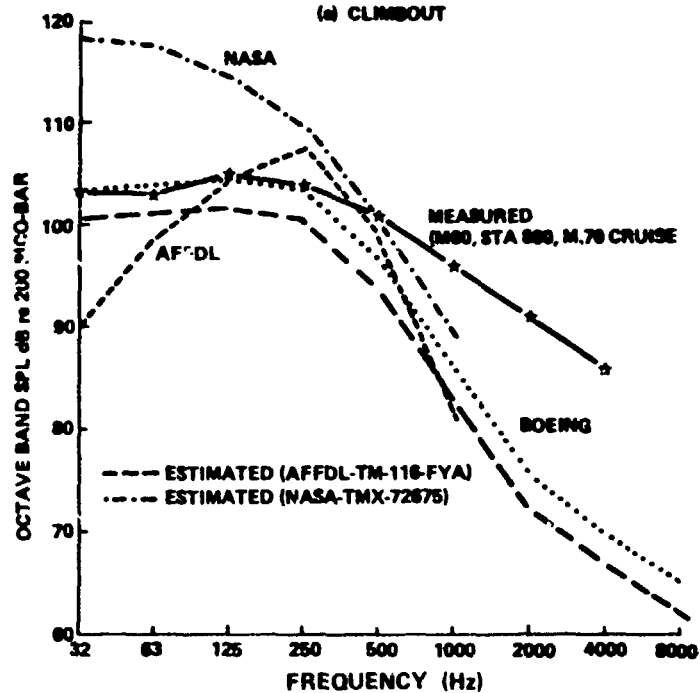


Figure 46 Effect of USB Flap Position on Interior Noise Spectra



(a) CLIMBOUT



(b) CRUISE

Figure 47 Comparison of Estimated and Measured Interior Noise Levels

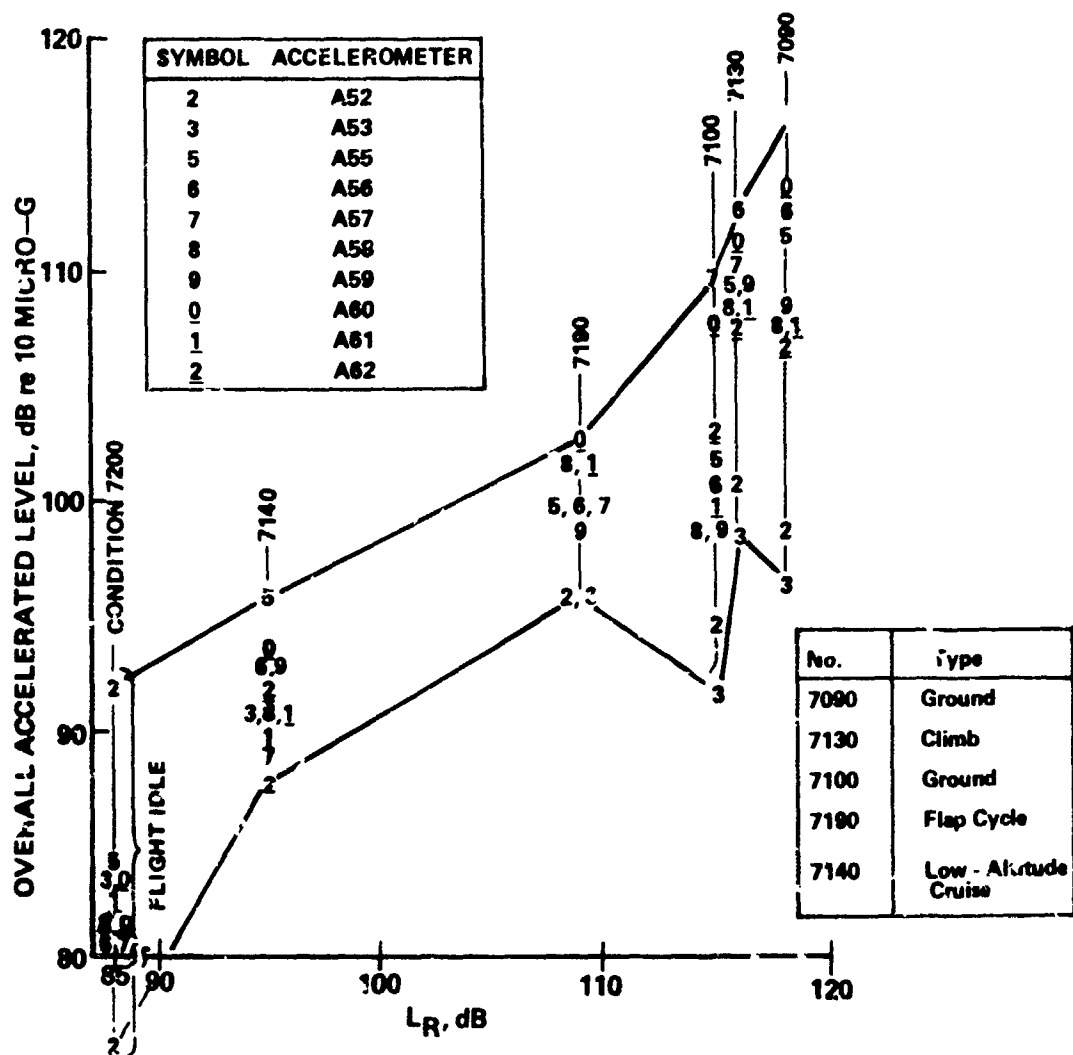


Figure 4f: Overall Fuselage Vibration Levels vs L_R Noise Measure



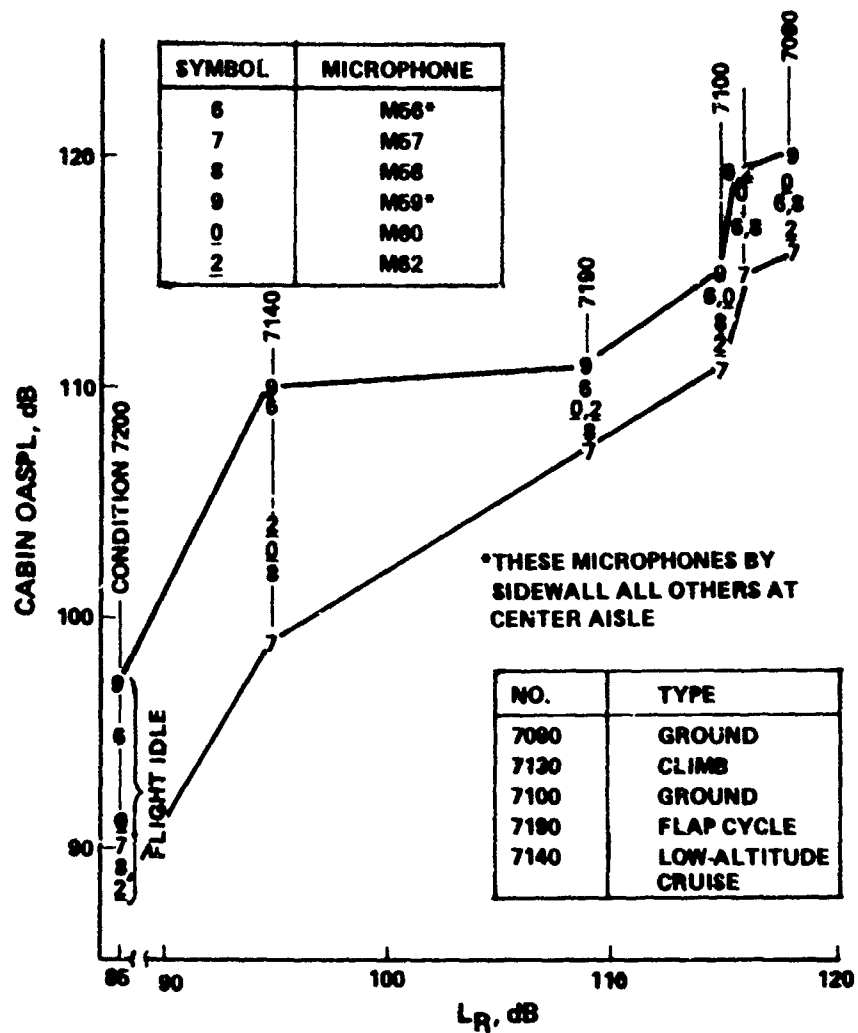


Figure 50 Cabin OASPL vs L_p Noise Measure

Intercomparing the three figures, a general level increase with increasing L_R can be noted. However, beyond this feature any further similarity between overall acceleration levels and exterior or interior fuselage noise overall levels is difficult to discern.

Figures 51, 52, and 53 show one-third octave band acceleration behavior at three selected fuselage points, and for each the corresponding acoustic behavior of a close-by exterior fuselage point (Table IX). In each case, spectra are given for five airplane conditions, summarized in Table X. These figures show that, as the exterior fuselage noise field intensifies, so does the intensity of the fuselage vibration. Acceleration and exterior noise change consistently from condition 7090 to 7100. This is encouraging, since the only difference between these two conditions is engine power setting, lower at 7100 than 7090. More data appear to be needed to clarify other trends that may be present.

Figure 54 shows the comparison between aft cabin interior noise (at M60) and fuselage wall vibration at the 10 points where wall normal motion was monitored. Test conditions are the same as those of Figures 51, 52, and 53. Behavior at the four low-speed conditions (7090, 7100, 7130, and 7190) is quite similar. As might be expected, the similarity is particularly good at conditions 7090 and 7100. Behavior at the one cruise condition, 7140, does not follow the pattern of the others.

It appears that the amount of reduced acceleration data is too small to yield clear patterns. A large body of raw acceleration data is available, and, on being reduced, might be expected to yield similar patterns observed in acoustic data.

4. CONCLUDING REMARKS

Full-scale ground and flight test measurements have been successfully accomplished on the prototype YC-14 to describe the cabin noise environment of an upper-surface-blown, propulsive lift transport. These tests complete efforts to establish a full-scale data base for further analysis.

Based upon preliminary analysis, the following acoustic trends have emerged.

- Spatially, the highest noise levels on the exterior fuselage and in the cabin occur aft of the engine nozzle exit plane, hence, where the exhaust flow approaches closest to the fuselage.
- Extension of the USB flaps causes the aft exterior fuselage noise pattern to simply rotate down. Raising of the vortex generators produces distinctive additional high-frequency noise. Within the cabin, noise levels increase smoothly with USB flap angle. Low-frequency increases are apparently due to flap disturbances, and higher frequency increases are due to the wing mounted vortex generators.
- Interior and exterior noise levels show a tendency to correlate with engine mixed exhaust relative jet velocity, except at cruise where levels are higher than would be anticipated based on relative velocity.

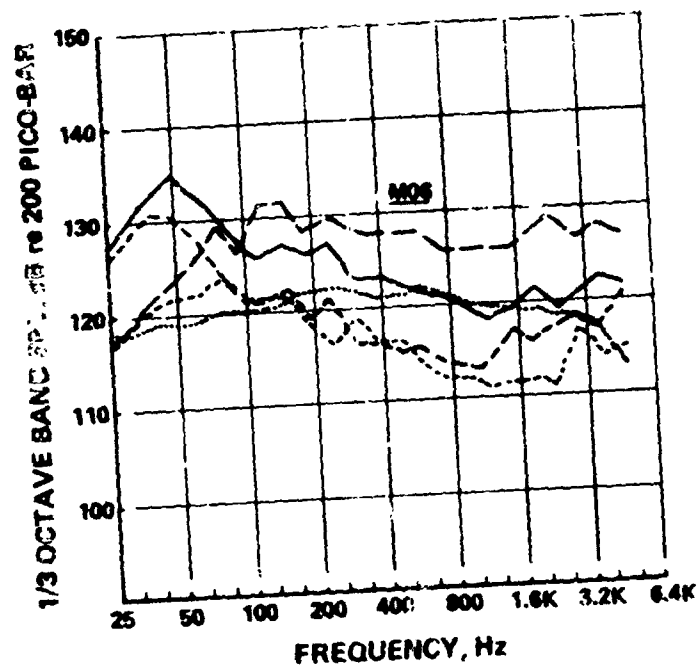
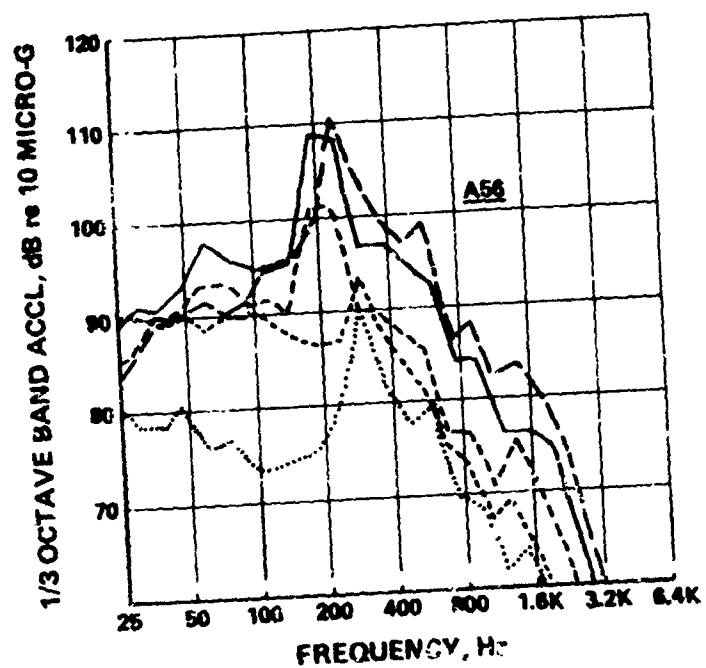
Trends for fuselage acceleration are presently far less distinguishable. This is felt to be due to the small body of reduced vibration (compared to reduced acoustic) data. However, overall acceleration levels do show a modest trend to correlate with engine mixed exhaust relative jet velocity.

Table IX Skin Accelerometer/Exterior Microphone Sets

Figure	Skin accelerometer	Exterior microphone
51	A56 @ BS 830,WL179	M06 @ BS 825,WL180
52	A57 @ BS 890,WL182	M13 @ BS 875,WL220
53	A60 @ BS 890,WL263	M20 @ BS 875,WL254

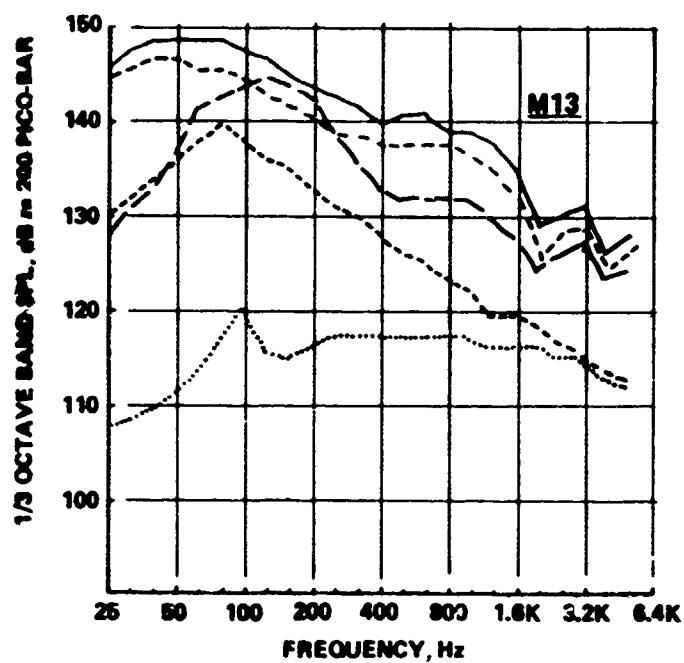
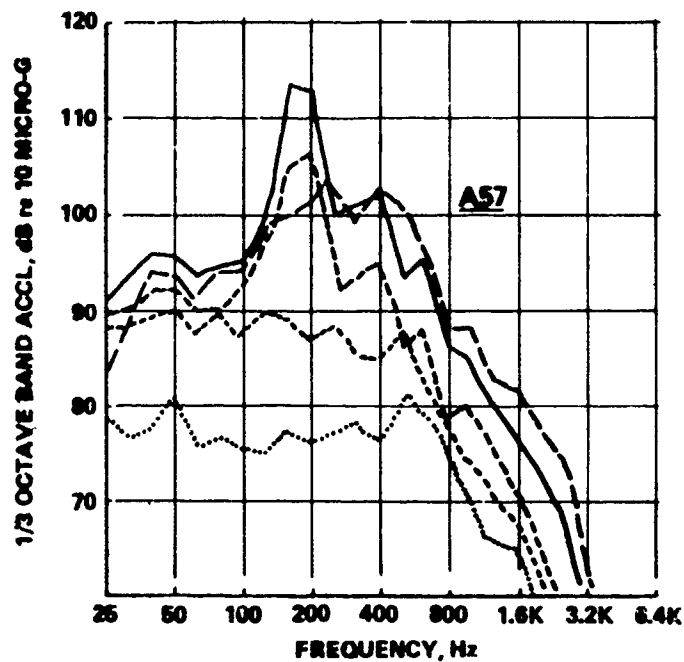
Table X Selected Condition Characteristics

Symbol	Condition	Type	Alt, ft	Speed, f/s	VMIX, f/s	N ₁ , RPM	USB, DEG	LR, dB
—	7090	Ground	0	0	870	3,110	0	118
— —	7130	Climbout	3,500	270	1,100	3,800	0	116
— — —	7100	Ground	0	0	756	2,740	0	115
— — — —	7190	Flap cycle	11,000	210	830	2,950	8	110
— — — — —	7140	Low Altitude cruise	10,600	490	788	2,440	0	95



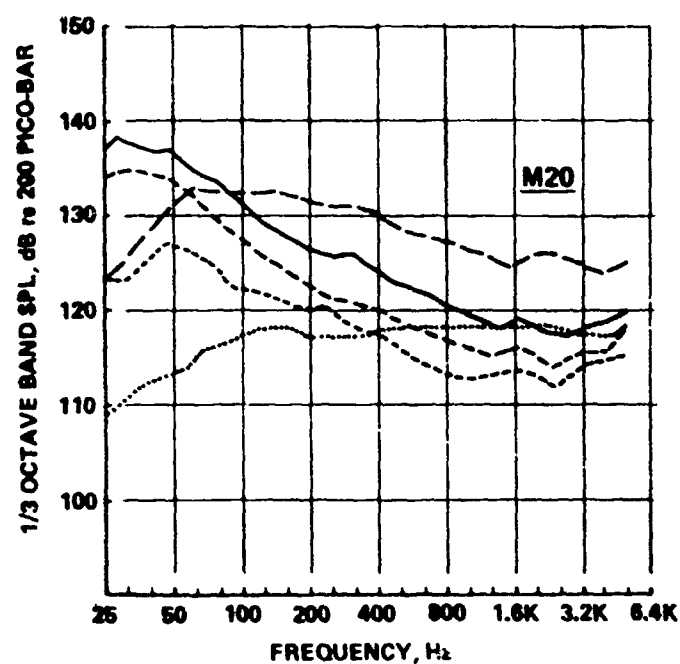
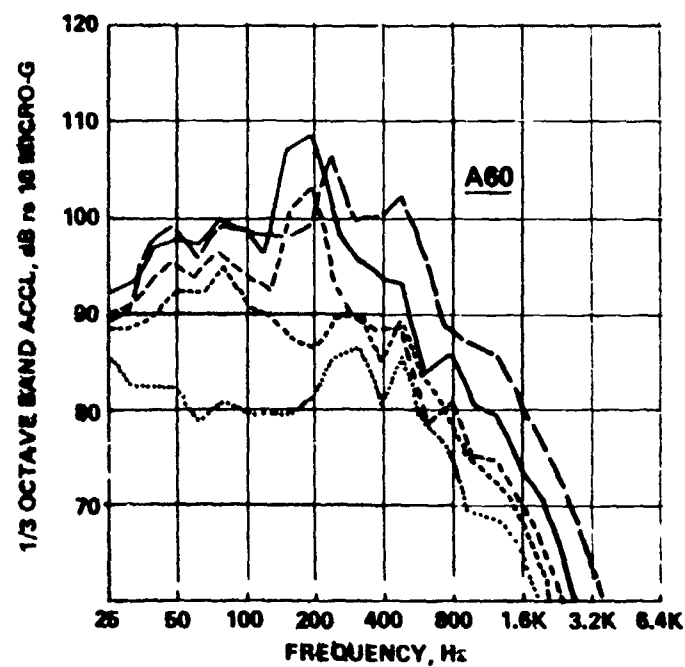
CONDITION	TYPE	L_{H}
— 7080	GROUND	118
- - - 7130	C.LIMB	116
- - - 7100	GROUND	116
- - - 7140	FLAP CYCLE	110
..... 7140	LOW-ALTITUDE CRUISE	95

Figure 51 Skin Vibration/Exterior Sound at A56/M06



CONDITION	TYPE	L _R
— 7090	GROUND	118
- - - 7130	CLIMB	116
- - - - 7100	GROUND	115
- - - - - 7190	FLAP CYCLE	110
..... 7140	LOW-ALTITUDE CRUISE	95

Figure 52 Skin Vibration/Exterior Sound at A57/M13



CONDITION	TYPE	L_R
— 7090	GROUND	118
- - - 7130	CLIMB	116
- · - · 7100	GROUND	115
· · · · 7190	FLAP CYCLE	110
· · · · · 7140	LOW-ALTITUDE CRUISE	95

Figure 53 Skin Vibration/Exterior Sound at A60/M20

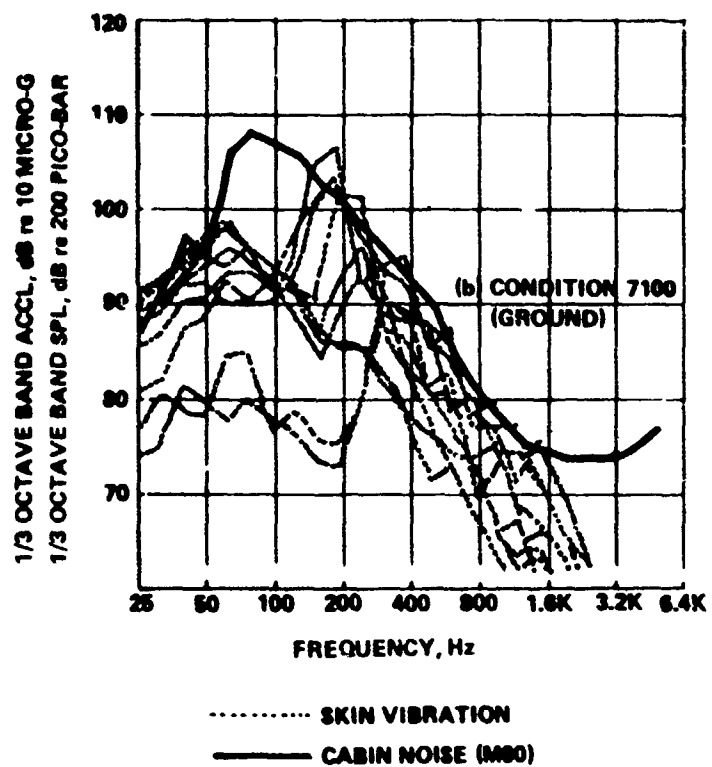
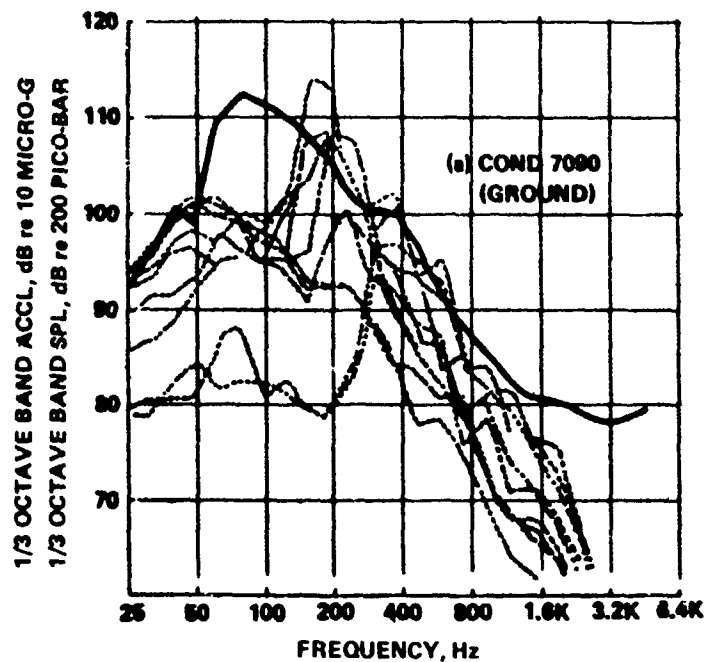
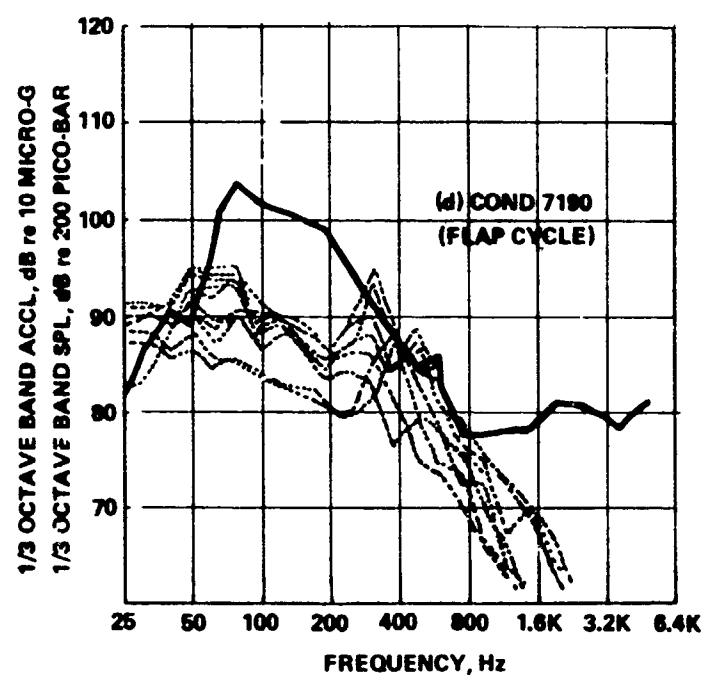
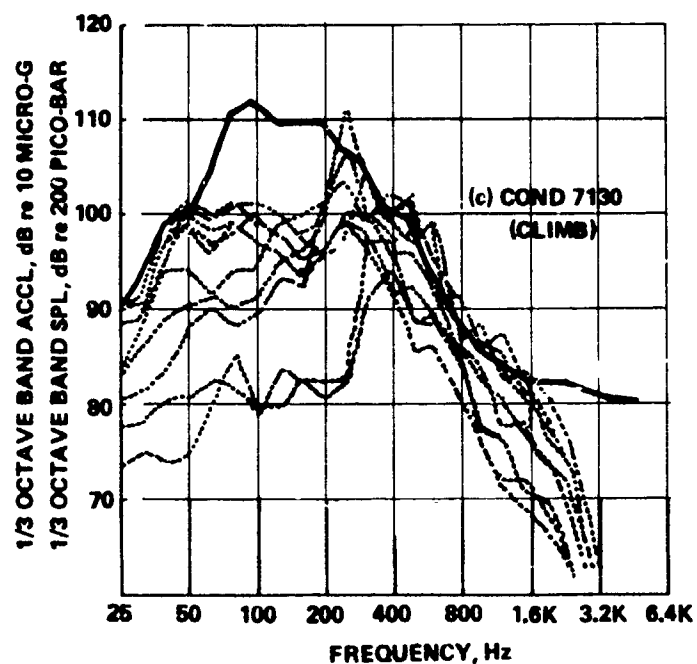


Figure 54 Comparative Behavior of Skin Vibration and Cabin Noise



----- SKIN VIBRATION
 ——— CABIN NOISE (M80)

Figure 54 Comparative Behavior of Skin Vibration and Cabin Noise (Continued)

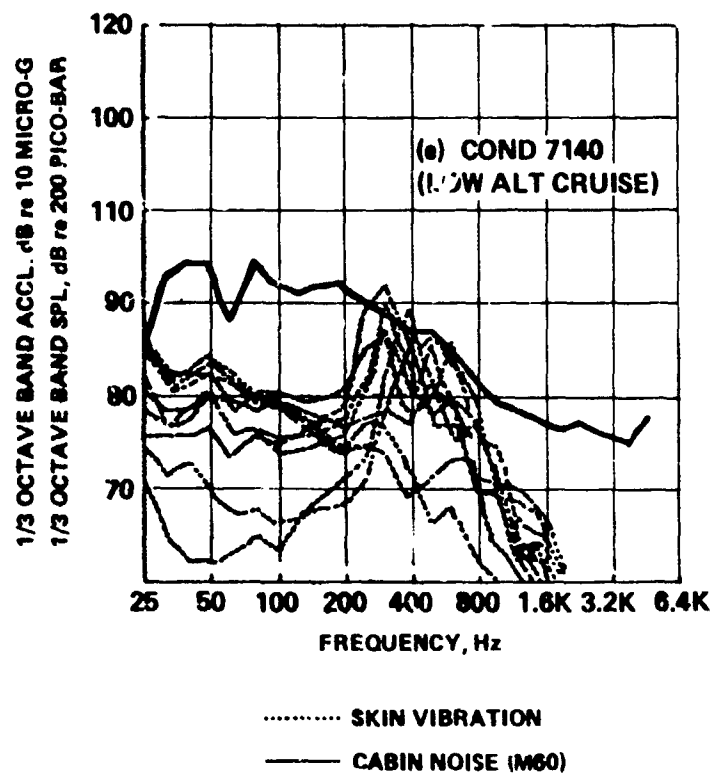


Figure 54 Comparative Behavior of Skin Vibration and Cabin Noise (Concluded)

APPENDIX

REFERENCE ACOUSTIC ANALYSIS MATERIAL

This appendix is an abridged version of the Results and Conclusions section of Reference 5. It is presented here as supporting material to Paragraph VI-2 of the present report.

While narrowband (PSD) as well as one-third octave and OASPL analyses of microphone signals, and one-third octave, RMS, and narrowband (PSD) analyses of accelerometer signals were accomplished as a part of this contract (all of which may be found in Reference 6) essentially only one-third octave and OASPL microphone data are discussed herein.

Concerning the relationship between test condition numbers and one-third octave (and complementing OASPL) and OASPL time history analysis numbers, note that interior noise measurement test conditions are identified with a number of the form

7.01.001.0XY.Z

For example (referring to Section IV of this document and Table A-I), the test condition number for the 22,000-ft Mach 0.70 cruise condition was

7.01.001.015,

while that for the first FLAPS 20 takeoff condition was

7.01.001.013,

and for the second FLAPS 20 takeoff condition, performed on another flight, was

7.01.001.013.1, etc.

One-third octave analyses, of which there are often several for the same test condition, particularly for transient type conditions, are identified by a four-digit number. This is of the form

7XYW,

where X and Y are the same as those appearing in the test condition number. For test conditions for which only a single one-third octave analysis has been made (used for steady-state conditions), then

W = Z.

In the case of test conditions for which several one-third octave analyses have been made, the W need no longer be equal to Z. In this case, the reader must refer to Table A-I for exact details. As an example (referring to Table A-I), analysis condition 7130 characterizes the (reasonably stable) climbout portion of test condition 7.01.001.013, while analysis conditions 7131, 7132, 7133, 7134, 7135, and 7136 cover intervals of test condition 7.01.001.013.1 from brake release through establishment of stable climbout, etc.

Table A-1 One-Third Octave Analysis Log

[illegible]

OASPL time history analyses typically cover the full span of a particular test condition. They are identified by a shortened version of the number of the test condition they deal with; e.g.,

7.XY.W,

as compared to the full test condition number form

7.01.001.OXY.W.

1.1 GENERAL INTERIOR NOISE ENVIRONMENTS

Figures A-1 and A-2 and Table A-II summarize measured interior noise OASPLs and airplane configuration for many of the flight and ground ambient conditions investigated during this contract effort. With engines on, the spread of OASPLs can be more than 35 dB, ranging from a low of about 86 dB at the aft end of the troop compartment at ground idle to a high of about 122 dB, again at the aft end of the troop compartment, at brake release. During flight operations, the highest levels occur at the aft end of the troop compartment, the lowest levels on the flight deck.

The highest levels occur at brake release (condition 7132). Within 20 sec, these levels drop from 2 dB to 5 dB, by which time the airplane has lifted off and stabilized in an aggressive climbout configuration (condition 7136). Climbout levels are then experienced for about 4 min, at which time the airplane will have easily reached 15,000 ft.

The approach noise levels (condition 7220) correspond essentially to a low capability STOL configuration, with USB flaps locked at 20° , an approach speed of 180 ft/sec (106 knots), and a glide slope (GS) of only about 3° . By comparison, a design STOL approach would involve USB flap angles of 40° to 60° , an approach speed of 135 to 150 ft/sec (80 to 90 knots), and a glide slope of 6° .

Data for a "simulated STOL approach" (condition 7183) are summarized in Figure A-2. The USB flaps were close to 40° , airplane speed was 170 ft/sec, and the glide slope (GS) was 6° .

By comparison, overall levels for the simulated STOL approach are 2 dB to 4 dB higher than those for the low-capability STOL approach.

Levels experienced during go-around summarized in Figure A-2, condition 7184, are about the same as those shown for climbout.

Three conditions aimed at defining interior ambient levels are also shown in Figure A-2. Condition 7010 corresponds to engines off, but electrical distribution systems (which are located at the front of the troop compartment and under the flight deck floor) on. Condition 7080 corresponds to engines at ground idle and electrical distribution systems on. Condition 7200 is for the airplane airborne, engines at idle, electrical systems on, and the air conditioning/pressurization systems on.

Figures A-3 through A-11 summarize one-third octave spectral behavior of YC-14 interior noise (as well as OASPL behavior both along the center aisle and within 18 in. of the sidewall) for conditions summarized in Figure A-2. Spectra are shown only for selected microphones.

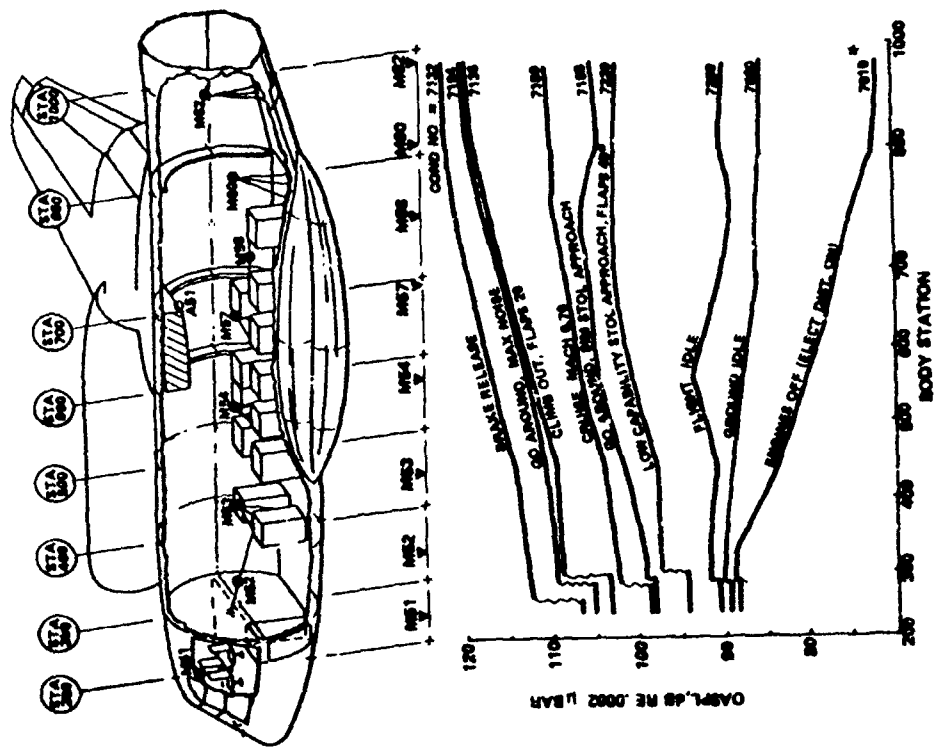


Figure A-2 Cabin Noise OASPL Distribution

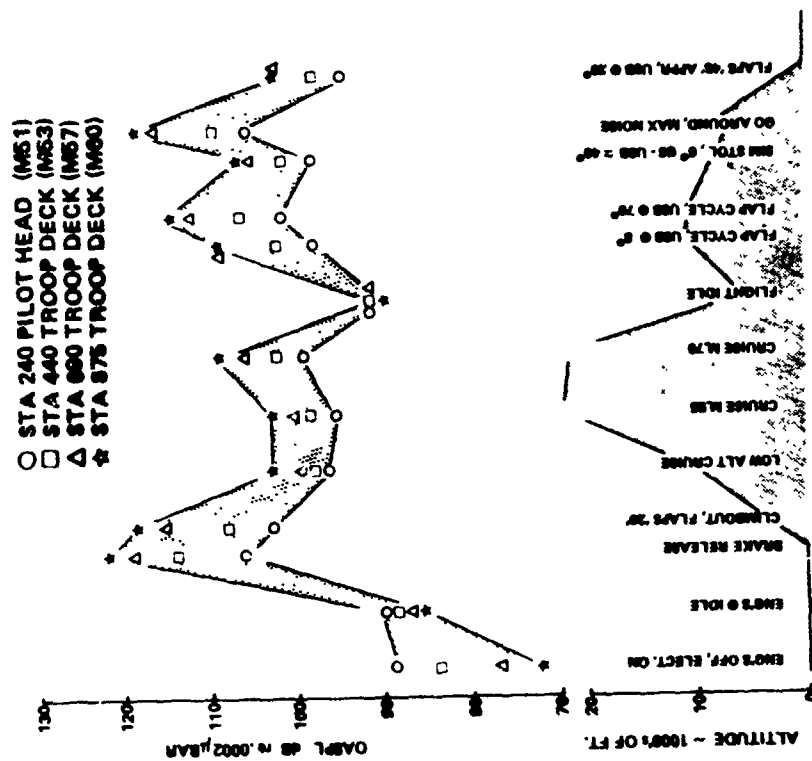



Figure A-1 Summary of Cabin Noise OASPL

Table A-II Summary of Condition Numbers and Airplane Parameters for Conditions Indicated in Figures A-1 and A-2

Condition description	Condition number	Airplane parameters				
		Alt, ft	Speed, f/s	N ₁ RPM	VMIX, f/s	USB  , deg
Engines off, electrical systems on	7010	0	0	0	0	0
Ground idle	7080	0	0	810	220	0
Brake release	7132	0	40	3,540	1,100	0
Climbout, flaps '20'	7136	100	220	3,710	1,050	0
Low altitude cruise	7140	11,570	490	2,440	790	0
Cruise, Mach 0.55	7170	22,170	570	2,690	910	0
Cruise, Mach 0.70	7150	22,370	725	3,240	1,140	0
Flight idle	7200	6,670	300	1,380	450	0
Flap cycle, USB @ 60°	7190	11,050	215	2,950	830	8
Flap cycle, USB @ 70°	7192	10,700	215	2,950	830	70
Simulated STOL, 6° GS, USB @ 40°	7183	8,300	170	2,200	560	41
Go-around, max noise	7184	7,700	215	3,670	1,100	18
Approach, flaps '45', USB @ 20°	7220	800	180	2,200	560	0

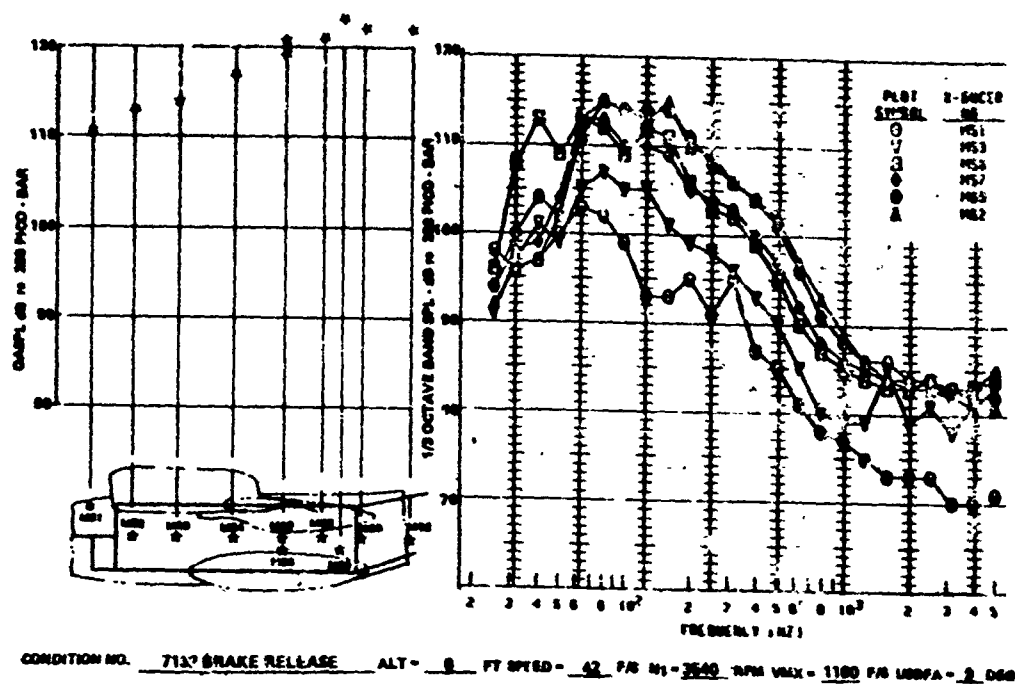


Figure A-3 Summary of Cabin Noise

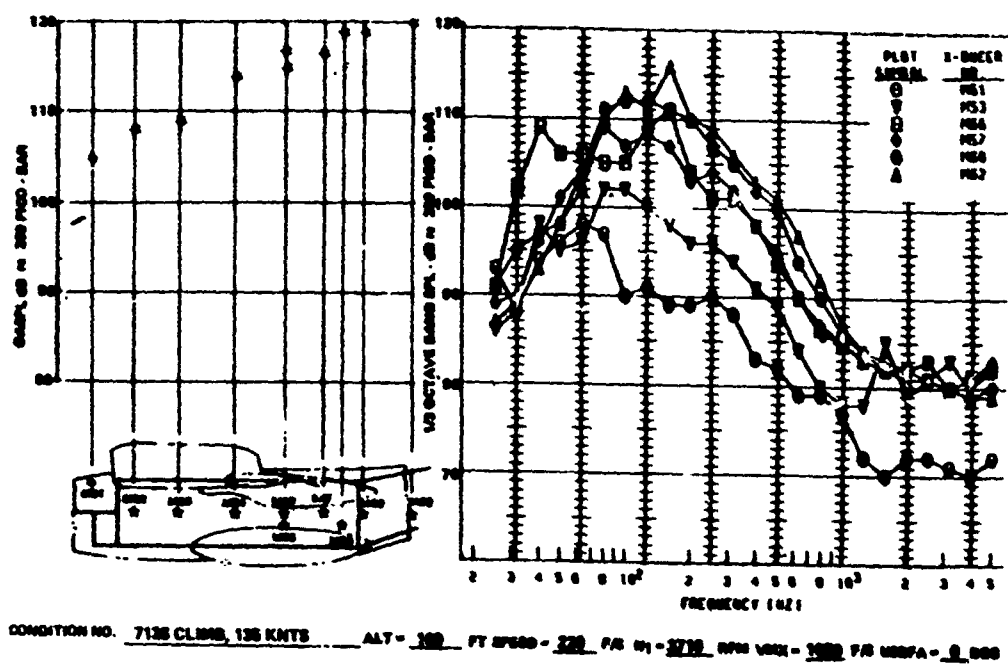
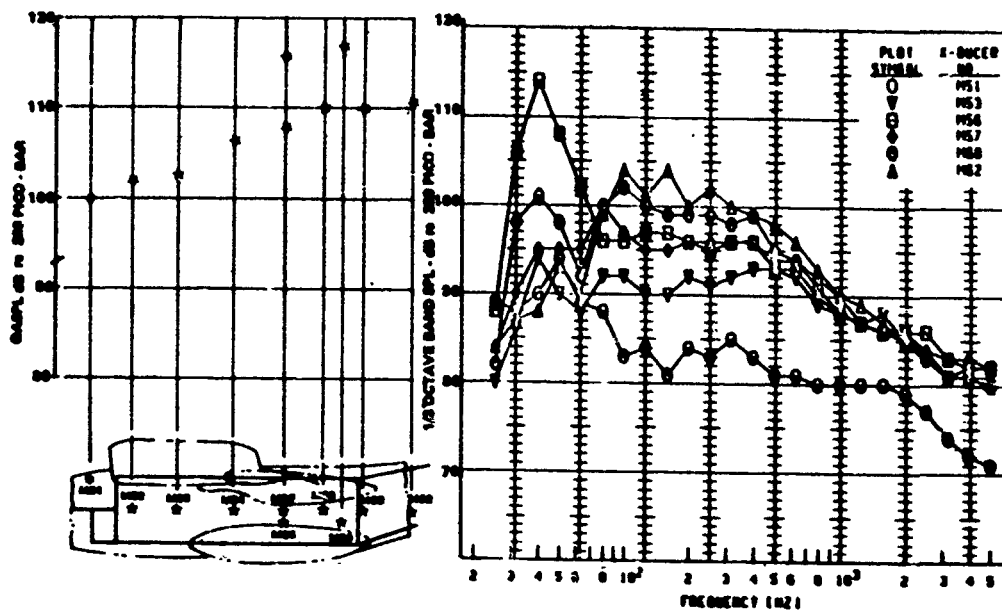
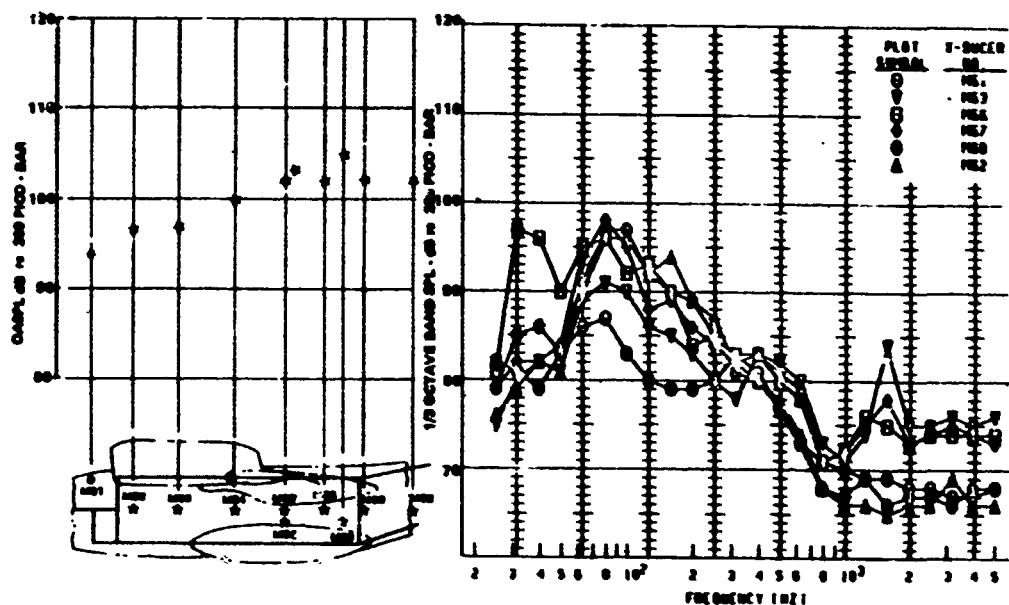


Figure A-4 Summary of Cabin Noise



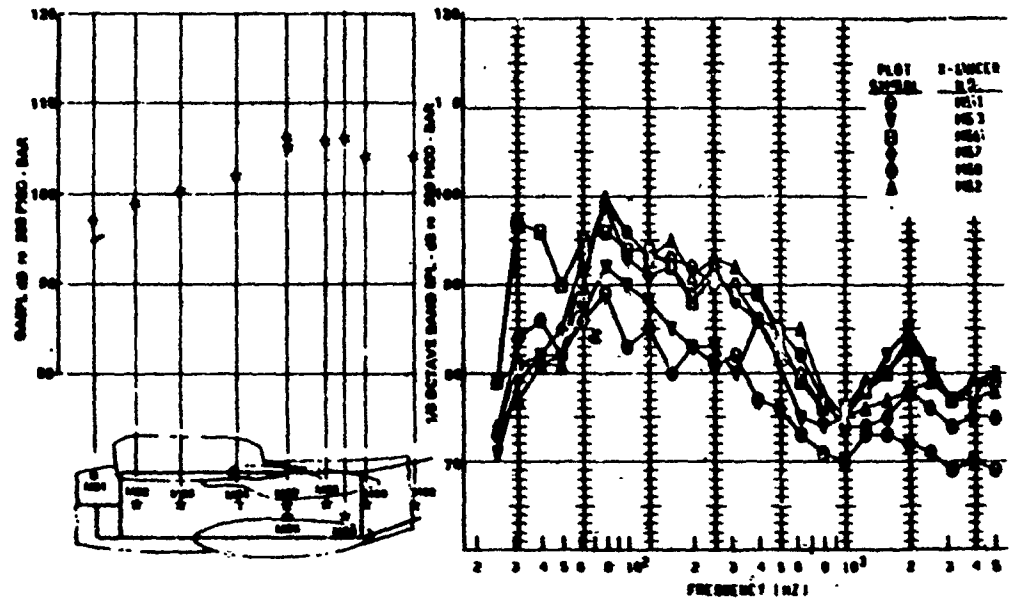
CONDITION NO. 7189 CRUISE ML70 ALT- 22270 FT SPEED- 724 F/S M_1 - 322.7 RPM VIBX- 1141 F/S USRFA- 0.000

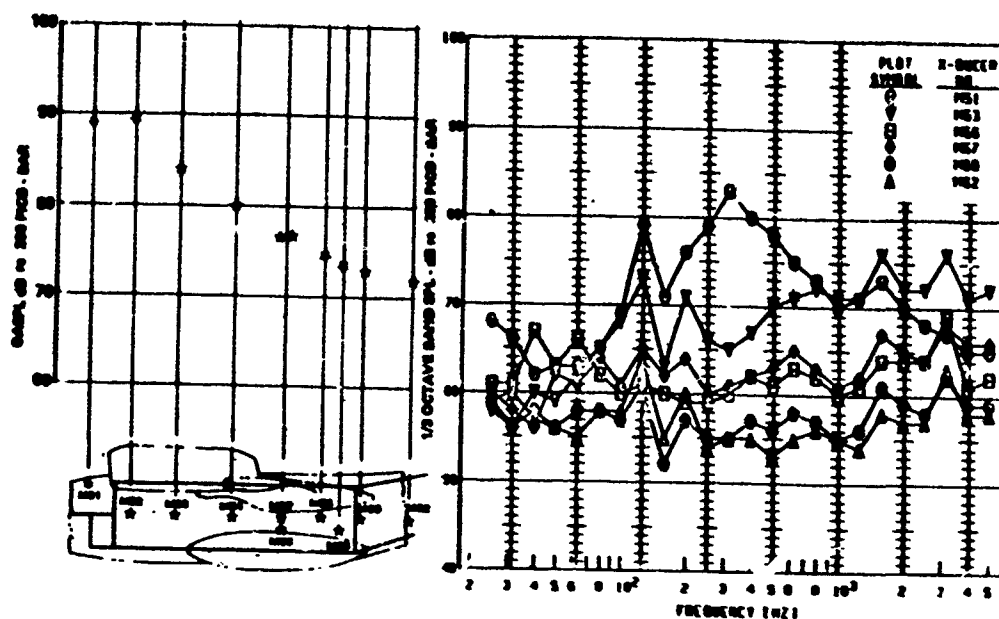
Figure A-5 Summary of Cabin Noise



CONDITION NO. 7220 APPR, FLPS 45 ALT- 000 FT SPEED- 100 F/S M_1 - 2200 RPM VIBX- 000 F/S USRFA- 20.000

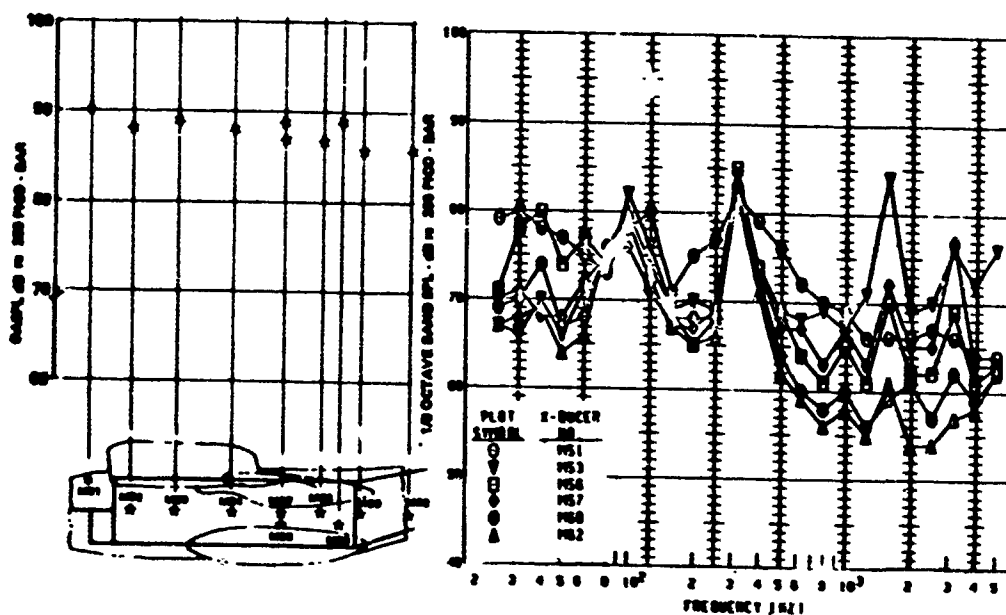
Figure A-6 Summary of Cabin Noise





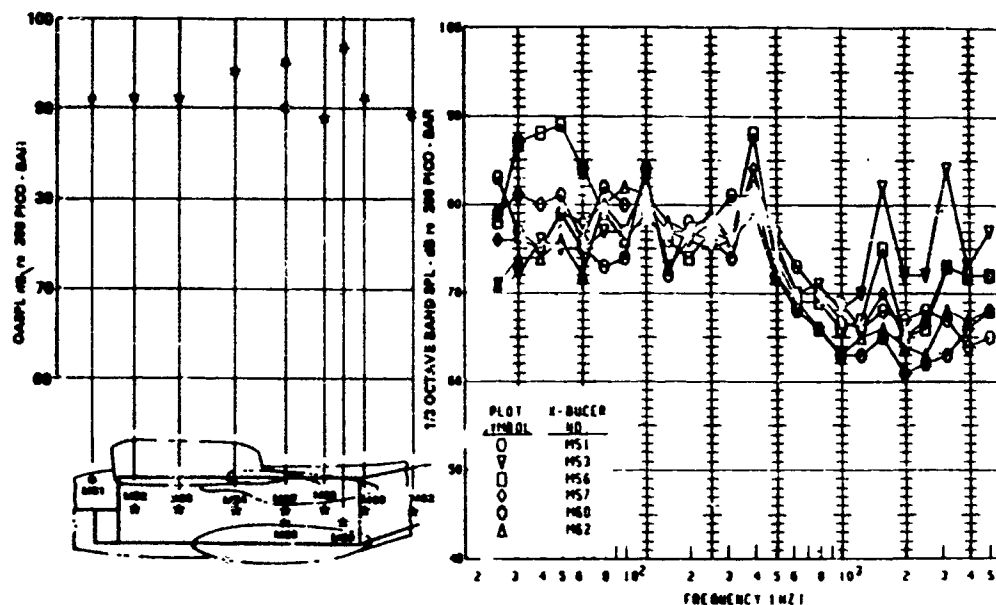
CONDITION NO. 7616 DEAD A/P AMBIENT ALT - 0 FT SPEED - 0 P/R n_1 - 0 RPM V/RX - 0 P/R L/RPA - 0 DDB

Figure A-9 Summary of Cabin Noise



CONDITION NO. 7616 BOTH ENG'S GROUND ALT - 0 FT SPEED - 0 P/R n_1 - 812 RPM V/RX - 225 P/R L/RPA - 0 DDB

Figure A-10 Summary of Cabin Noise



CONDITION NO. 7288 AMB. A/C PRESS ON ALT - 8579 FT SPEED - 302 F/N N1 - 1377 RPM VMCX - 447 F/N UBBFA - 8.066

Figure A-11 Summary of Cabin Noise

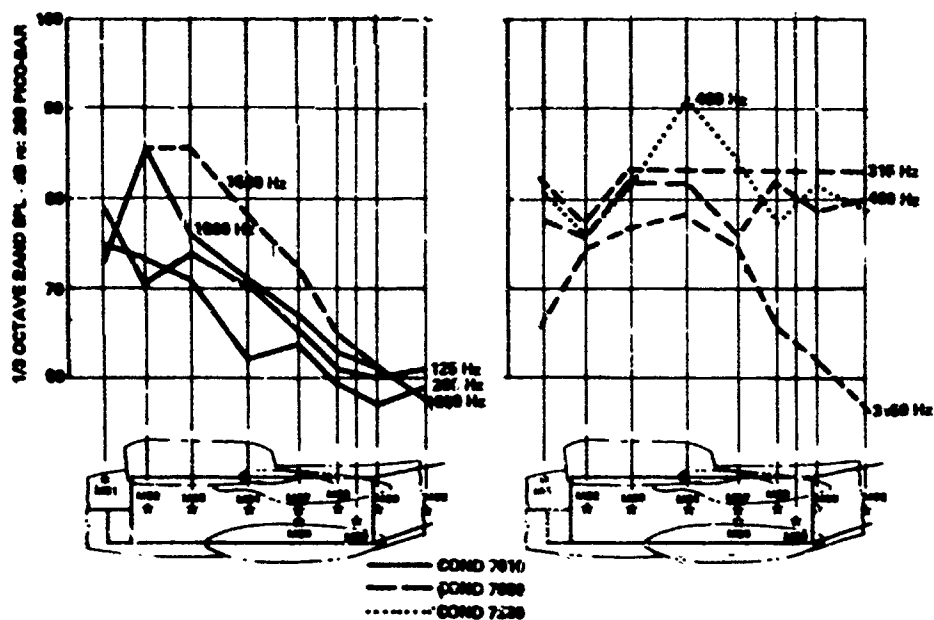


Figure A-12 Distribution of Dominant One-Third Octave Band (Ambient) Noise Levels Along Cabin Center Aisle

Omitting the ambient noise conditions for the moment, spectra for a given condition have similar shapes from front to rear of the airplane. M55 near the sidewall, and nearby center aisle microphone M60, show distinctively higher levels in the 30 Hz through 50 Hz bands than microphones forward of the wing. This effect is currently not fully understood, although some sort of room mode effect is suspected.

Levels on the flight deck follow closely those in the forward portion of the troop compartment from 25 Hz to 60 Hz. In the higher bands, levels on the flight deck typically are 5 dB to 10 dB below those at the front of the troop compartment for the loudest conditions (takeoff, climbout, cruise, and maximum noise portion of the go-around). At approach, flight deck and forward troop compartment levels are about the same.

Figures A-9, A-10, and A-11 summarize interior noise felt to indicate primarily ambient noise behavior. These suggest that ambient levels on the flight deck and in the troop compartment are set by electrical distribution system noise dominated by energy concentrated in the 125 Hz, 200 Hz, and 1600 Hz one-third octave bands. Engine auxiliary systems (e.g., hydraulics, air conditioning, etc.) are suspected to be responsible for energy concentrated in the 100 Hz, 315 Hz (which shifts to 400 Hz as engine speed is increased from ground to flight idle), and 3150 Hz one-third octave bands. Referring to Figure A-12, electrical distribution system noise (typically in the 125 Hz, 200 Hz, and 1600 Hz bands) can be seen to originate at the front of the troop compartment, largely in the electronic equipment bay. Hydraulic noise in the other indicated bands originates further back in the troop compartment, near stations 600-700 where hydraulic lines and reservoirs are situated.

A.2 GENERAL EXTERIOR FUSELAGE FLUCTUATING PRESSURE ENVIRONMENT

Figure A-13 summarizes measured exterior fuselage fluctuating pressure levels—often to be referred to as exterior noise levels—for most of the flight conditions shown in Figure A-1.

With engines on, external fuselage OASPLs can fall anywhere between 105 dB and 158 dB. During flight, levels are all above about 115 dB. As expected, the lowest levels occur on the forward part of the airplane, and the highest levels on the sides (and upper sidewalls) aft of the USB flaps. The highest levels are observed during such high-power, low-speed operations as takeoff/climbout and go-around. During Mach 0.70 cruise at 22,000 ft, levels between 142 dB and 129 dB are observed.

OASPLs for two groups of the flush-mounted exterior fuselage microphones for various conditions are summarized in Figure A-14. Group one, consisting of M1, M3, M5, M6, M14, and M16, is distributed lengthwise along the fuselage from forward of the wing, beneath it, to well aft of the trailing edge of the USB flaps. Group two, consisting of M12, M20, M13, M14, and M15, is distributed circumferentially from the top of the fuselage down to just above the top of the main landing gear wheel well fairing.

In almost every case, the OASPL at M1 is 1 dB to 6 dB higher than at M3. This is almost totally due to much more high-frequency noise energy at M1 than at M3. It is expected that this high-frequency energy is produced by the fan of the engine, which is in the direct view of M1 but is blocked from the view of M3 by the nacelle.

As was the case for interior noise, the highest exterior noise levels occur at brake release (condition 7132). By the establishment of climbout (condition 7136), levels are down from 2 dB to 7 dB. Levels for the maximum noise portion of go-around (condition 7184) are, as for interior noise, about the same as for climbout.

Exterior levels for Mach 0.70 cruise (condition 7150) come next in the scale. However, the variation of levels along the fuselage lacks the strong rise aft of the USB flap trailing edge experienced in other conditions, except for flight idle (condition 7200). Circumferentially, the Mach 0.70 cruise levels also lack the extreme gradients observed for other conditions, again except for flight idle.

Levels for the low capability STOL (USB at 20°) approach condition 7220 and the simulated STOL approach (condition 7183) are essentially the same, except at microphones M13, M14, and M16. Not unexpectedly, this appears to be a USB flap position flow turning effect, which is strongly observed on the fuselage because of the close-in location of the engine to the fuselage. For low-speed operations, the exhaust flow stream trailing off (nearly tangent to the upper surface of) the USB flaps produces locally high fluctuating pressure levels on the fuselage where the flow sheet geometrically intersects the fuselage surface. For low USB angles (20° or less), the flow sheet passes close to M13 and M16. At 40°, the sheet appears to pass below these two microphones but is now close to M14. (This behavior is examined again in Section A.4). Note that for high-speed operation, such locally high levels do not occur. A suggestion is that, for such operations, the exhaust sheet is further away or approaches closely only further aft on the fuselage, out of the range of transducers installed for this test program.

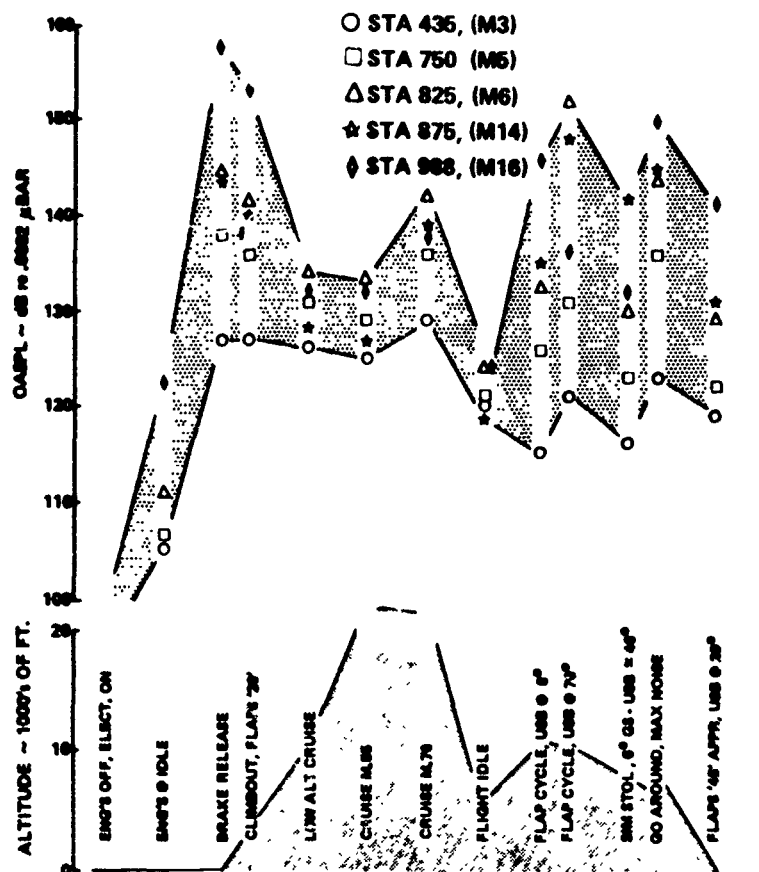


Figure A-13 Summary of Exterior Fuselage Noise OASPL

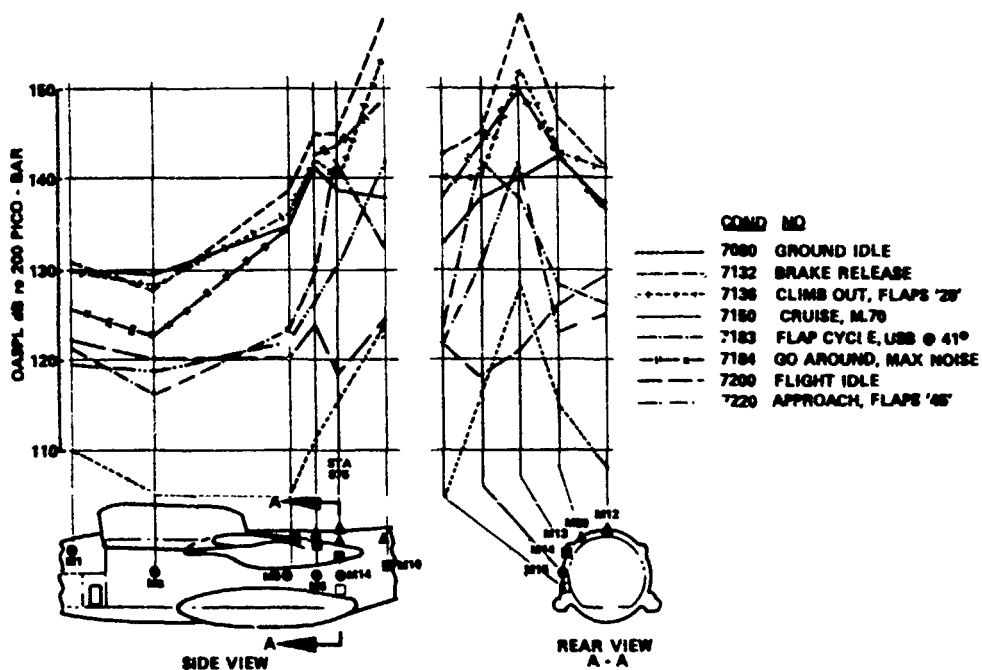


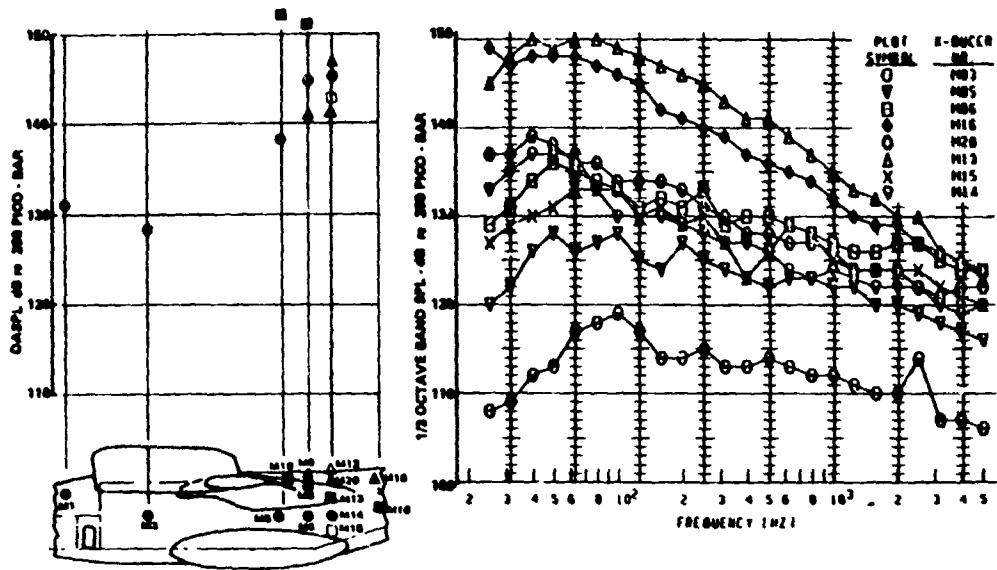
Figure A-14 Summary of External Fuselage Noise Activity

A negligible fore-to-aft noise level gradient is observed only in the case of flight idle (condition 7200). One reason could be that only in the case of flight idle is engine exhaust noise perhaps negligible compared to turbulent boundary layer (TBL) fluctuations over most of the fuselage. It could be that, even in the case of high speed operation such as Mach 0.70 cruise (condition 7150), engine exhaust noise is for a significant portion of the fuselage as important as or more so than TBL fluctuations.

Figures A-15 through A-22 summarize spectral and OASPL behavior of fuselage exterior noise. Note that spectra are shown only for a selected subset of the exterior fuselage microphones. These exterior fuselage noise figures complement interior noise Figures A-3 through A-11.

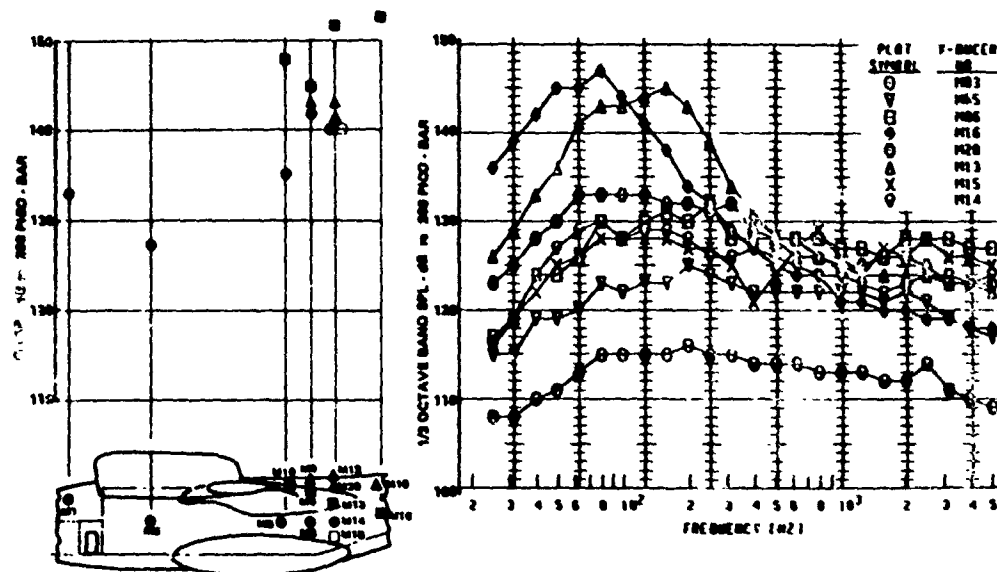
Of particular interest in Figures A-15 through A-22 are.

- Noticeable low-frequency reductions from brake release to climbout.
- Rich low-frequency content of spectra for climbout and approach as compared to cruise or flight idle (Figure A-22). Cruise and flight idle spectra contain more high-frequency energy than spectra at other conditions.
- Similarity in shape of spectra for brake release/climbout/go-around (maximum noise) and for approach.



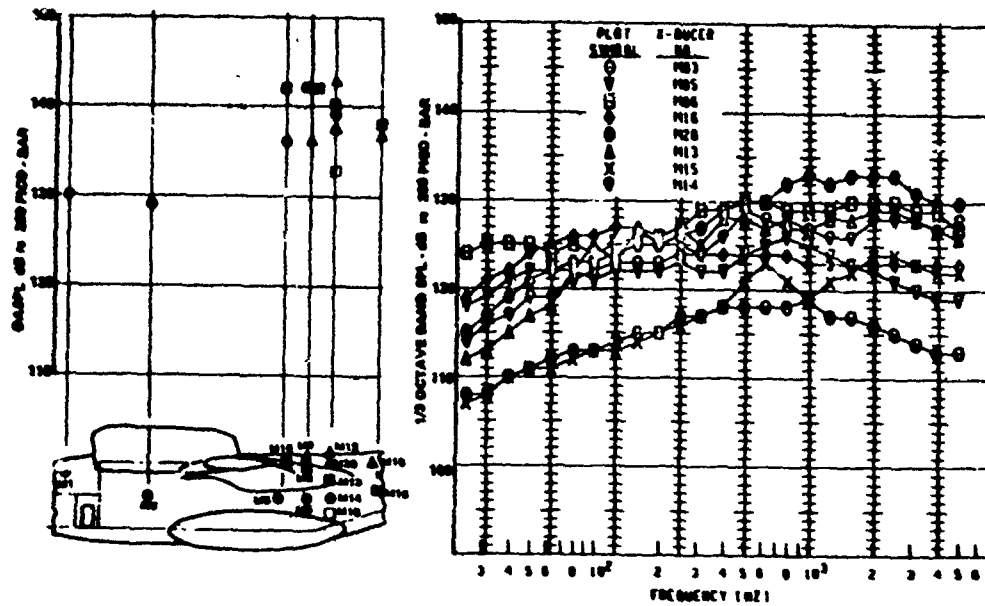
CONDITION NO. 7132 BRAKE RELEASE ALT - 0 FT SPEED - 42 F/S N1 - 540 RPM VMAX - 1100 F/S UBRFA - 9 DEG

Figure A-15 Summary of Exterior Noise



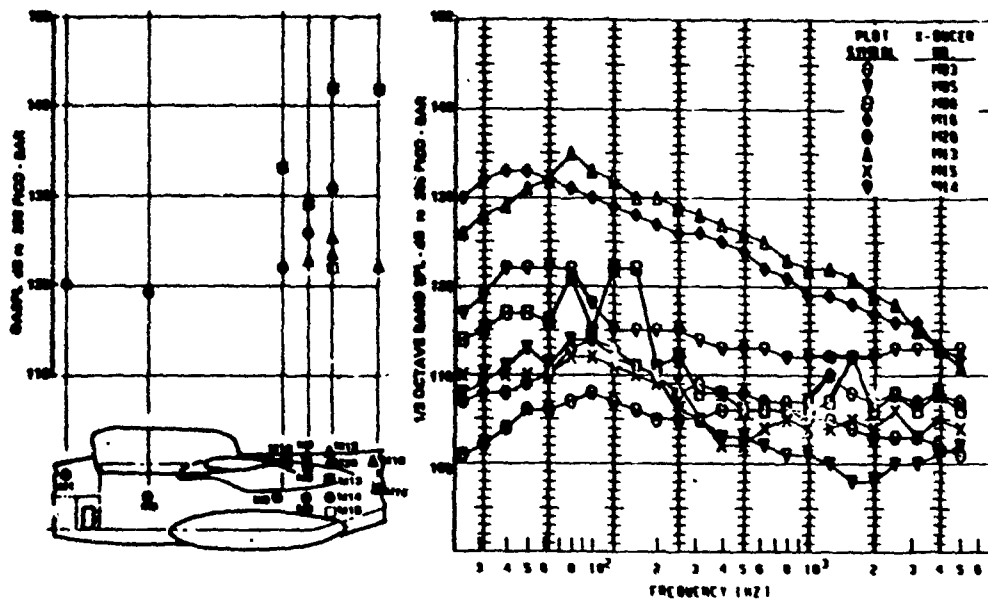
CONDITION NO. 7136 CLIMB 135 KNTS ALT - 100 FT SPEED - 220 F/S N1 - 3710 RPM VMAX - 1000 F/S UBRFA - 9 DEG

Figure A-16 Summary of Exterior Noise



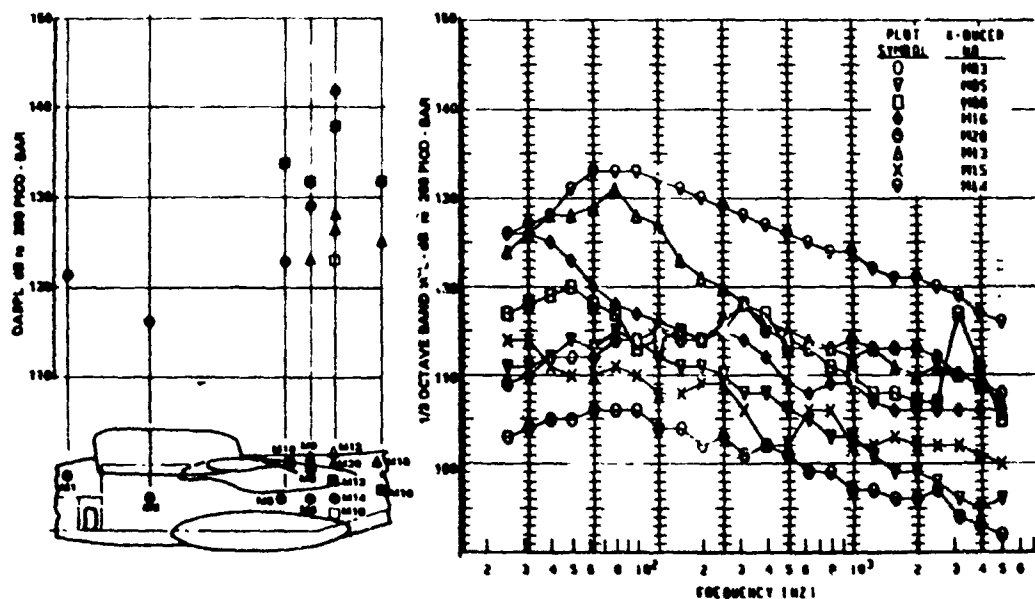
CONDITION NO. 7188 CRUISE M70 ALT - 22270 FT SPEED - 174 F/S M1 - 3222 RPM VMAX - 1141 F/S USBFA - 0 DEG

Figure A-17 Summary of Exterior Noise



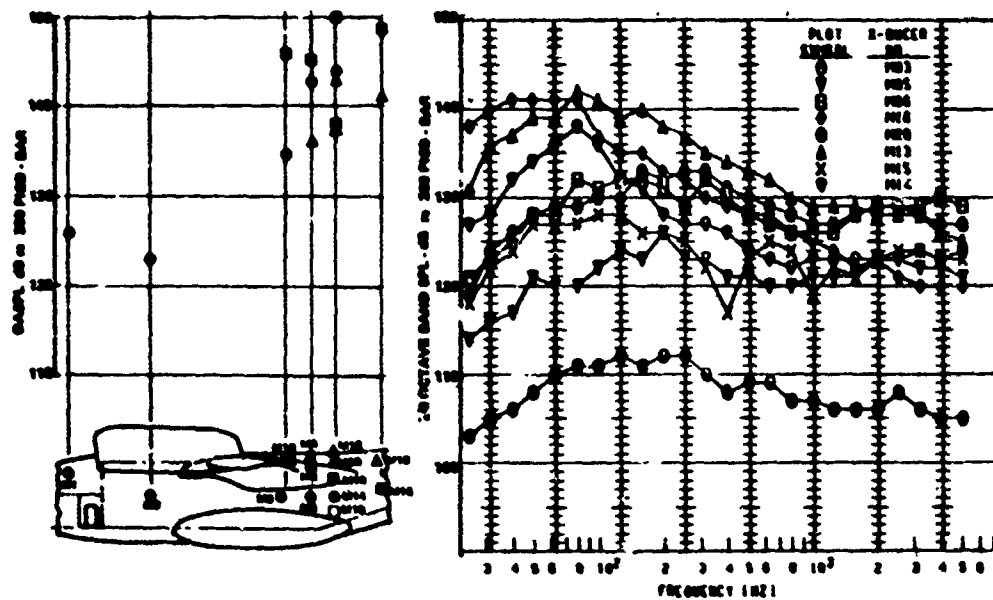
CONDITION NO. 7226 APPRO FLPS 65 ALT - 800 FT SPEED - 180 F/S M1 - 2200 RPM VMAX - 800 F/S USBFA - 20 DEG

Figure A-18 Summary of Exterior Noise



CONDITION NO. 7183 GO AROUND 8° G.S. ALT - 8700 FT SPEED - 170 F/M M1 - 2200 RPM VMAX - 200 F/M LMBFA - 41 DEG

Figure A-19 Summary of Exterior Noise



CONDITION NO. 7754 GO AROUND MAX NOISE ALT - 7700 FT SPEED - 214 F/M M1 - 3070 RPM VMAX - 1200 F/M LMBFA - 30 DEG

FIGURE A-20 SUMMARY OF EXTERIOR NOISE

Figure A-20 Summary of Exterior Noise

A.3 INTERIOR VERSUS EXTERIOR FUSELAGE NOISE

Figure A-23 provides a very simple indication of the relationship between exterior and interior noise.

- Conditions for which exterior fuselage levels are high are the same conditions for which interior noise levels are high, and vice versa, and
- A nominal difference between a mean interior sound power level and a mean exterior fuselage fluctuating pressure power level is 30 dB. This value is roughly appropriate to all flight conditions shown.

While the contents of Figure A-23 are encouraging in their regularity, there remains far more work to bring understanding of interior versus exterior noise even to the level of understanding of exterior noise and of interior noise demonstrated in Sections A.1 and A.2. The work in these two sections on the separate problems of interior noise and exterior noise represents necessary ground work to attacking effectively the coupled problems.

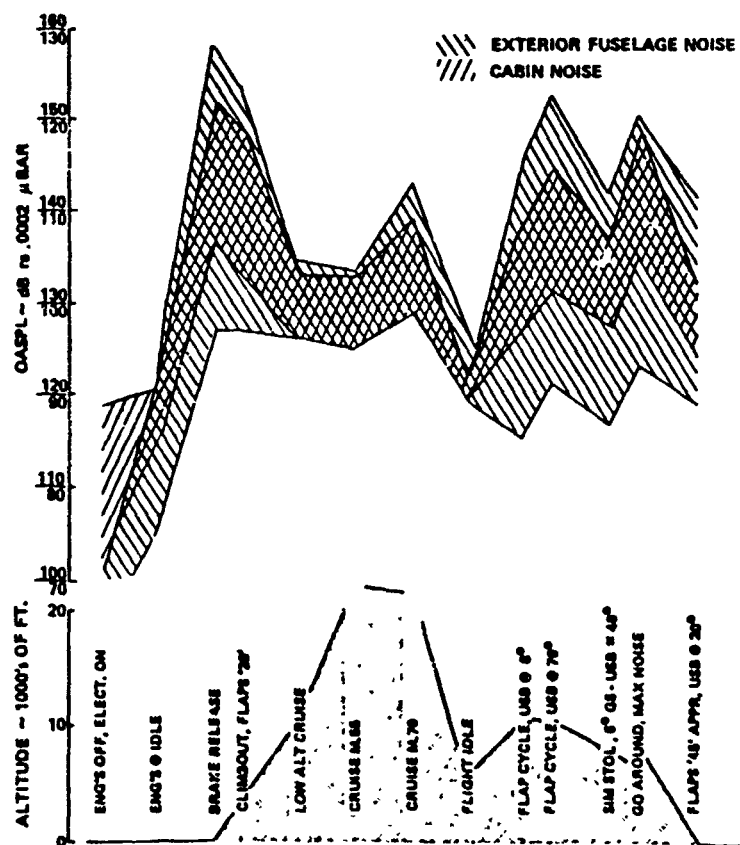


Figure A-23 Summary of Cabin Noise OASPL vs Exterior Fuselage Noise OASPL

A.4 USB PROPULSION SYSTEM EFFECTS

Only the most obvious special USB propulsion system effect, namely USB flap position dependency, has been examined.

USB flap position effects have been easy to spot, primarily because of the close-in location of the engine/USB flap system to the fuselage. Because of this arrangement, the exhaust flow sheet trailing off the USB flaps produces locally high fluctuating pressure levels on the fuselage where it geometrically intersects the fuselage surface. This behavior is observed for all conditions except flight idle and the various cruise conditions. When the USB flaps are retracted, the region of distinctively high fluctuating pressure levels covers microphones M13 and M16, but not M20 just above, or M15 just below M13. As the USB flaps are lowered, the levels on M14, and M15, and finally M6 increases, while the levels on M13 and M16 decrease.

This is illustrated in Figure A-24, which displays time histories of the exterior fuselage fluctuating pressure OASPLs obtained from the first flap cycle test (condition 7.01.001.019) data. Corresponding time histories of airplane parameters, particularly USB flap position, are shown in Figure A-25. Figure A-24 further suggests that the width of the region in which the highest pressure fluctuations occur is quite narrow. This is further illustrated by Figure A-26.

An additional feature suggested by curves in these figures is that exterior noise levels appear to be highly sensitive to the status of the vortex generators (VGs). OASPLs for microphones at more remote parts of the fuselage—as M3, M5, and even M8 and M20, for example—are as much as 5 dB higher when the VGs are up than when they are down.

Interior noise OASPL time histories for the flap cycle test condition are shown in Figure A-27, and OASPL distributions corresponding to a few USB flap/VG position combinations are shown in Figure A-28. In general, interior noise levels are about 5 dB higher with the USB flaps fully extended than with these same flaps fully retracted.

The effect of VGs and flap position is demonstrated quite effectively in the one-third octave spectra of both exterior and interior microphones. Figures A-29 through A-33 show spectra for exterior microphones M3, M5, M6, M14, and M16, which are distributed along the side of the fuselage from in front of the wing to underneath the wing and on the back to well aft of the USB flap system. Figures A-34 through A-37 show spectra for exterior microphones M12, M20, M13, and M15, which are distributed circumferentially from the top of the body down to just above the top of the main landing gear fairing. Finally, Figures A-38 through A-42 show spectra for interior microphones M51, M53, M57, M59, and M60, which are distributed from the flight deck aft to the back of the troop deck.

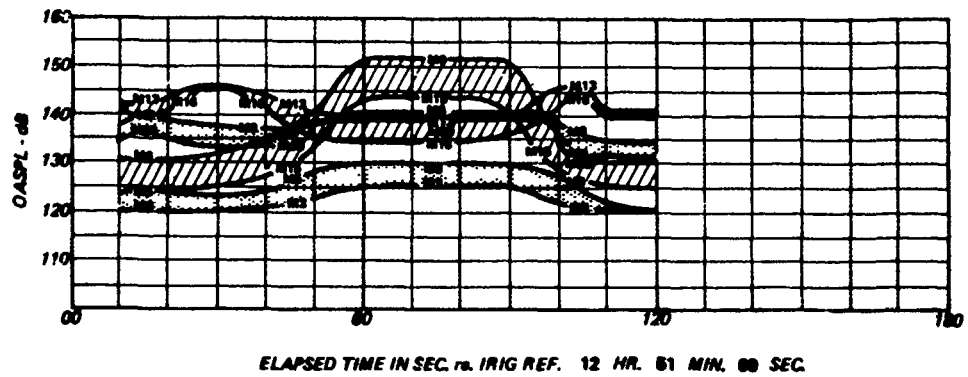
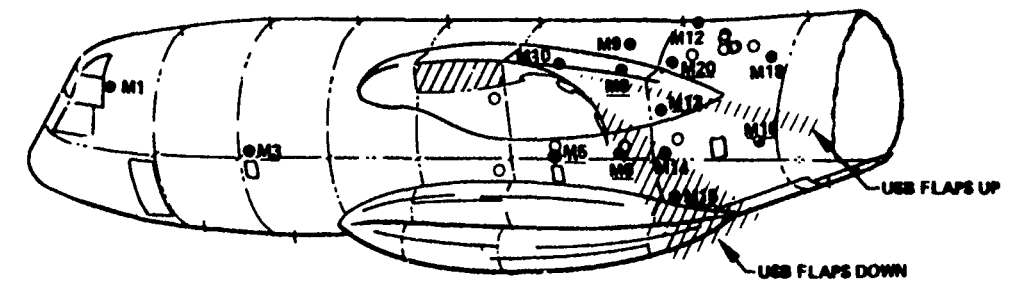


Figure A-24 Exterior Noise Level Time Histories; Condition 7.01.001.019 (Flap Cycle)

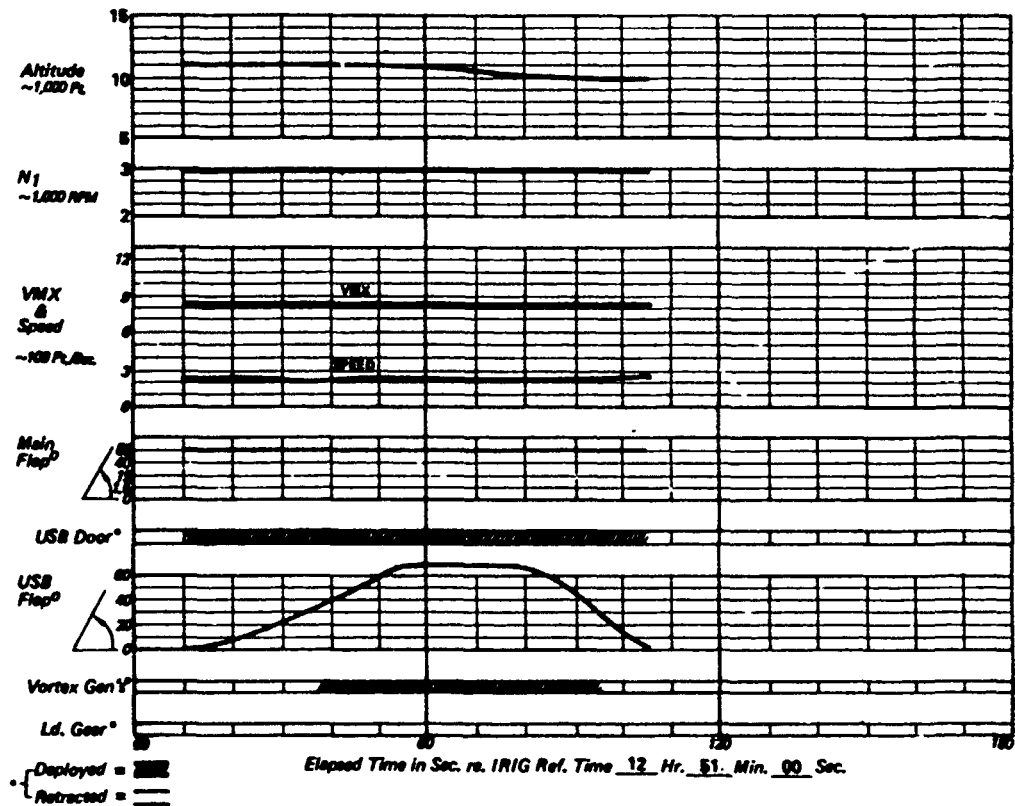


Figure A-25 Airplane Parameter Time Histories; Condition 7.01.001.019 (Flap Cycle)

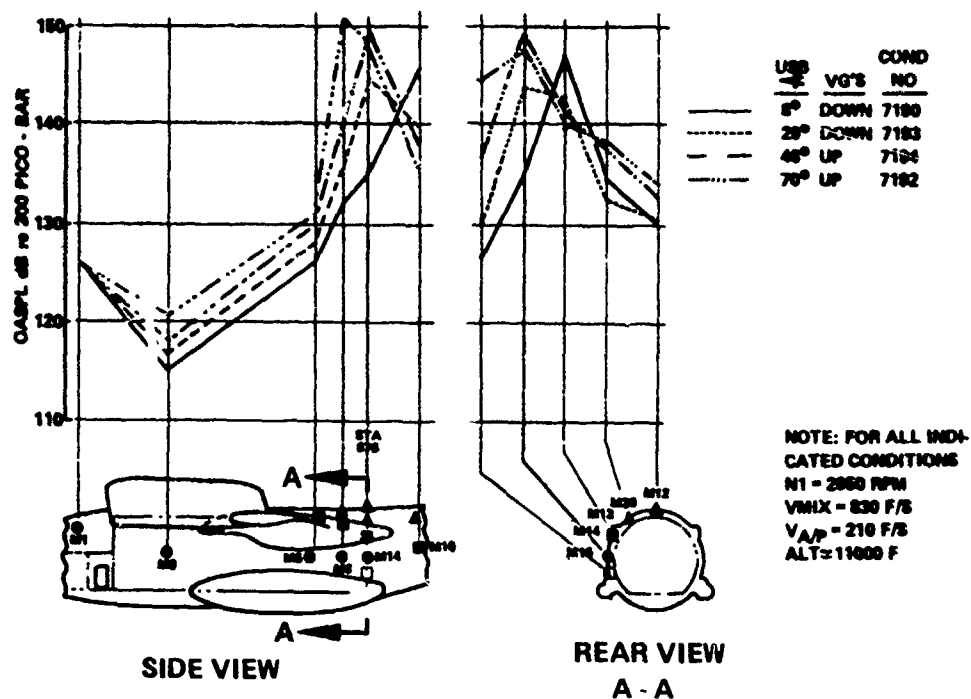


Figure A-26 Effect of USB Flap Position on External Fuselage OASPLs

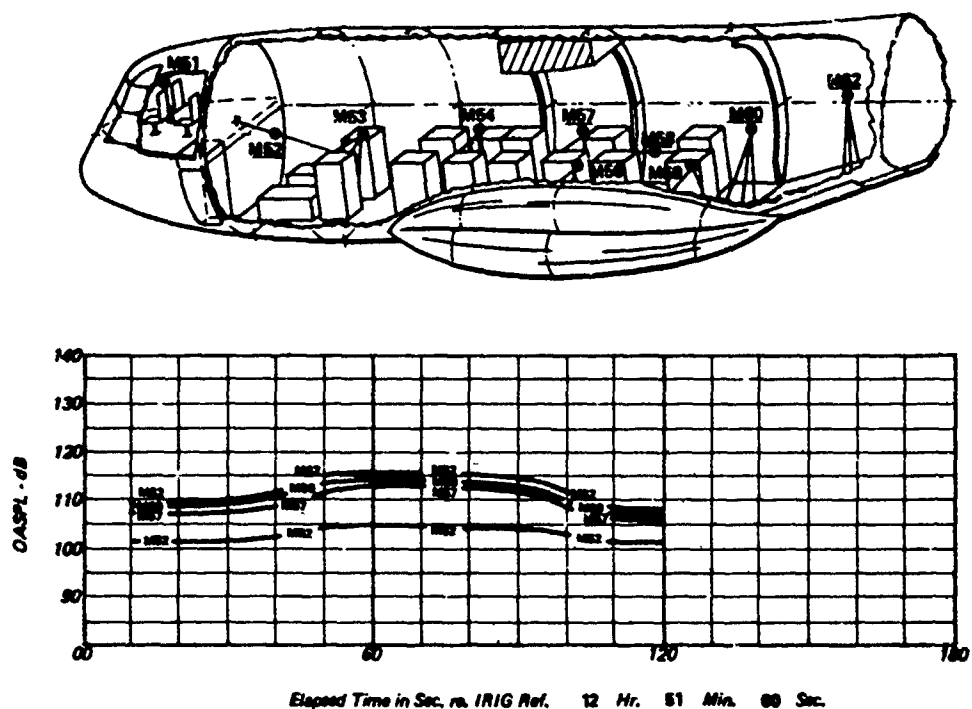


Figure A-27 Cabin Noise Level Time Histories; Condition 7.01.001.019 (Flap Cycle)

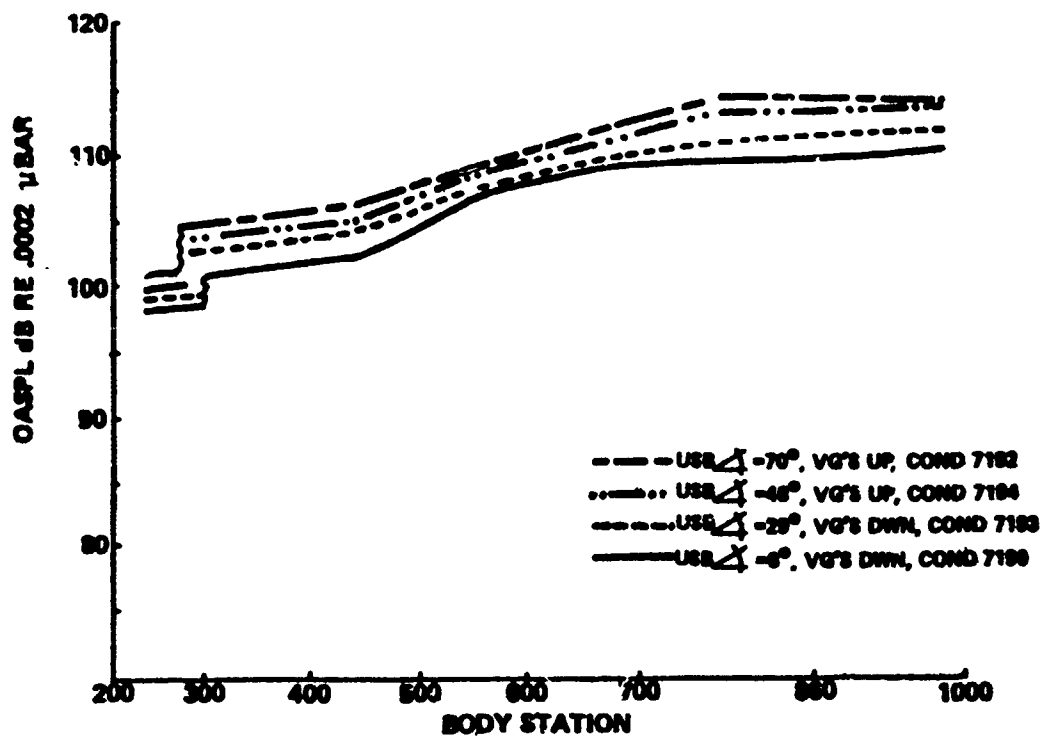
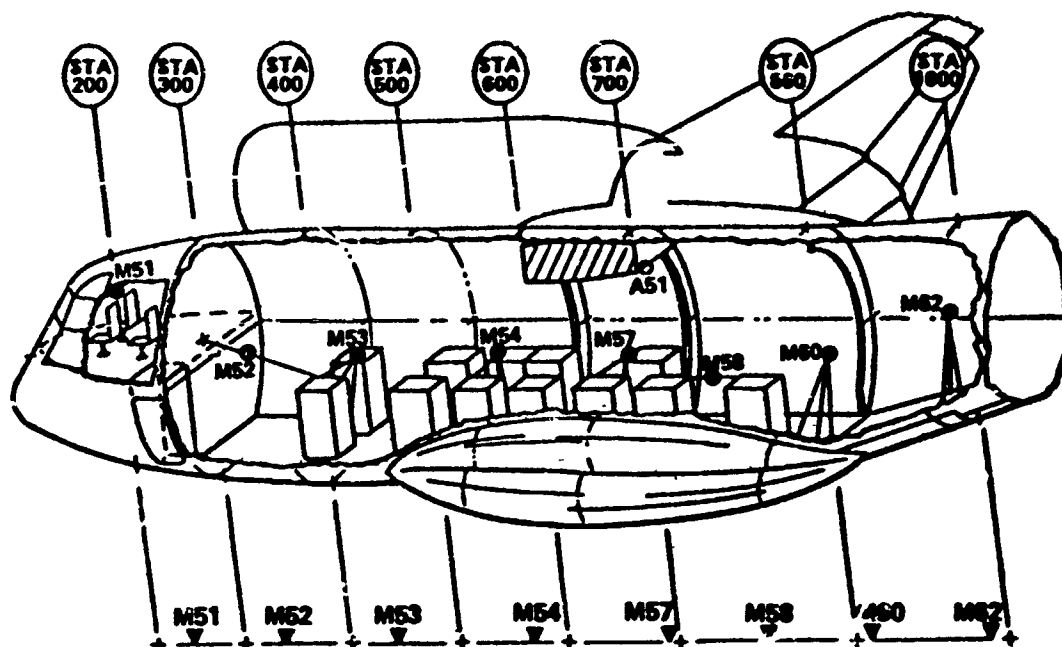


Figure A-28 Effect of USB Flap Position on Cabin OASPLs

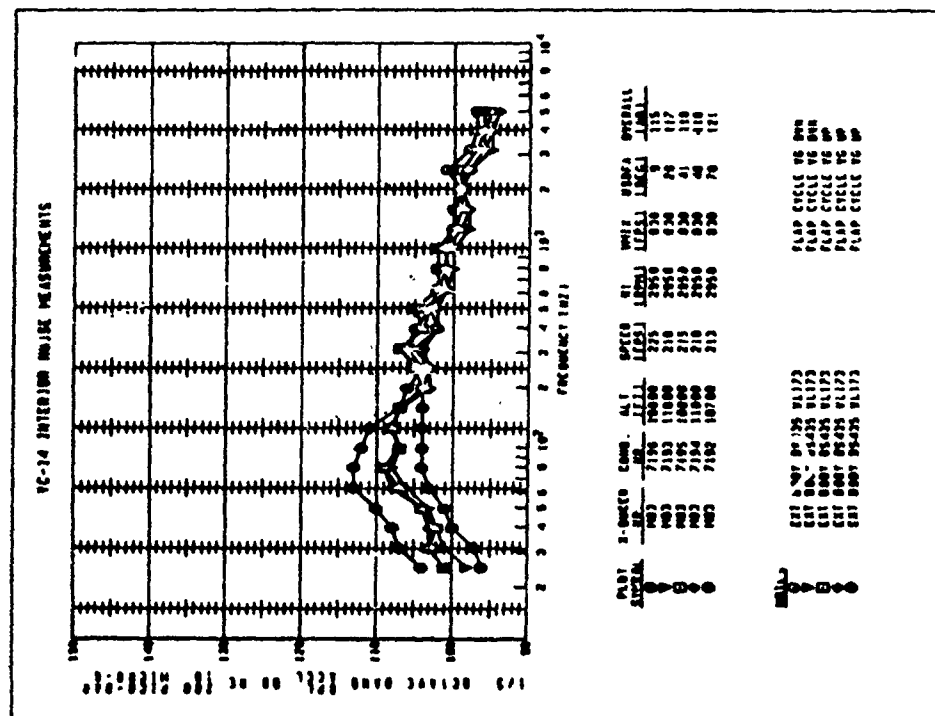


Figure A-29 One-Third Octave Spectra, M03, Flap Cycle

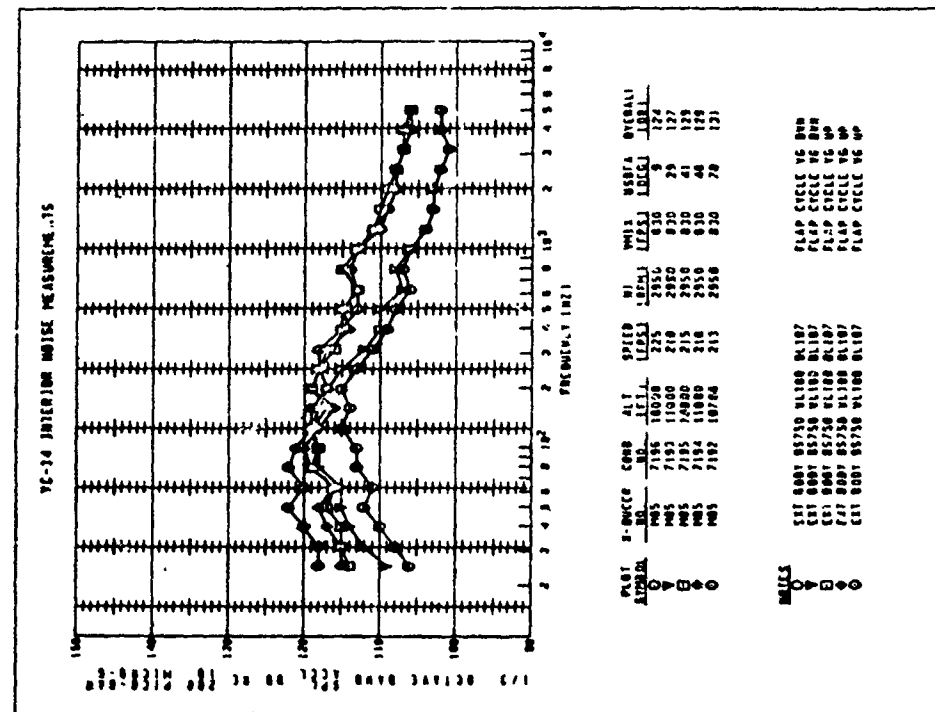


Figure A-30 One-Third Octave Spectra, M05, Flap Cycle

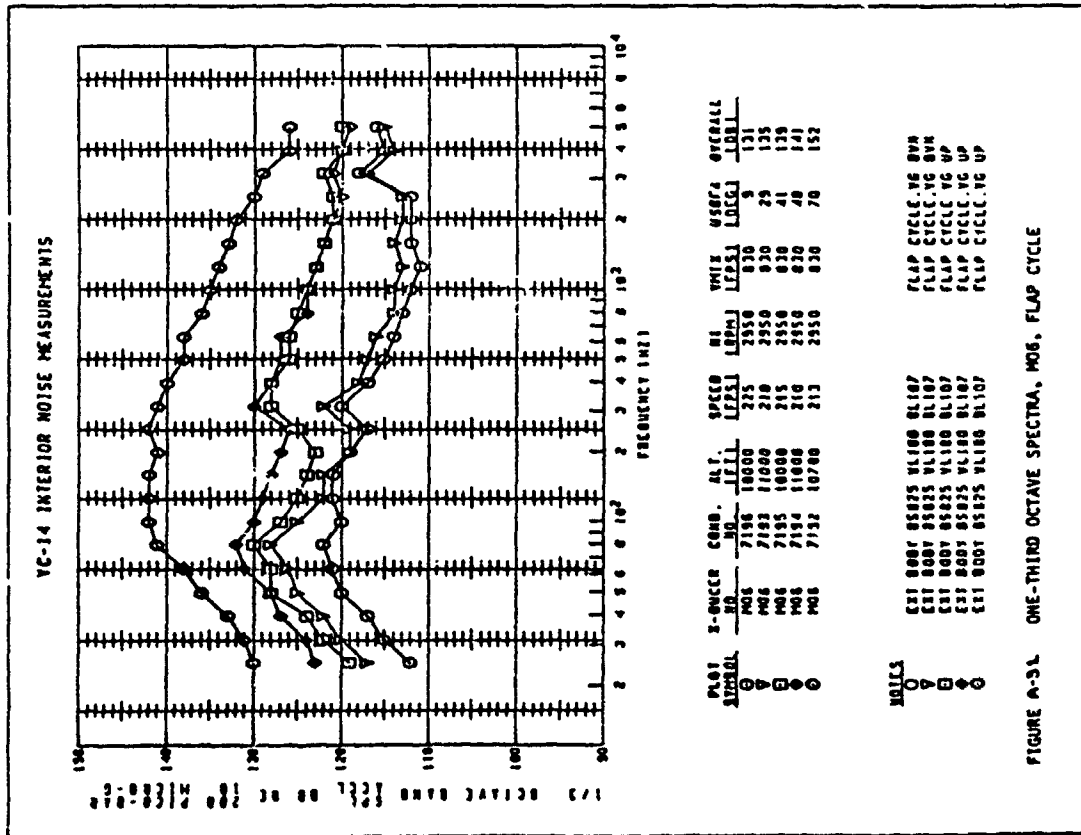


FIGURE A-31 ONE-THIRD OCTAVE SPECTRA, M06, FLAP CYCLE

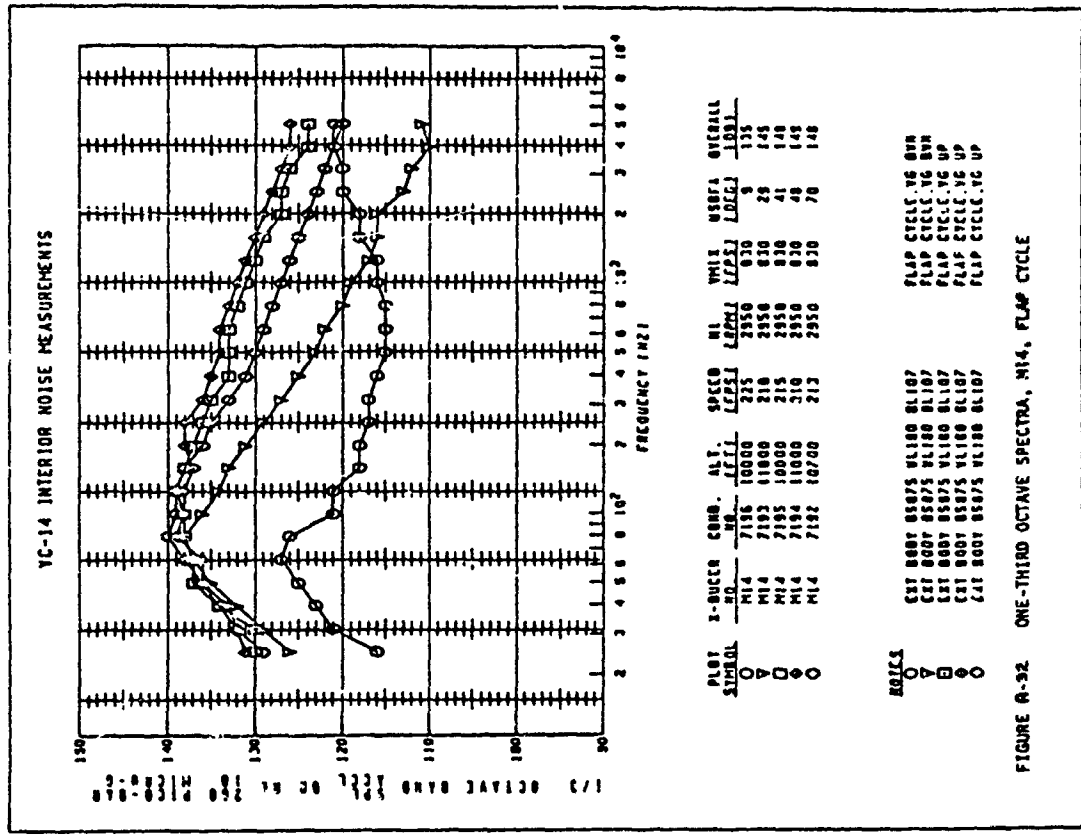
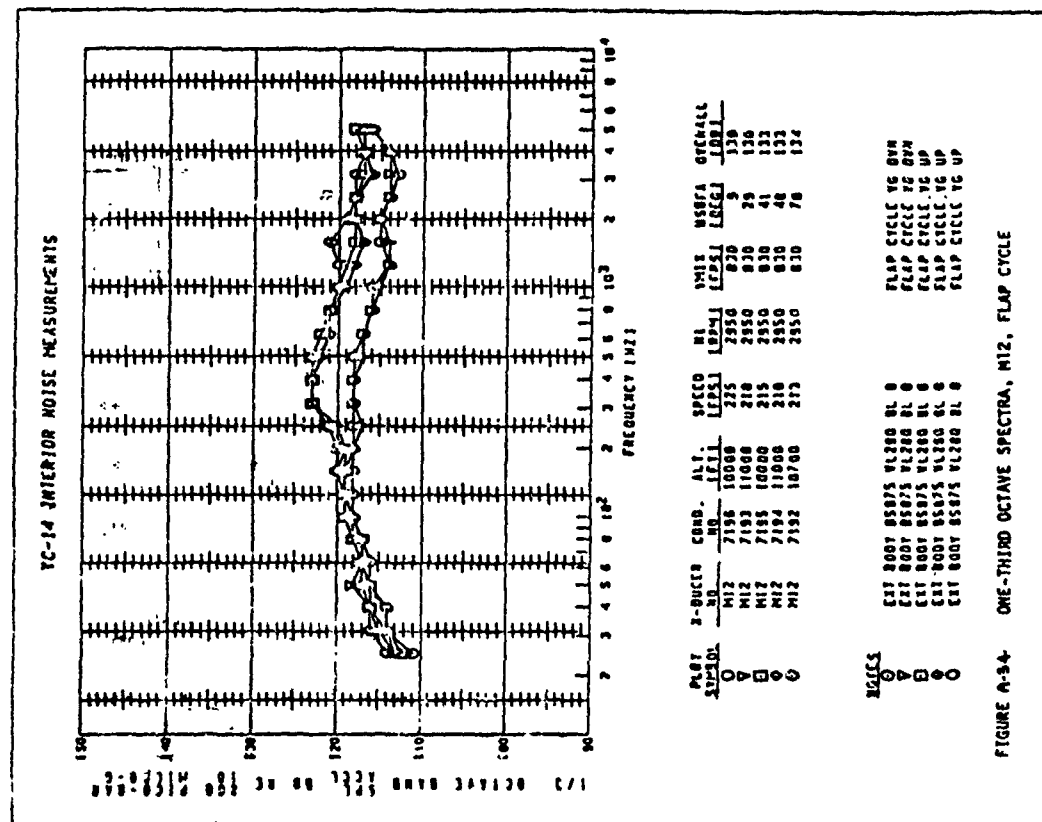
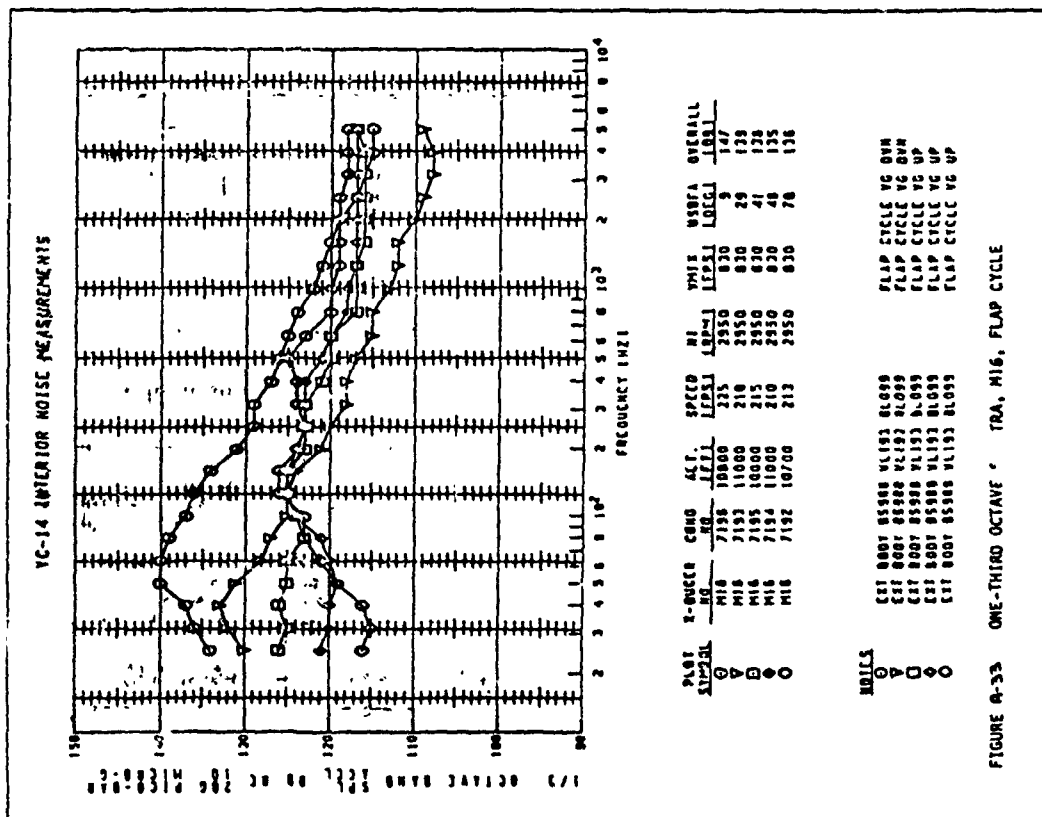
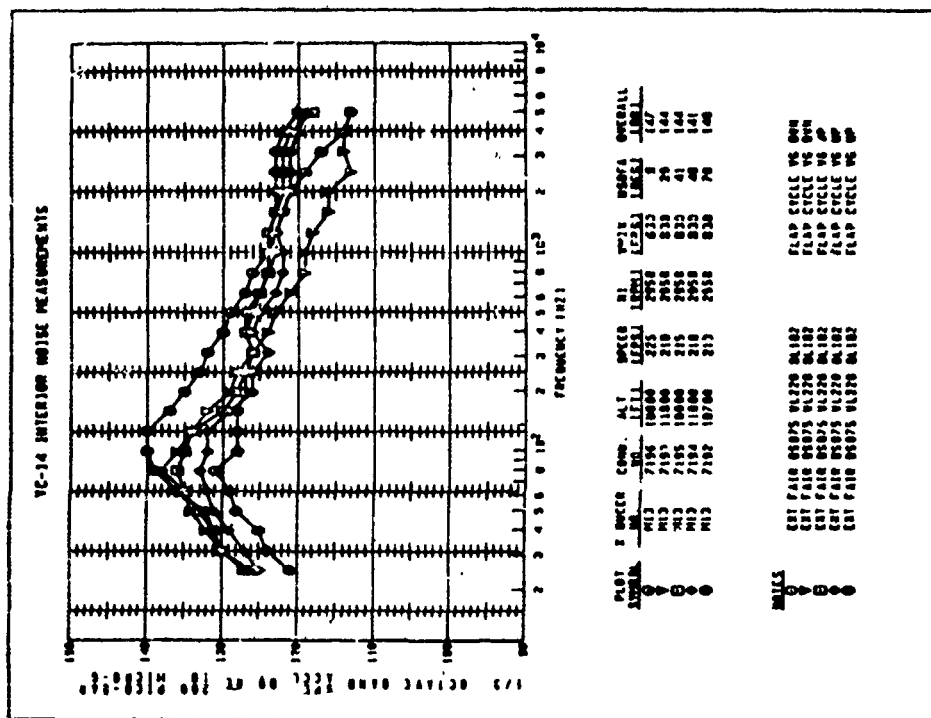
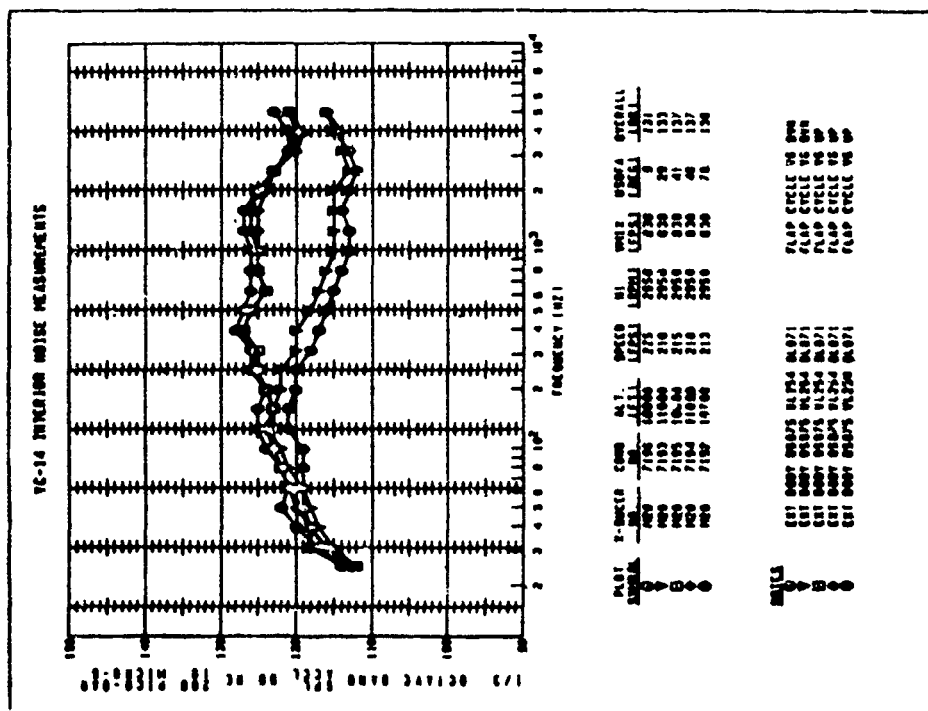


FIGURE A-32 ONE-THIRD OCTAVE SPECTRA, M14, FLAP CYCLE





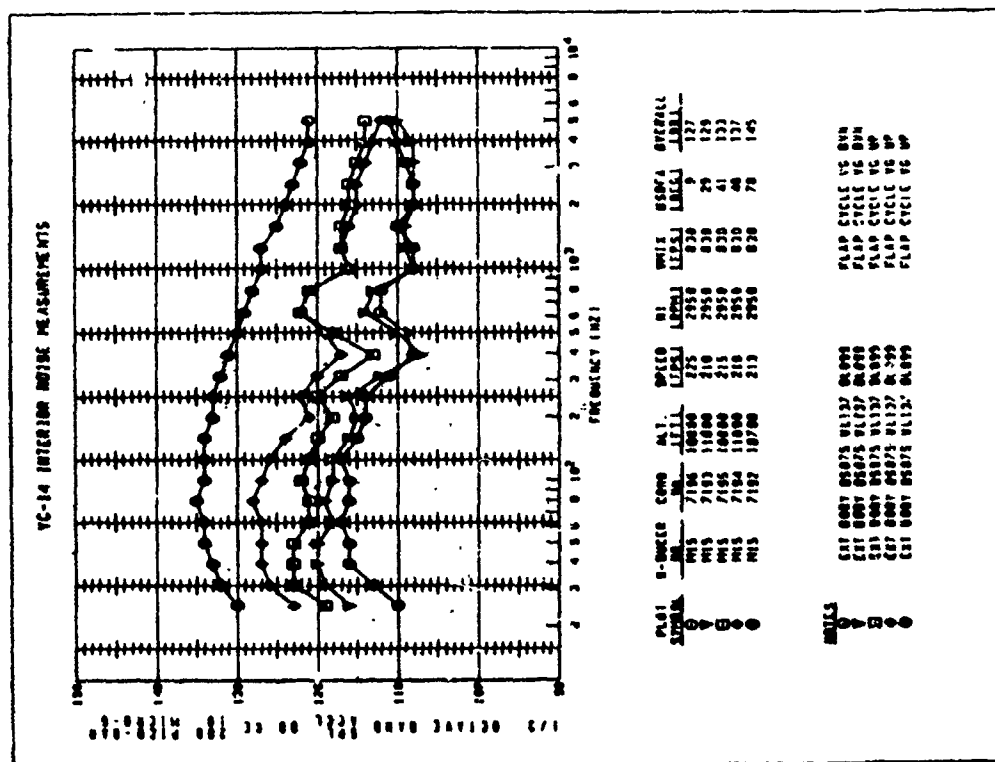


Figure A-37 One-Third Octave Spectra, M15, Flap Cycle

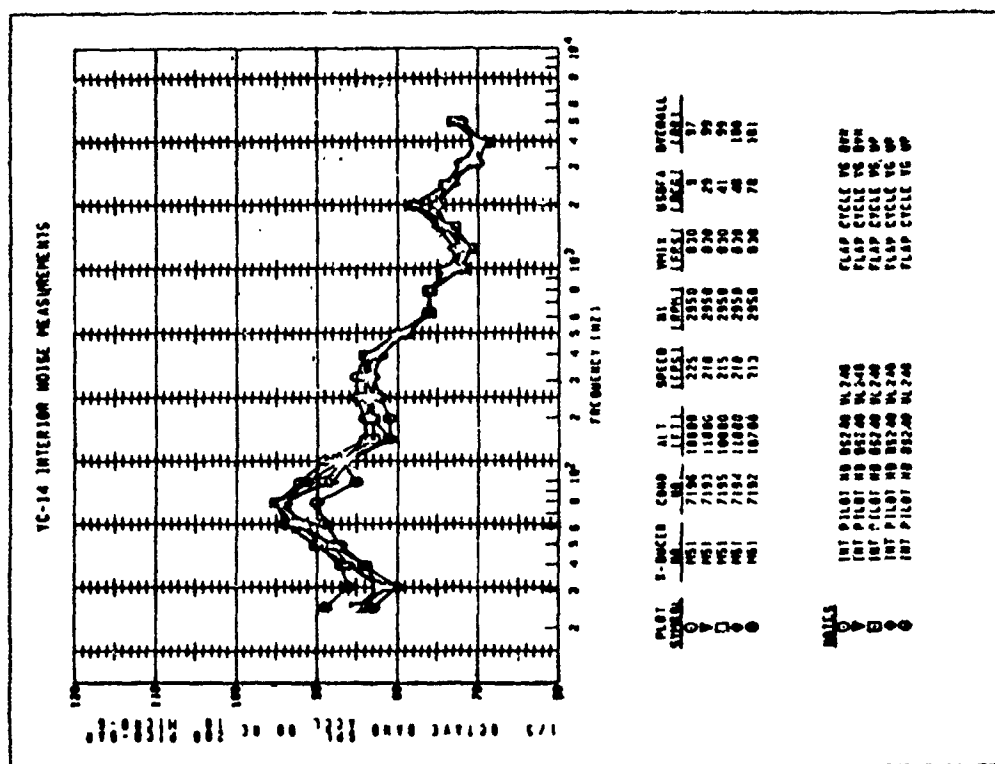
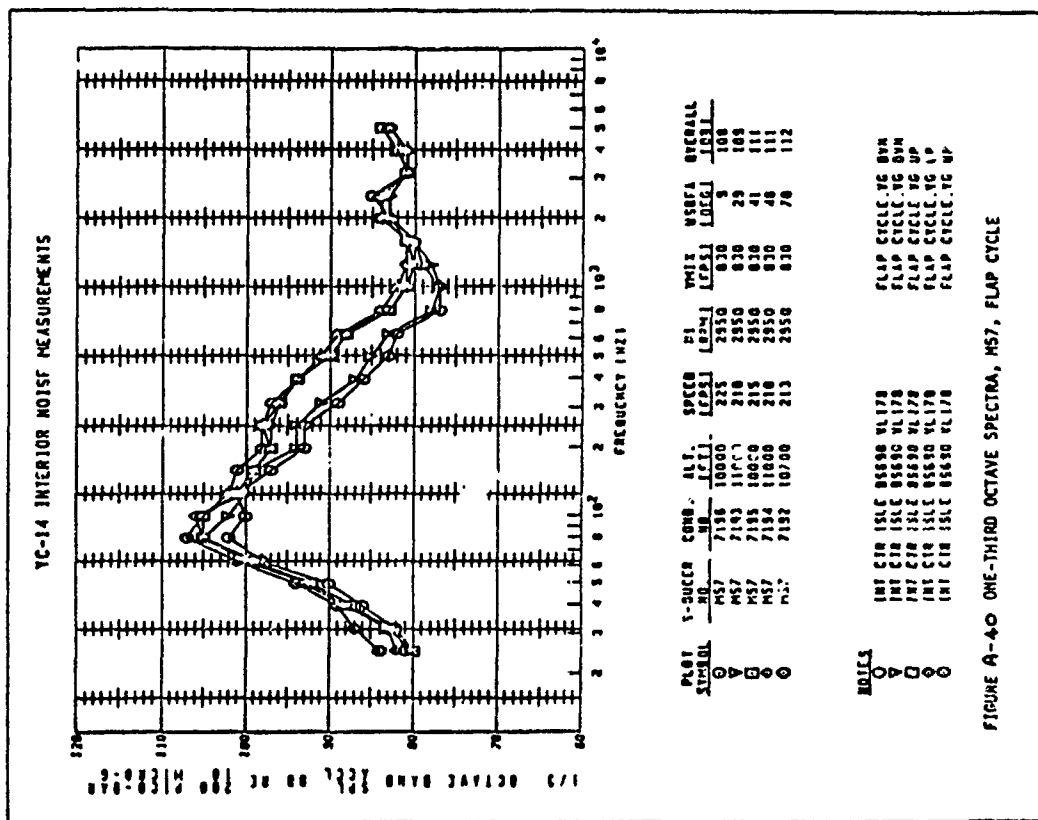
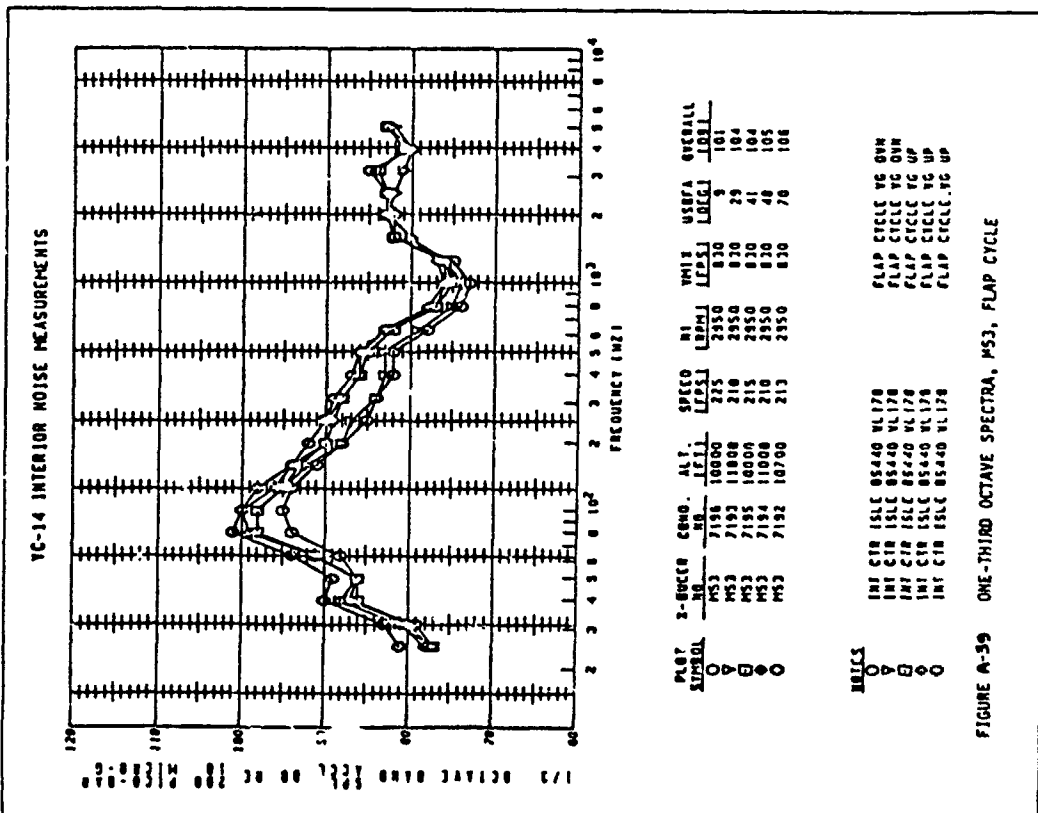
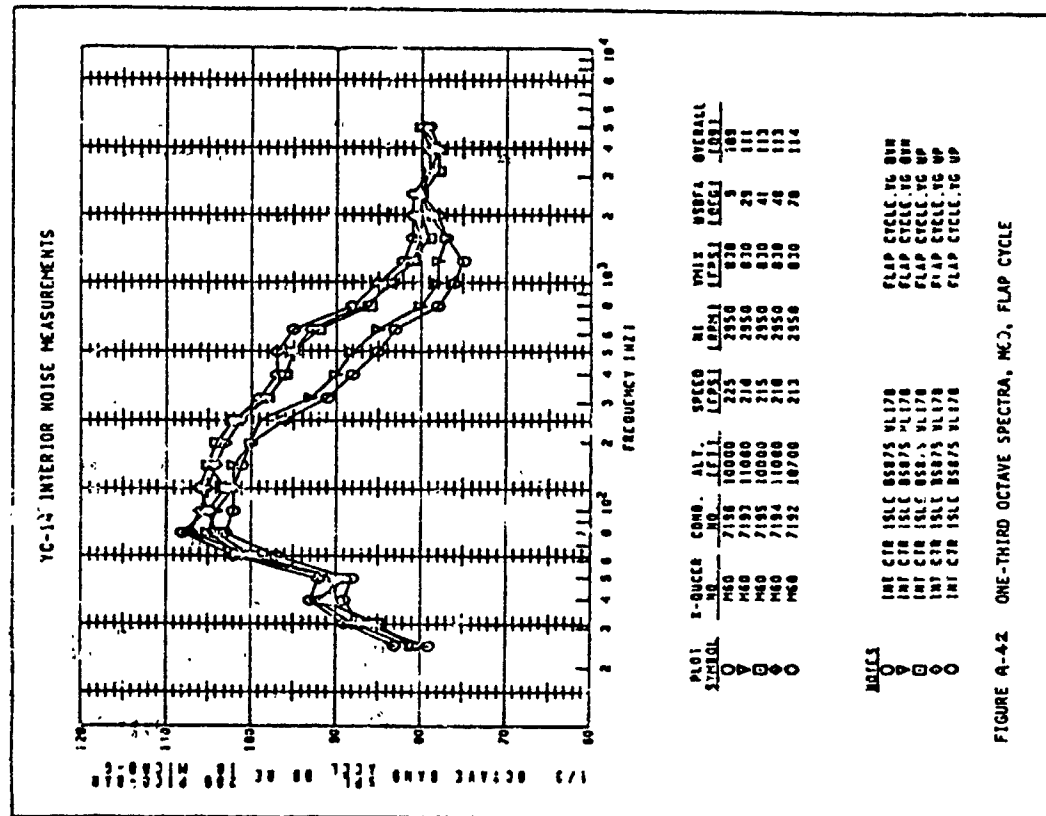
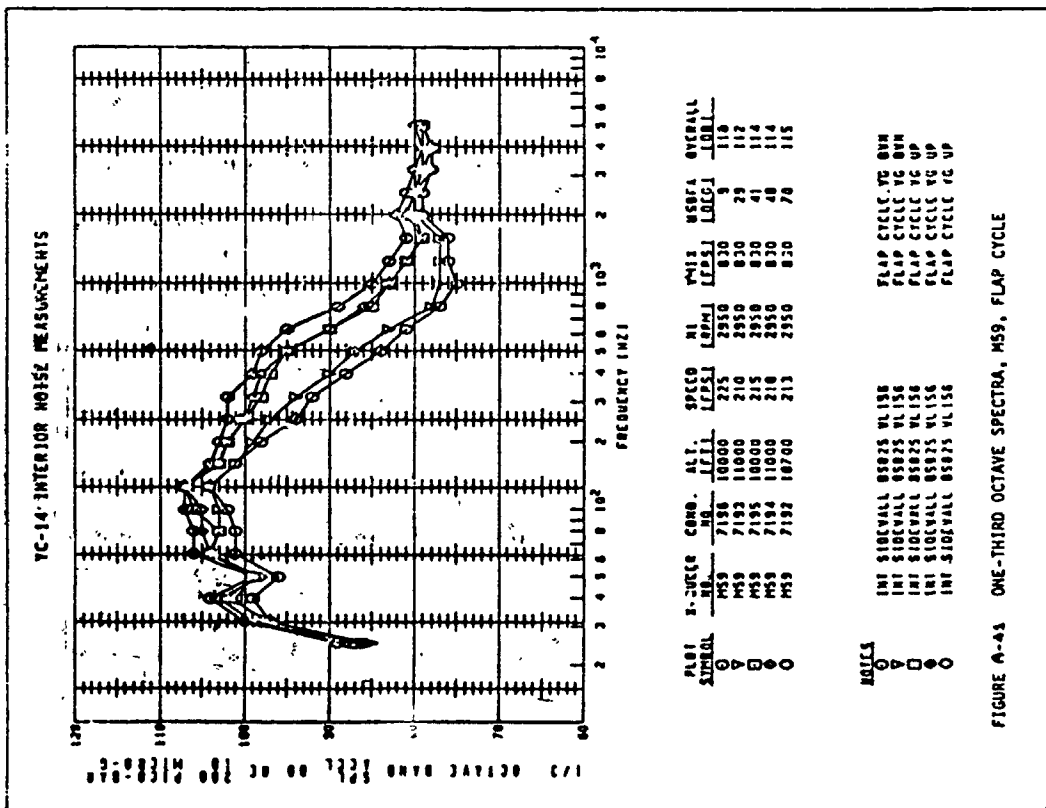


Figure A-38 One-Third Octave Spectra, M51, Flap Cycle





A review of these figures suggests that:

- For M3, M5, and M6 (except with USBs at 70°), which are all below and/or forward of the trailing edge of the USB flap system, noise in the bands below about 125 Hz appears to increase smoothly as the USB flaps are deployed, while noise in the bands above about 250 Hz increases when the VGs are raised.
- For M12 and M20, which are above and to the rear of the USB flaps, low-frequency noise increases are not observed, but the higher frequency noise increases apparently associated with raising of the VGs are observed.
- For M13, M14, M15, M16 and M6 (with USBs at 70°), which are on the portion of the fuselage over which the engine exhaust sheet sweeps (close to) as the USBs are deployed, the above low- and high-frequency effects are more difficult to assess. Broadband noise changes occur, which appear to be associated with the close approach of the exhaust flow sheet to and/or departure of the flow sheet from the near proximity of the above noted microphones.
- For interior microphones M51, M53, M57, M59, and M60, both low-frequency flap angle position-dependent noise and high-frequency VG position-dependent noise are observed. In the worst case, at the aft end of the troop deck, spectral levels up to the 125 Hz band increase about 5 dB as the flaps are deployed from 0° to 70° . Spectral levels above about the 250 Hz band increase from 3 dB to 10 dB when the VGs are deployed. Note that the low-frequency flap position dependent noise has a strong effect on OASPL, while VG dependent noise has a weaker effect. Just the opposite would be true for PSIL or dBA measures.

A.5 FLIGHT EFFECTS

Changes in exterior and interior noise associated primarily with changes in airplane speed at two very different portions of the YC-14 operating envelope are examined briefly.

- Those observed during high-power, relatively low-speed, accelerating brake-release-to-lift-off-to-climbout operations.
- Those observed with differing stable flight speeds best associated with cruise-style operations.

An extremely important difference between these types of operations is that takeoff is typically done at essentially a fixed high-power engine setting, while at cruise each speed operation is associated with a different power setting. Each power setting is fixed by the requirement of matching engine thrust to airplane drag.

Note also that during takeoff operations, the USB nozzle door is always open, outboard (but not USB) flaps are deployed, the landing gear are down at least through lift-off, and the cabin is typically unpressurized. By comparison, during cruise style operations, the USB nozzle door is closed, outboard flaps as well as USB flaps and landing gear are fully retracted, and at altitudes above about 7,000 ft the cabin pressurization system is in operation.

The reader should keep in mind, as he reviews high-power/low-speed OASPL data and subsequent one-third octave spectral data, that there are perhaps two other parameters in addition to forward speed that traditionally can effect exterior and interior noise. These are the position of the ground relative to the airplane, and the status of the landing gear, up or down. All three change radically during takeoff. In addition, airplane attack angle increases significantly at rotation (lift-off). The OASPL data presented does not offer much clarification as to how much of the observed noise changes is associated with the change in each of these parameters.

Figures A-43 through A-51 show one-third octave spectra for exterior microphones M3, M5, M6, M14, and M16, which are distributed along the side of the fuselage; and for M12, M20, M13, M14, and M15, which are distributed circumferentially.

Low-frequency noise levels up to about 200 Hz decrease with increasing airplane speed at microphones M13 and M16. These microphones experience the highest levels and, from previous discussions, would appear to be closest to the exhaust flow sheet stream. There also is a distinctive reduction in this frequency range that appears to be associated with motion away from the ground plane. Above 200 Hz, level reductions appear to relate strictly to motion away from the ground plane and/or retraction of the gear.

For the other microphones, levels roughly decrease inversely to frequency, with the greatest decreases occurring at the low frequencies. Above perhaps 500 Hz, there is often a slight increase in spectral levels with airplane speed. Apparent reductions that track with motion away from the ground and/or retraction of the landing gear are not obvious.

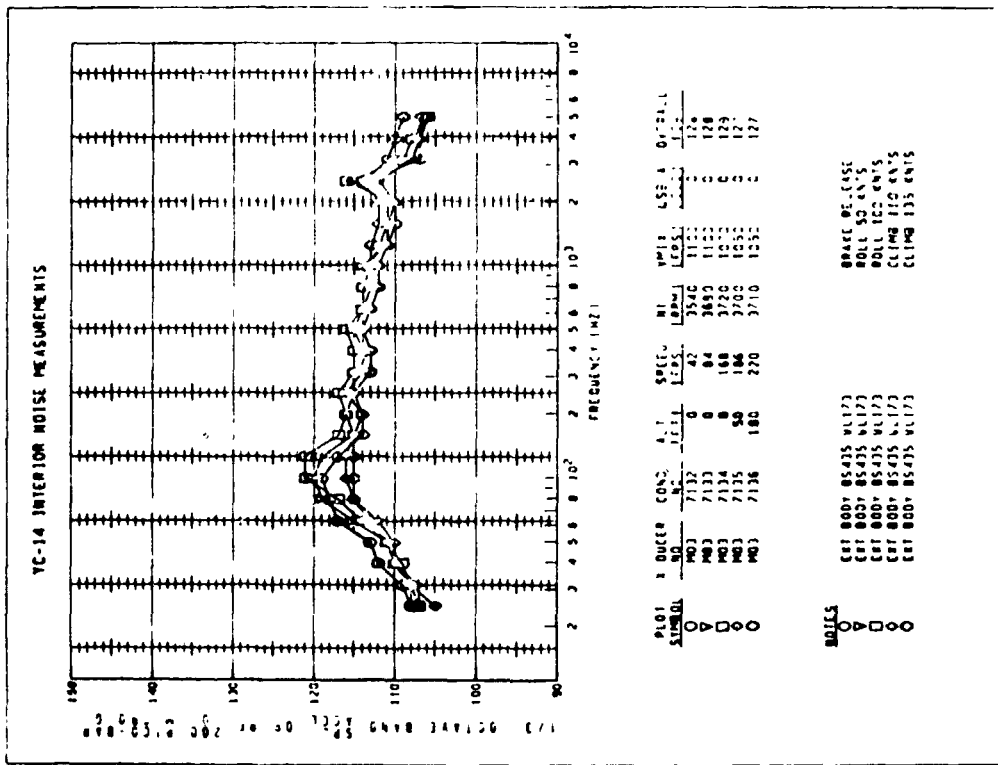


Figure A-43 One-Third Octave Spectra, M03, Takeoff

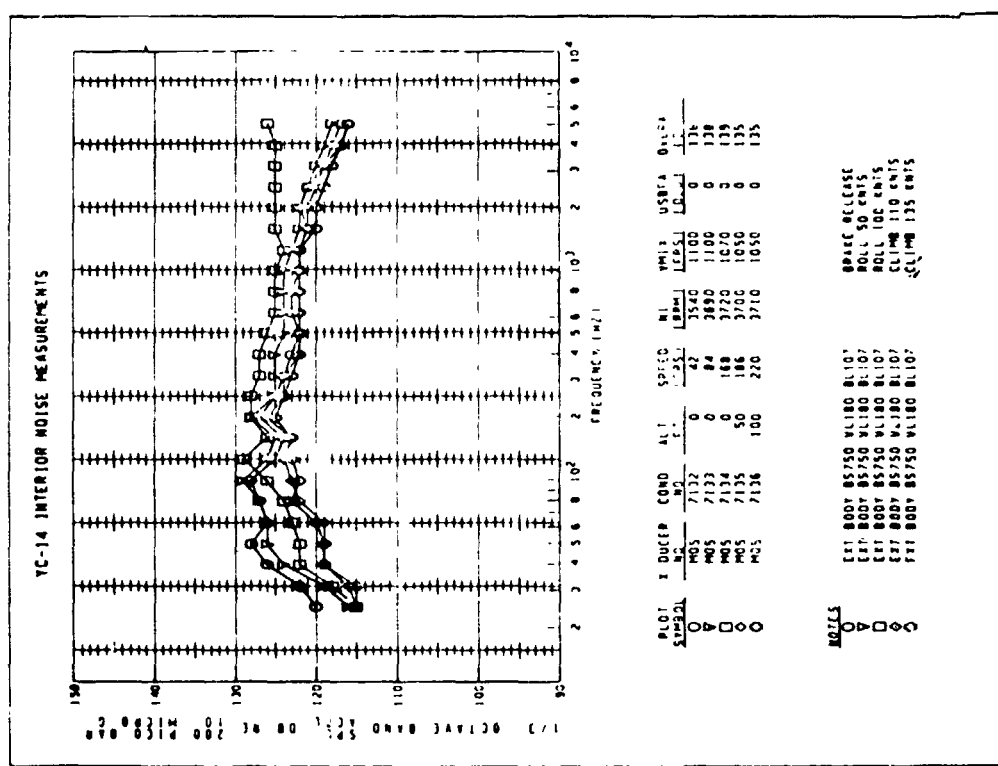


Figure A-44 One-Third Octave Spectra, M05, Takeoff

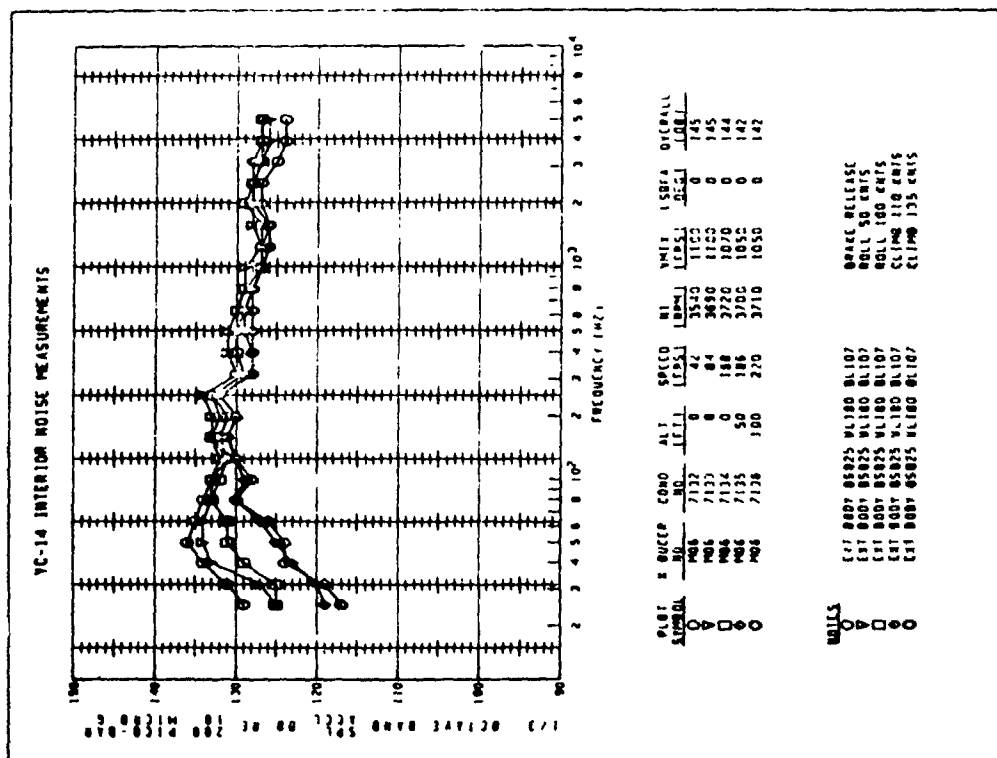


Figure A-45 One-Third Octave Spectra, M06, Takeoff

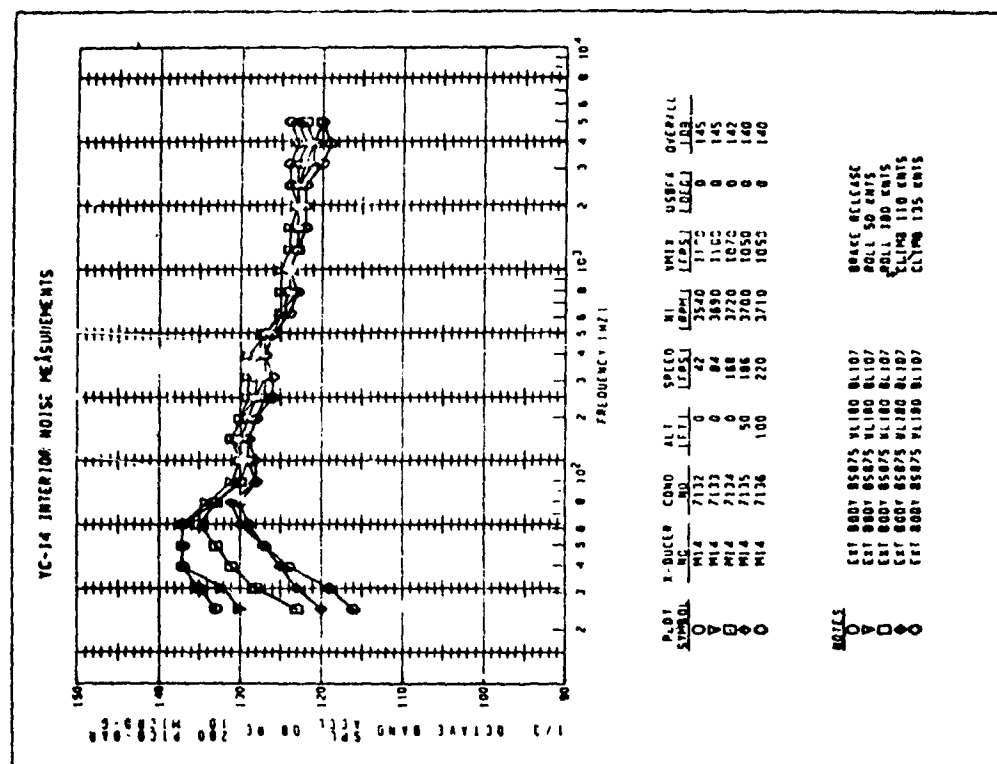


Figure A-46 One-Third Octave Spectra, M14, Takeoff

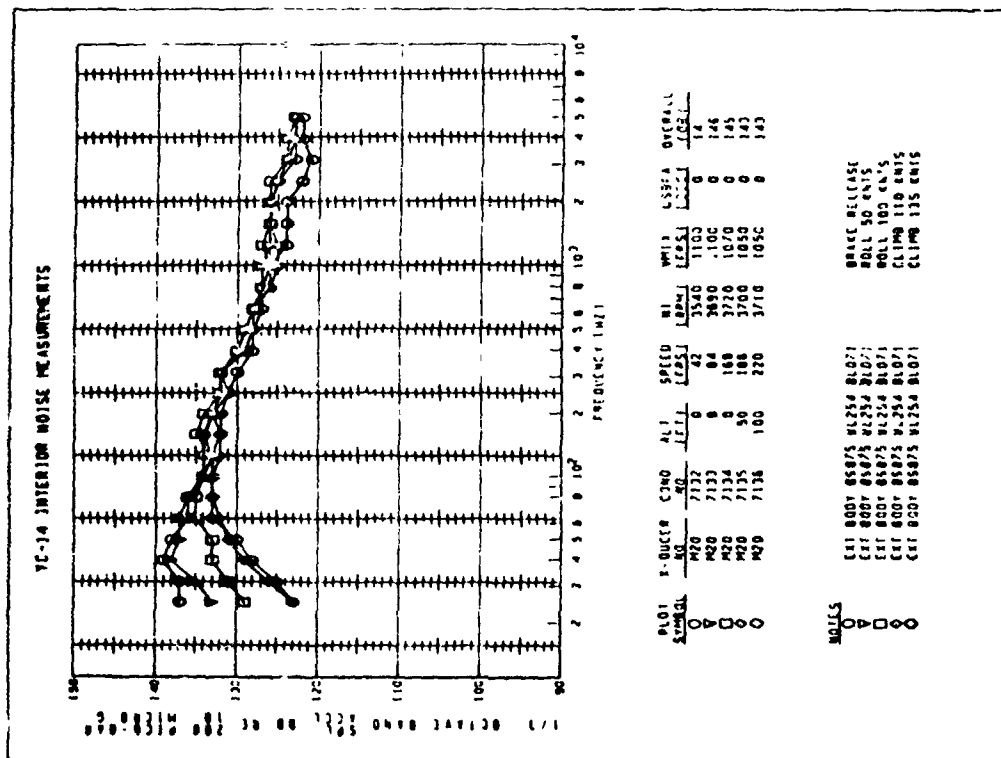


Figure A-49 One-Third Octave Spectra, M20, Takeoff

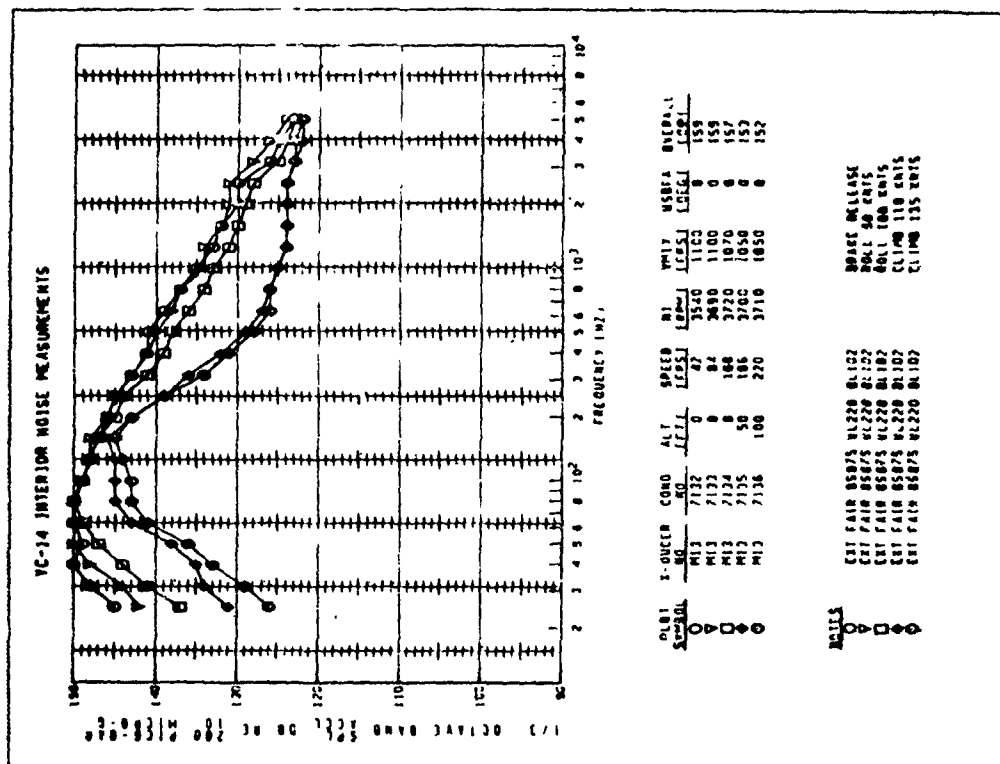


Figure A-50 One-Third Octave Spectra, M13, Takeoff

Figures A-52 through A-56 present spectra for interior microphones M51 on the flight deck, and for M53, M57, M59, and M60 distributed from front to back of the troop compartment. In the front of the airplane, significant reductions are limited to frequencies below about 500 Hz. However, as one moves toward the aft end of the troop compartment, the reductions can be seen to extend over the whole analyses spectrum; i.e., up to 5000 Hz. Note that on the exterior, reductions in the high-frequency portion of the spectrum occur only at M13 and M16.

For cruise type (stable speed) conditions, Figures A-57 and A-58 show respectively exterior and interior OASPL distributions for four level flight conditions and a flight idle condition.

Figures A-59 through A-67 show one-third octave band spectra for various exterior microphones. Other than the fact that all curves are essentially smooth, a consistent pattern relatable to either body position or dynamic pressure, etc., has as yet not been identified.

Figures A-68 through A-72 show one-third octave band spectra for various interior microphones. Variations with dynamic pressure become more noticeable as one moves aft. Note also the increasing activity in the 30 Hz, 40 Hz, and 50 Hz bands as one moves aft. Finally, recall that ambient noise from air conditioning, pressurization, hydraulic systems, etc., appears to influence interior noise levels, particularly on the flight deck during cruise operations. Curves in Figure A-68 should be viewed with this consideration in mind.

One of the results expected to show up easily in spectra for the various cruise-like conditions considered was an indication of the importance of engine noise relative to turbulent boundary layer noise. If such information is there, it has yet to be sorted out. Further work on this matter is felt to be most essential.

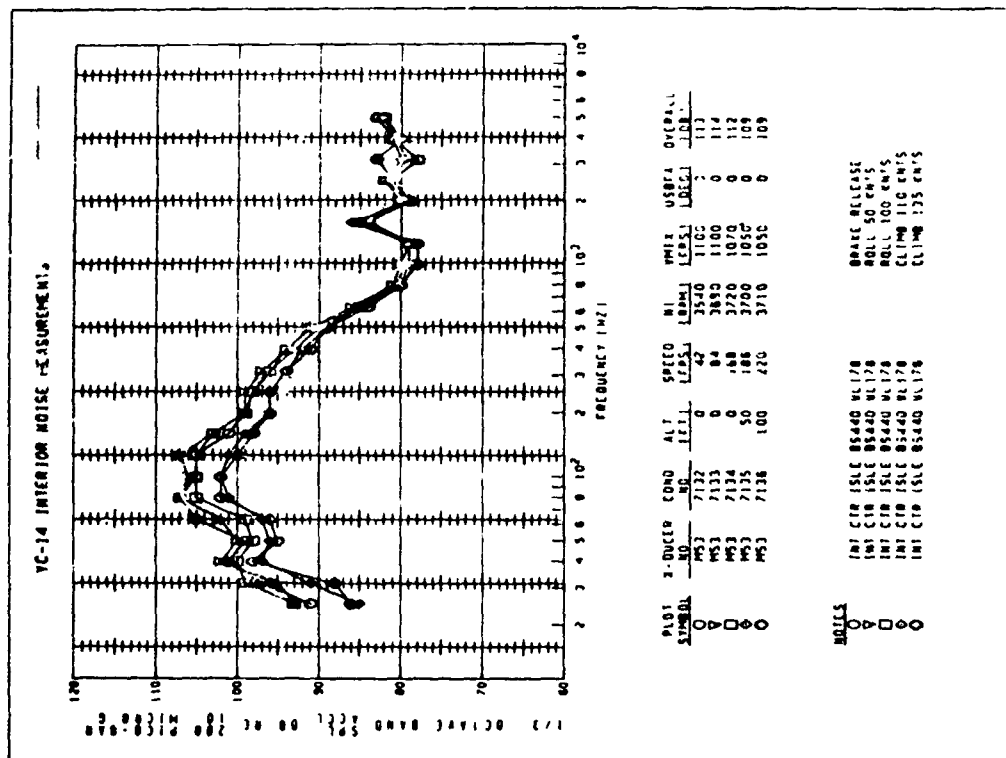


Figure A-53 One-Third Octave Spectra, M53, Takeoff

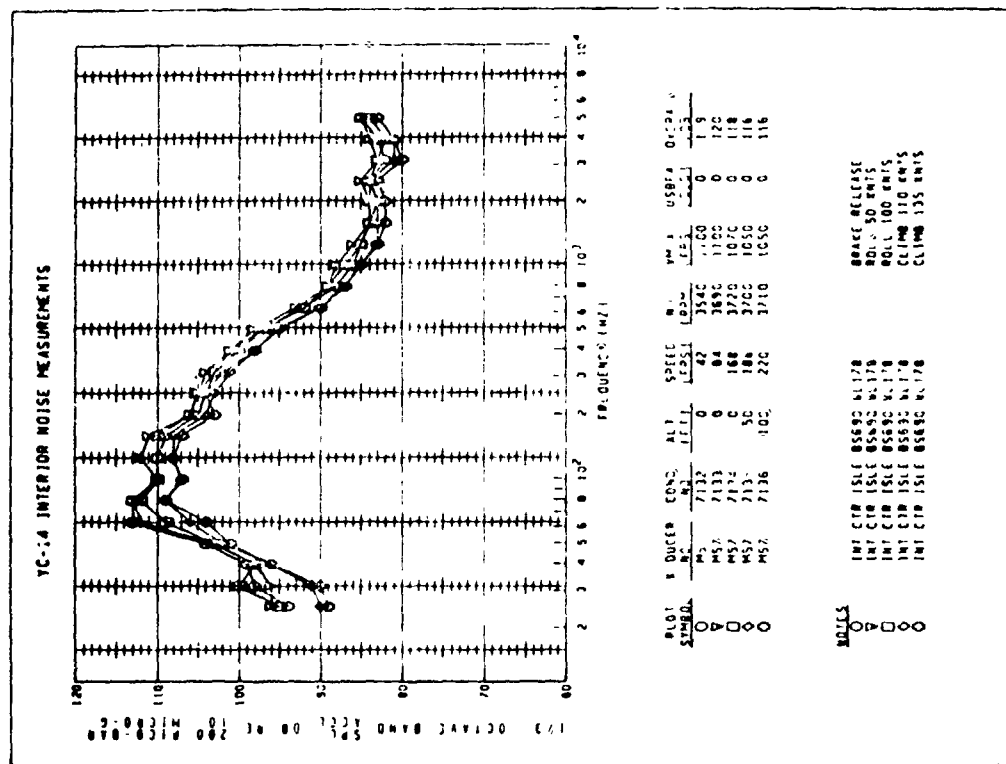


Figure A-54 One-Third Octave Spectra, M57, Takeoff

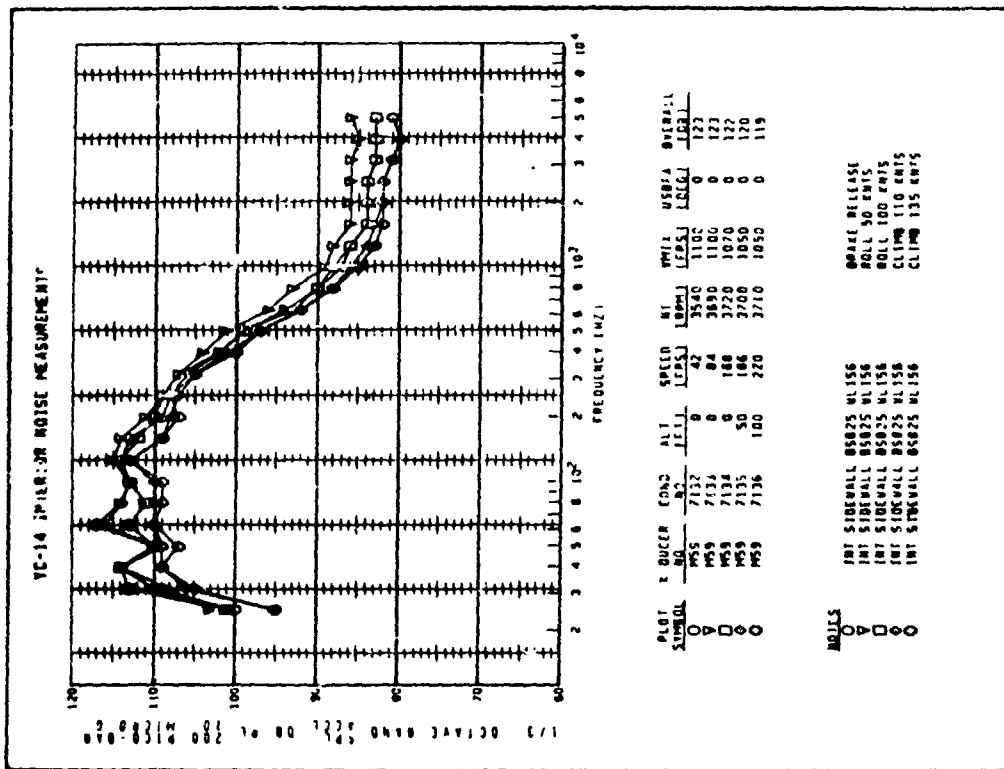


Figure A-55 One-Third Octave Spectra, M59, Takeoff

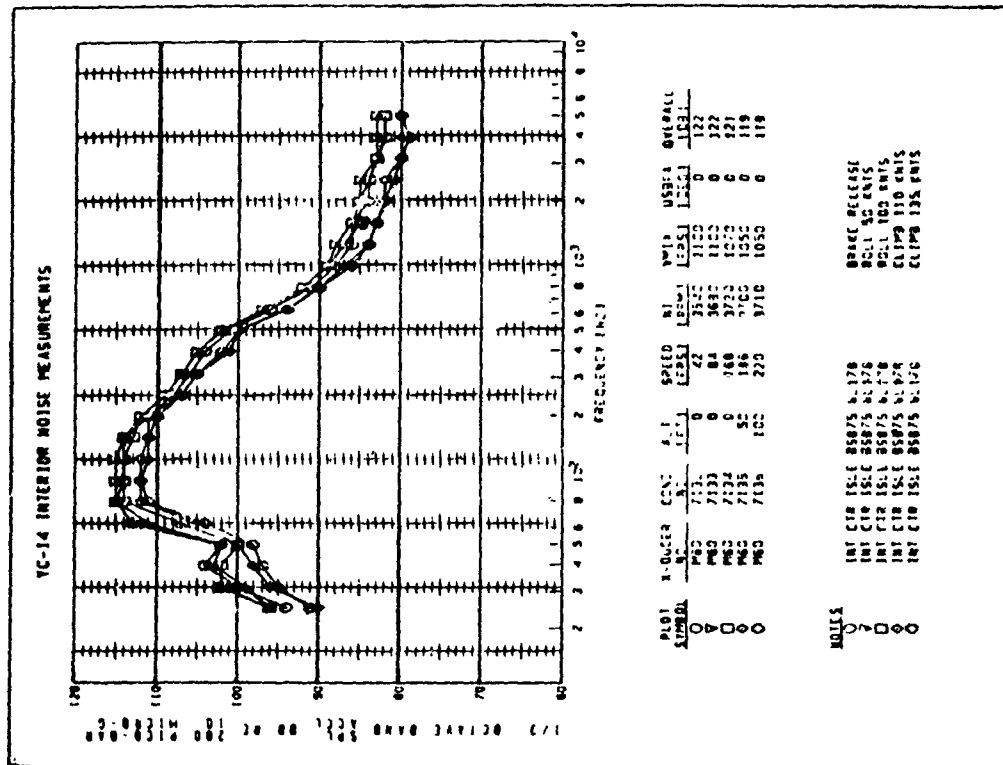


Figure A-56 One-Third Octave Spectra, M60, Takeoff

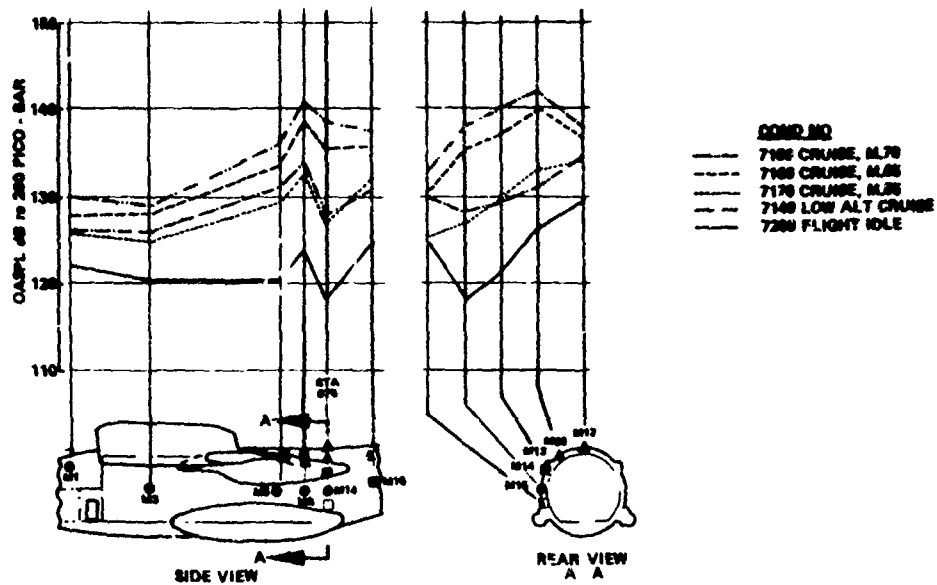


Figure A-57 Variation of External Fuselage OASPLs with Cruise Condition

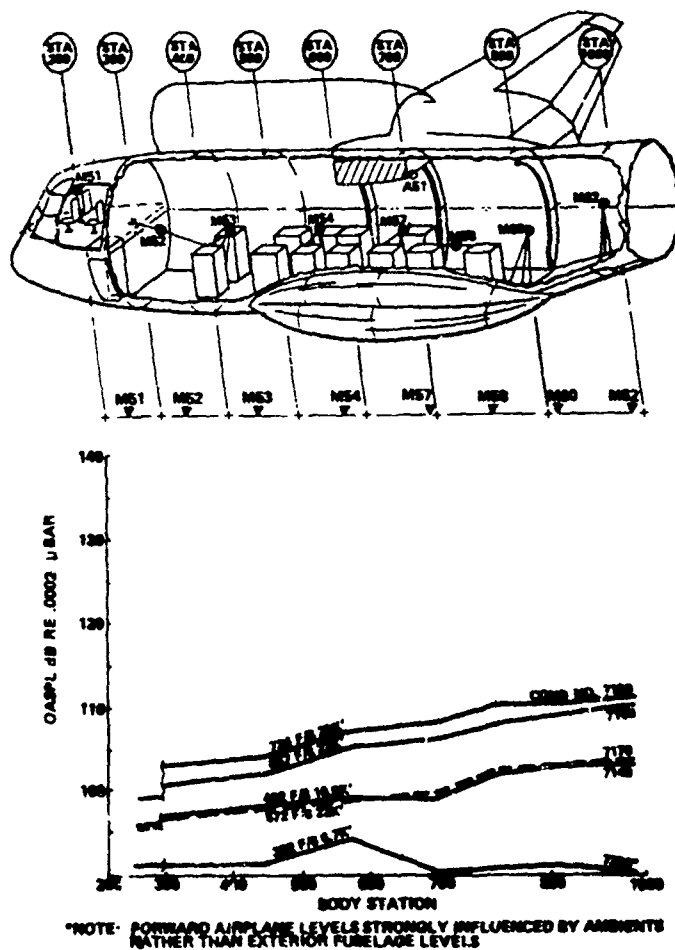


Figure A-58 Variation of Cabin OASPLs with Cruise Condition

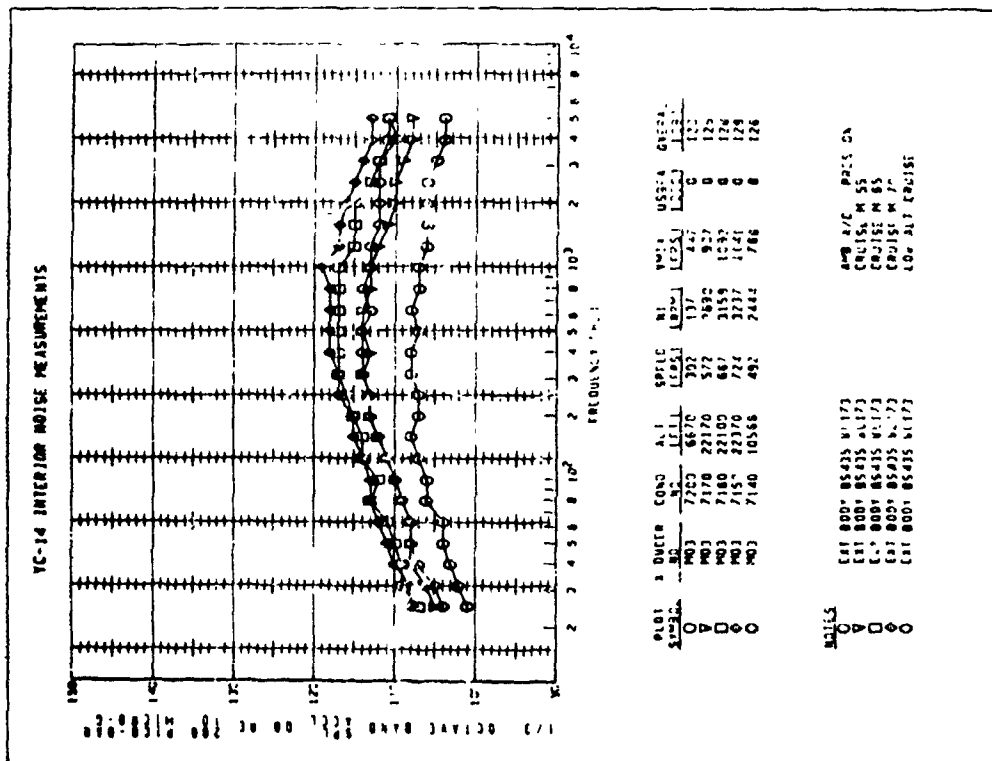


Figure A-59 One-Third Octave Spectra,
M03, Cruise Type Conditions

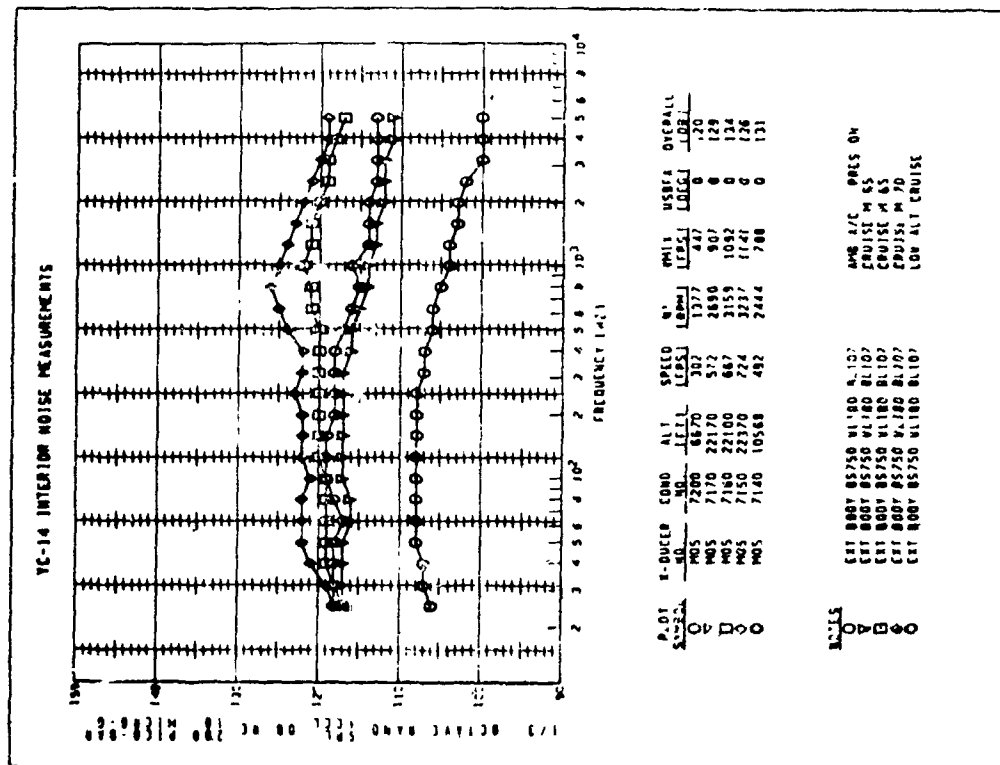


Figure A-60 One-Third Octave Spectra,
M05, Cruise Type Conditions

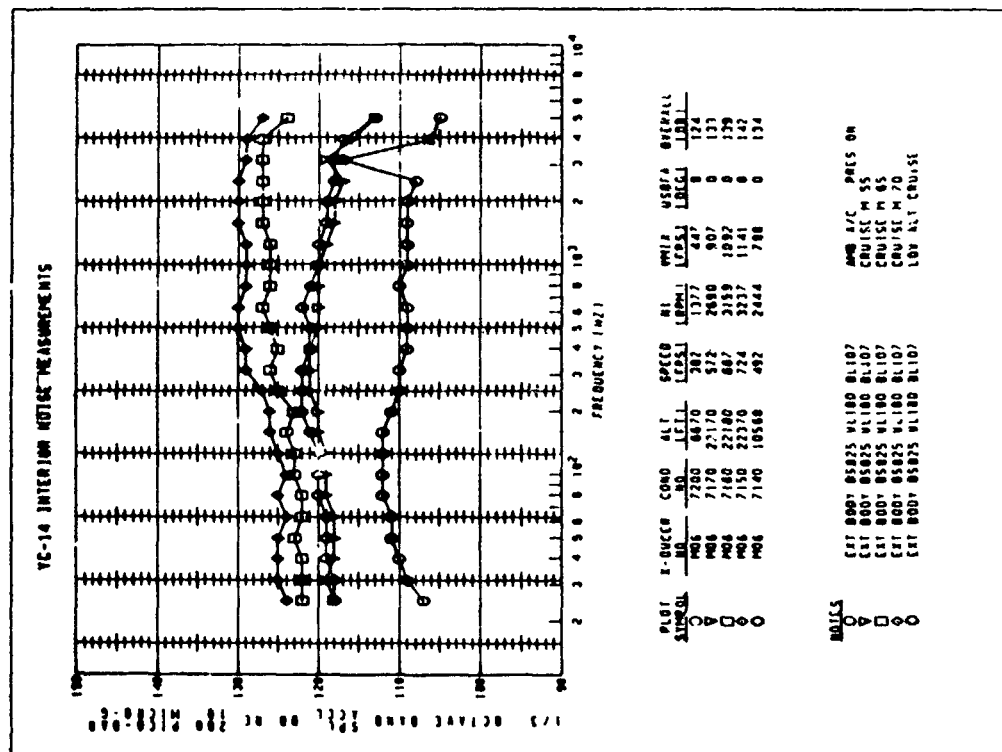


Figure A-61 One-Third Octave Spectra,
M06, Cruise Type Conditions

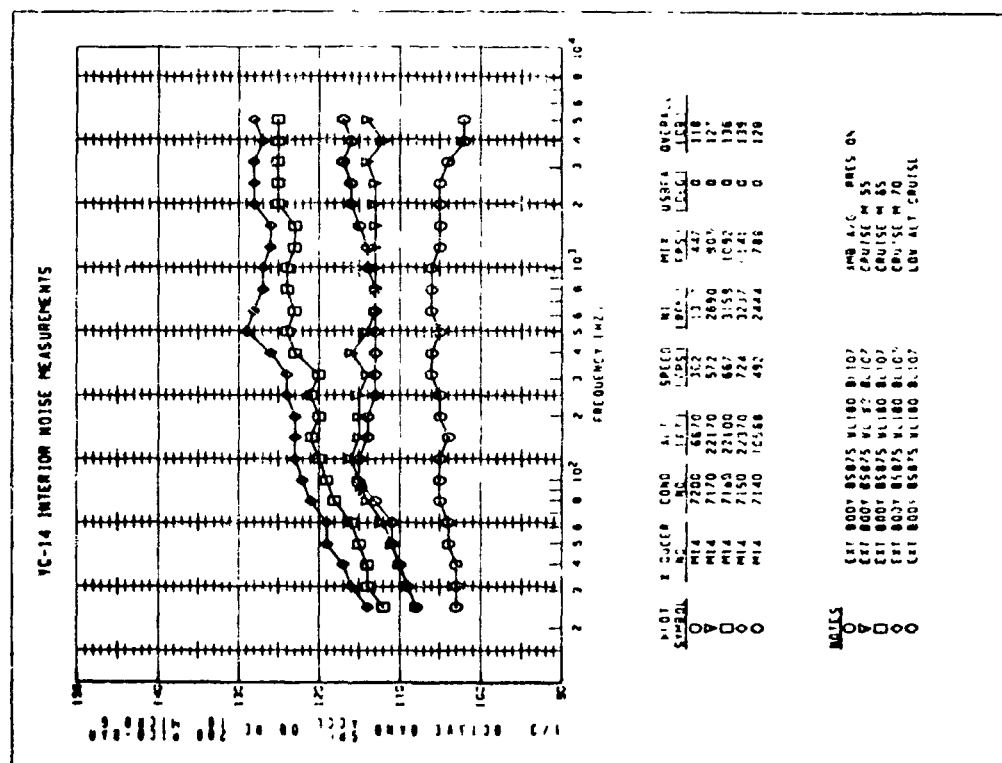


Figure A-62 One-Third Octave Spectra,
M14, Cruise Type Conditions

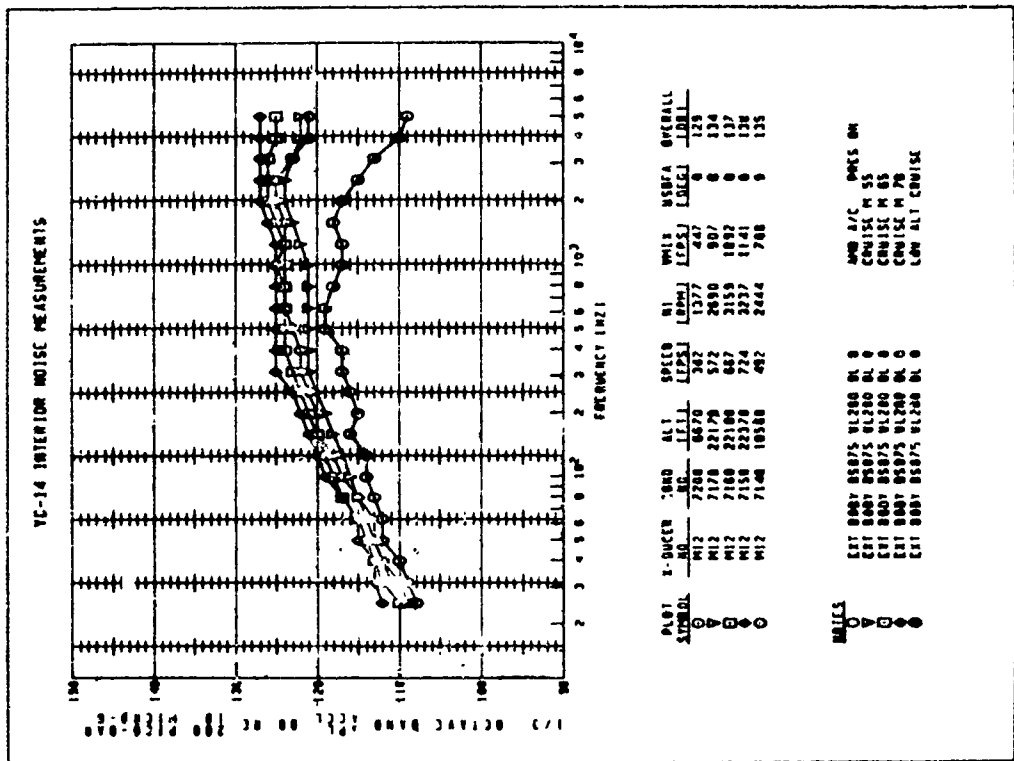


Figure A-64 One-Third Octave Spectra,
M12, Cruise Type Conditions

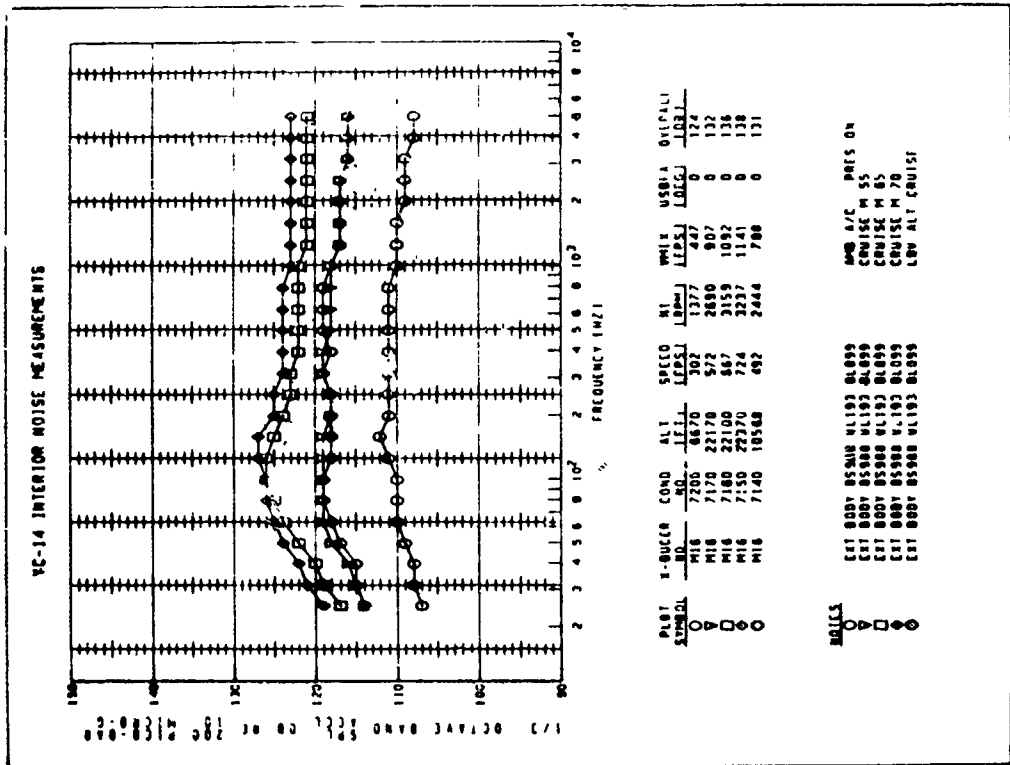


Figure A-63 One-Third Octave Spectra,
M16, Cruise Type Conditions

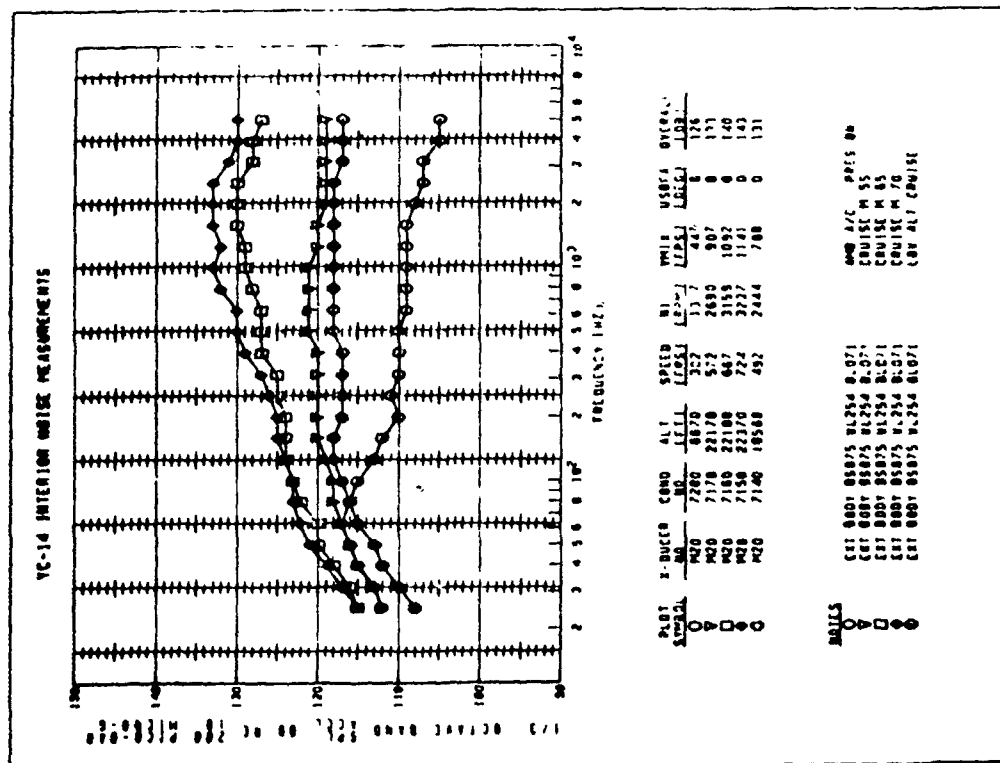


Figure A-65 One-Third Octave Spectra,
M20, Cruise Type Conditions

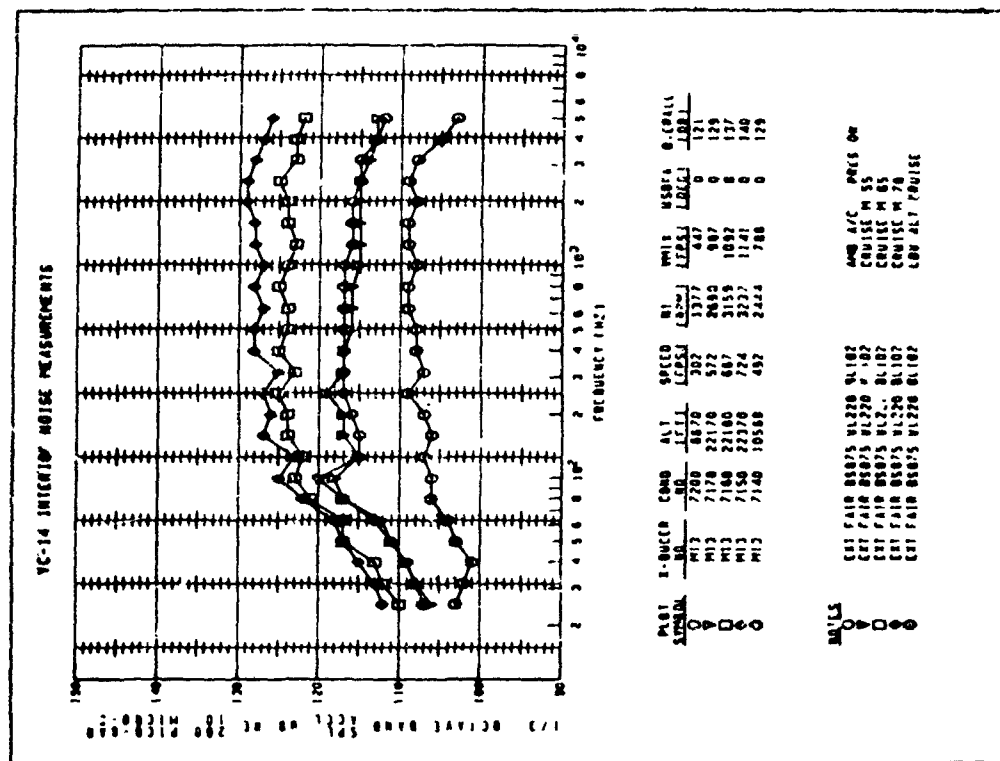


Figure A-66 One-Third Octave Spectra,
M13, Cruise Type Conditions

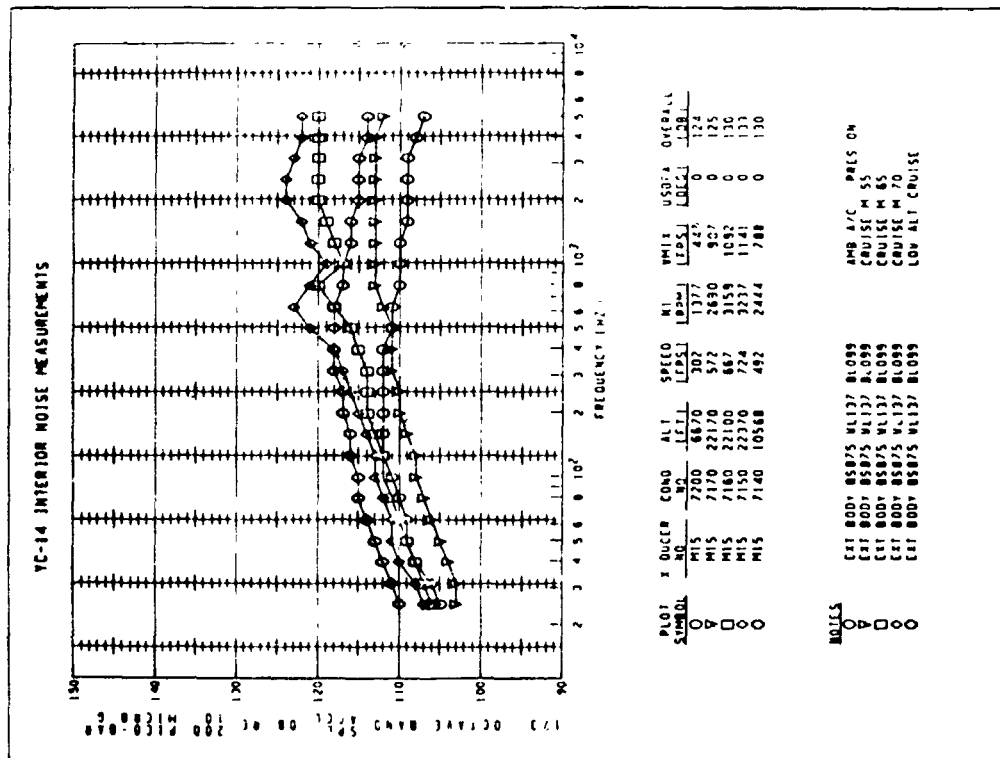


Figure A-67 One-Third Octave Spectra,
M15, Cruise Type Conditions

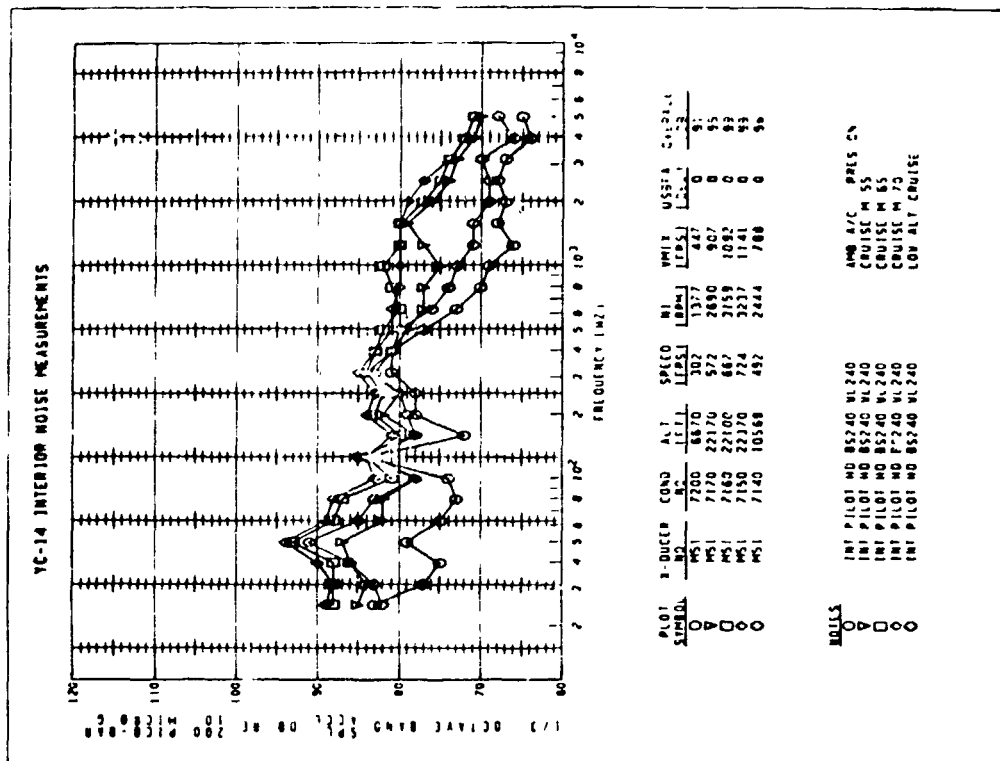


Figure A-68 One-Third Octave Spectra,
M51, Cruise Type Conditions

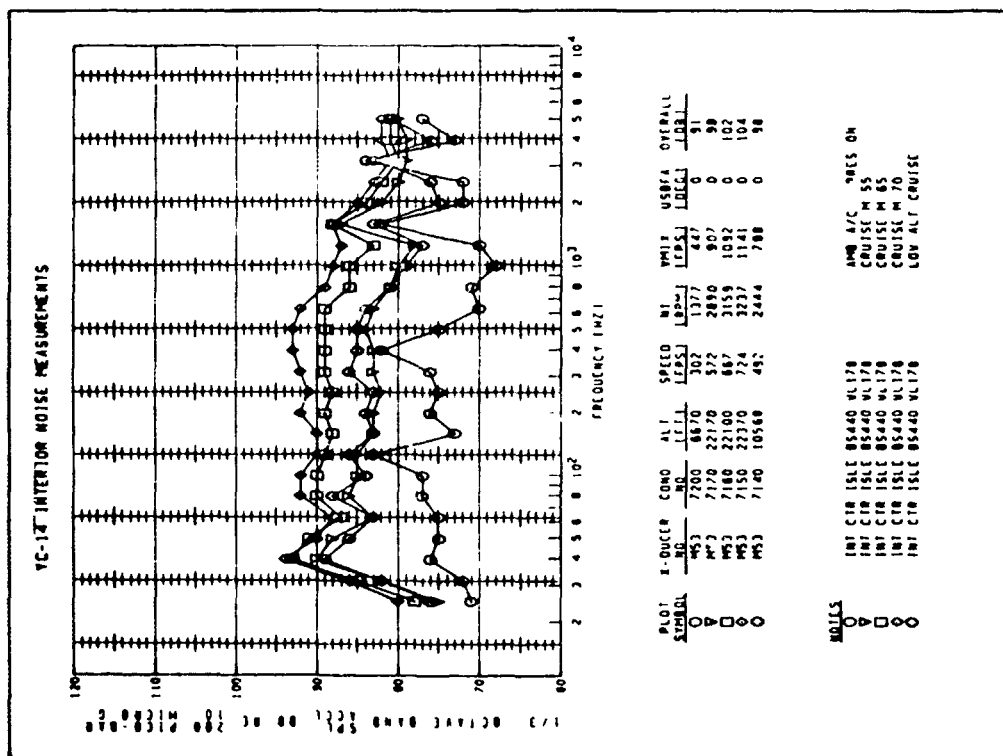


Figure A-69 One-Third Octave Spectra, M53, Cruise Type Conditions

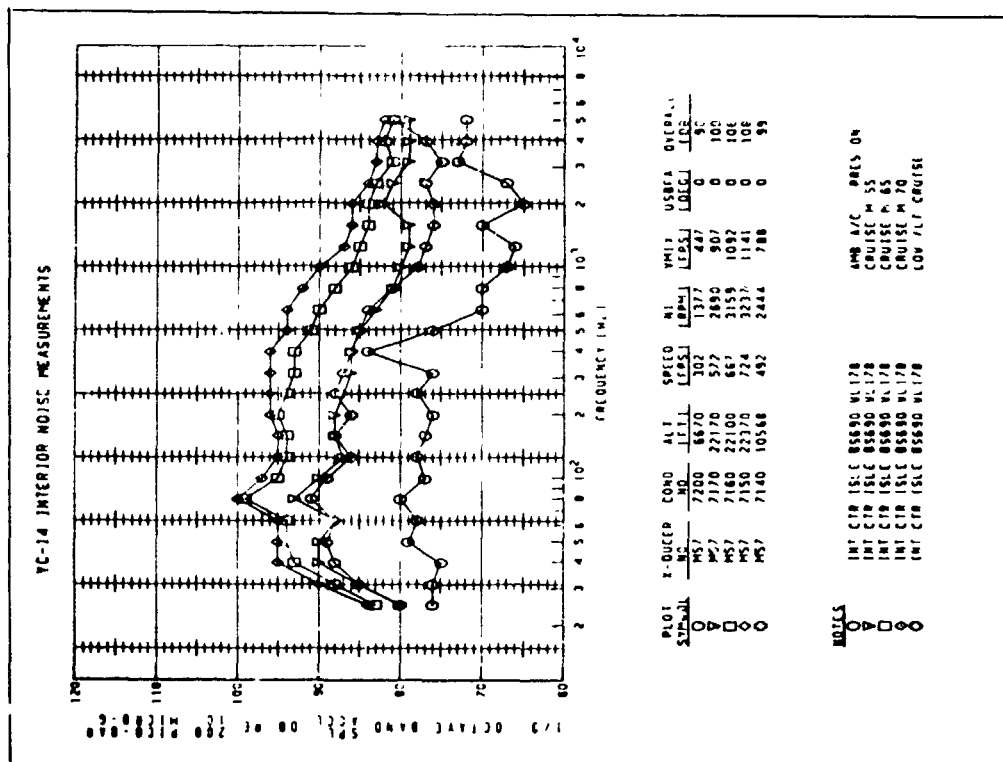


Figure A-70 One-Third Octave Spectra, M57, Cruise Type Conditions

A.6 COMPARISON WITH PREDICTIONS

During the last half of 1975, in response to estimates published by NASA (Reference 2) and by AFFDL (Reference 3), an improved set of estimates for the YC-14 was developed at Boeing (Reference 1). Octave band estimates for both exterior and interior noise levels at climbout, cruise, STOL approach, and maximum noise portion of go-around were formulated. The interior estimates were for the aft troop deck center aisle in the vicinity of station 860.

As a result of the current test program, data have become available for simply checking at least the interior noise estimates for climbout and almost as simply at cruise. To this end, comparisons with predictions for these two conditions are shown on Figures A-73 and A-74. One-third octave data, converted to octave band format for microphone M60 located on the center aisle of the aft troop deck at station 860, are used in both figures.

With regard to climbout (Figure A-73), condition 7130 data appear to be most appropriate. The airplane was at 3,500 ft, traveling at 160 knots with engines at full power ($N_1 = 3800$ RPM). For the climbout estimate in Reference 5, the airplane was taken to be at 5,000 ft, at a speed of 270 knots with engines at full power. As can be seen, measured levels fall below estimated levels for the first two bands. Estimate and measurement essentially agree at the 125 Hz, 250 Hz, and 500 Hz bands. For the higher bands, measured values exceed estimated values, due to lack of insulation in the cargo ramp doors and/or ambient equipment noise effects.

With regard to cruise, condition 7150 data (Mach 0.70, 22,000 ft cruise) come closest to the conditions of the cruise estimate. For the estimate in Reference 1, the airplane was taken to be cruising at Mach 0.70 at 33,000 ft, rather than 22,000 ft. Using the method of Reference 1, the estimate shown corresponding to 22,000 ft was obtained by increasing the estimate at 33,000 ft by 3 dB. This increase is equal to 20 LOG_{10} of the ratio of the air density at 22,000 ft to that at 33,000 ft.

As can be seen in Figure A-74, agreement between Boeing estimates and measured levels is very good up through the 250 Hz band. For the higher frequency bands, measured levels exceed estimated levels. Again, these differences are likely to be due to lack of insulation in the cargo ramp doors and/or ambient noise effects.

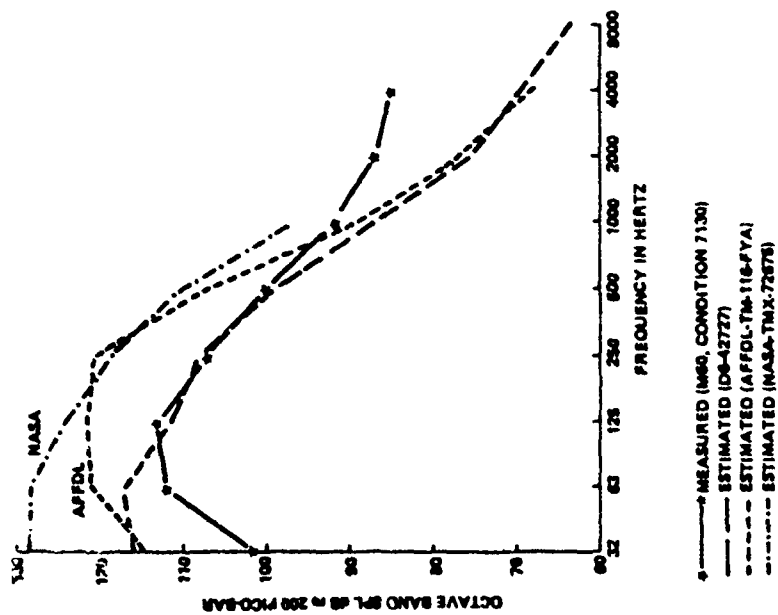


Figure A-73 Comparison of Measured and Estimated Interior Noise Climbout Levels

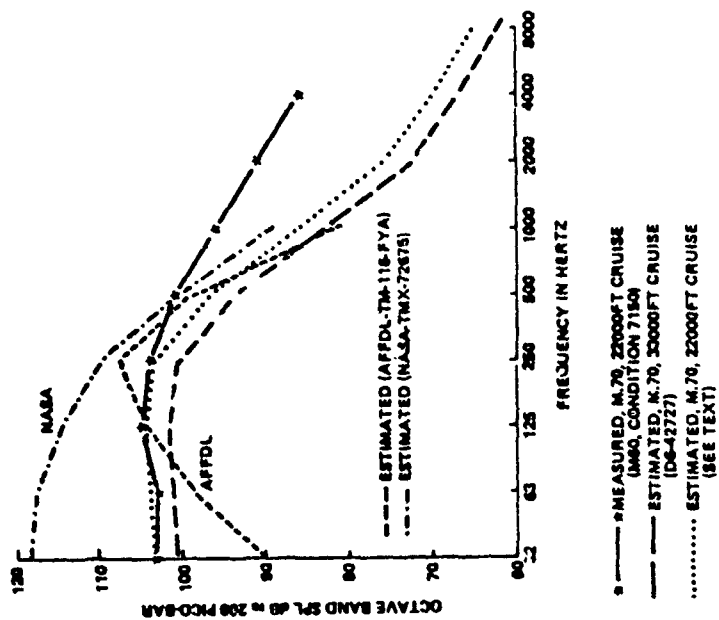


Figure A-74 Comparison of Measured and Estimated Interior Noise Cruise Levels

A.7 ANOMALIES

Among the data that have been acquired and reduced as part of the current test effort, a number of consistent but to date essentially unexplained patterns have been identified. In this section, data appropriate to three of these are presented. The three to be discussed are

- The pattern of two peaks observed in the 60 Hz to 200 Hz portion of one-third octave spectra for exterior microphone M8.
- The pattern of two peaks observed in the 80 Hz to 500 Hz portion of one-third octave spectra for exterior microphone M10.
- The pattern of the bump observed in the 30 Hz to 50 Hz portion of the one-third octave spectra for many of the microphones in the aft half of the troop compartment.

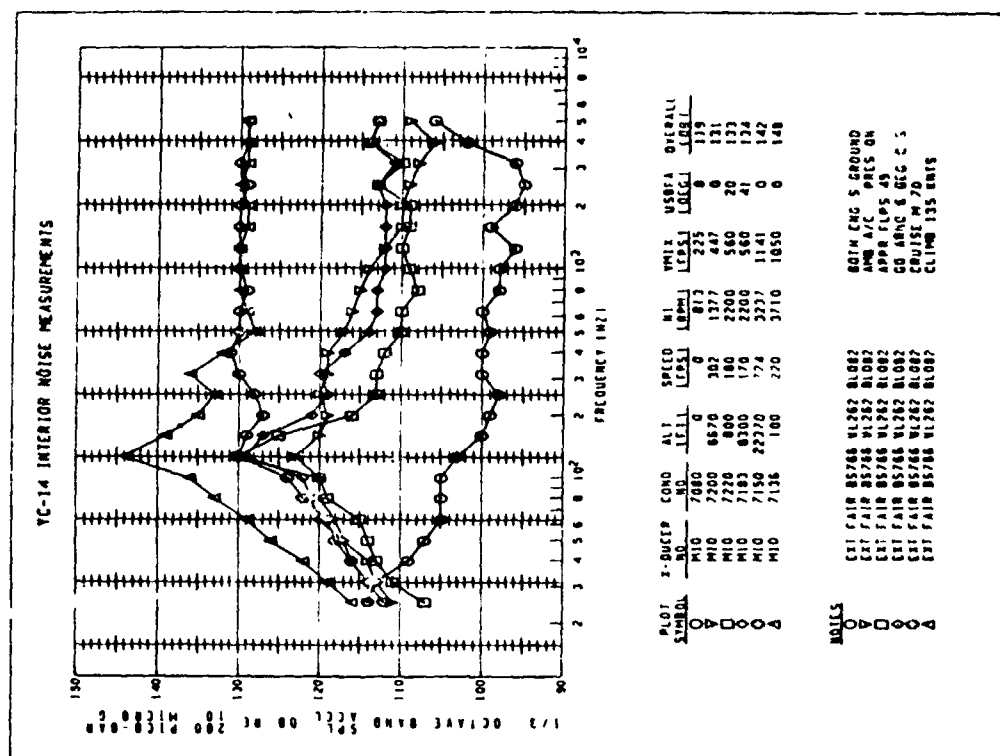
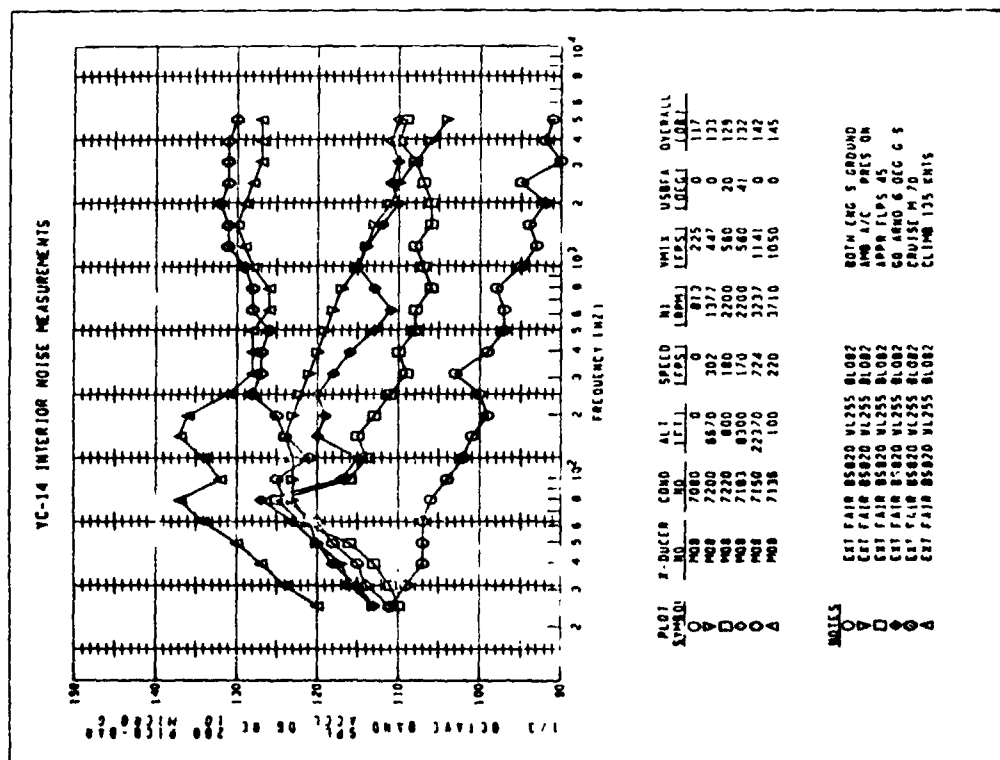
Spectra for M8 covering a selection of conditions examined (for other microphones) in previous sections are presented in Figure A-75. Corresponding spectra for M10 are presented in Figure A-76. Both M8 and M10 are Photocon 524 type microphones, flush mounted on the top of the wing body fairing. M8 is at station 860, and M10 is at station 766 just about on a body station line with the vortex generators.

In the case of M8, the two peaks are at 80 Hz, with a tendency to shift toward 100 Hz with increasing airplane altitude, and at 160 Hz. For M10, the peaks are at 125 Hz and 315 Hz. The peak at 315 Hz is much weaker than that at 125 Hz. For both sets, the peaks are strongest at low-speed/medium-to-high-power conditions, considerably weaker for cruise type conditions, and weaker yet at ground and flight idle conditions.

Figure A-77 compares spectra for M8 and M10 obtained during the Tulalip ground test program (Reference Boeing Document D745-10113-1) with spectra for a ground run (condition 7060) accomplished during the current test program. Note that for the Tulalip run, the USB flaps were fully extended and the VGs were up, while for condition 7060 the USBs were fully retracted, hence, VGs were down. These flap/VG differences likely account for the higher low- and high-frequency portions of the Tulalip spectra. Of greatest importance, however, is the absence of the peaks at 80 Hz and 160 Hz for M8 and at 125 Hz and 315 Hz for M10 in the spectra obtained at Tulalip. These comparisons encourage the view that the peaks in the spectra of M8 and M10 may not be indicative of the local exterior pressure field, and perhaps should be disregarded. Current evidence is not felt to be sufficient to justify this view.

Figure A-78 illustrates a peculiar bump first noted in the cruise spectra of interior microphones located in the aft half of the troop compartment. The bump is most pronounced for the two microphones by the sidewall (M56 and M59), and somewhat less pronounced—about 10 dB lower—for aisle microphones M58 and M60. Note that the bump is essentially absent in M62, the aft-most troop compartment microphone. Somewhat surprisingly, it is nearly absent from the spectra of M57 that is at the same station, but in the center aisle, as wall microphone M56.

This general bump behavior is, in fact, observed in essentially all engine-on operations considered in this program. Beyond this, it is observed when an independent source of exterior noise is utilized; e.g., the Sabre VI, and is illustrated in Figure A-79. A candidate partial explanation of this behavior could be low-frequency room modes.



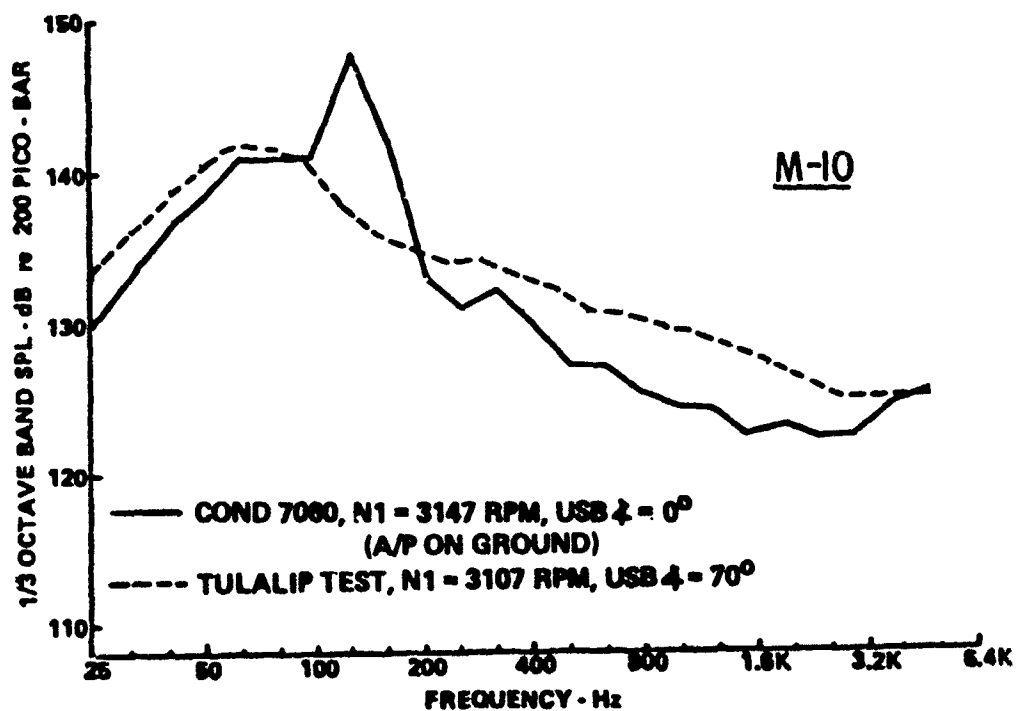
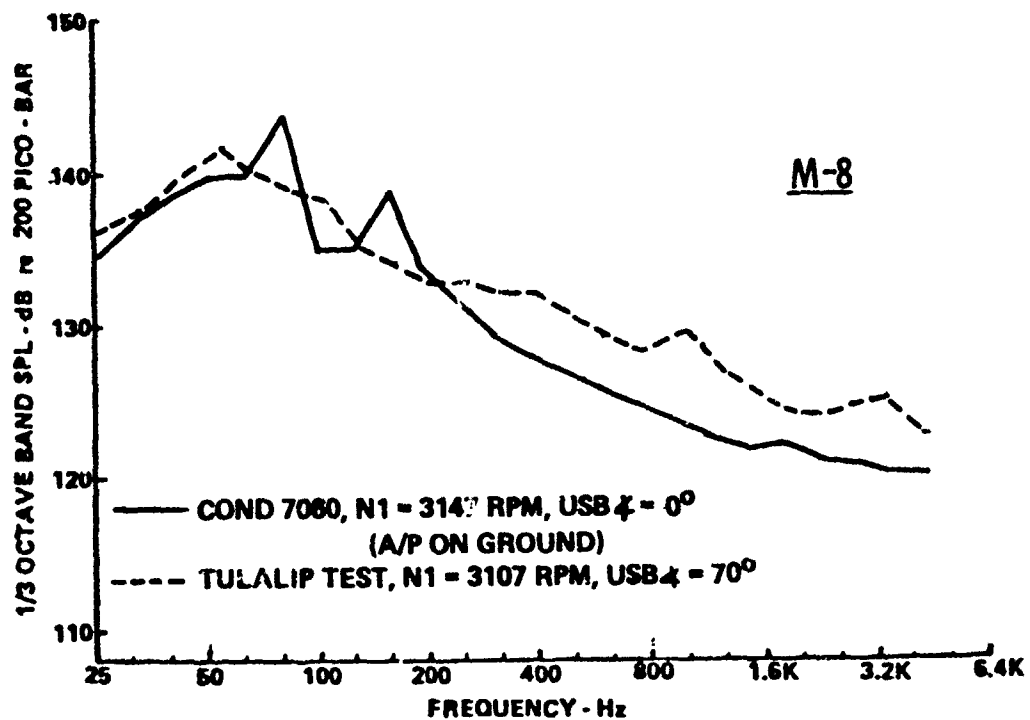


Figure A-77 Comparison of Microphone M8 and M10 Behavior—Current Test Program vs Tulalip Test Program

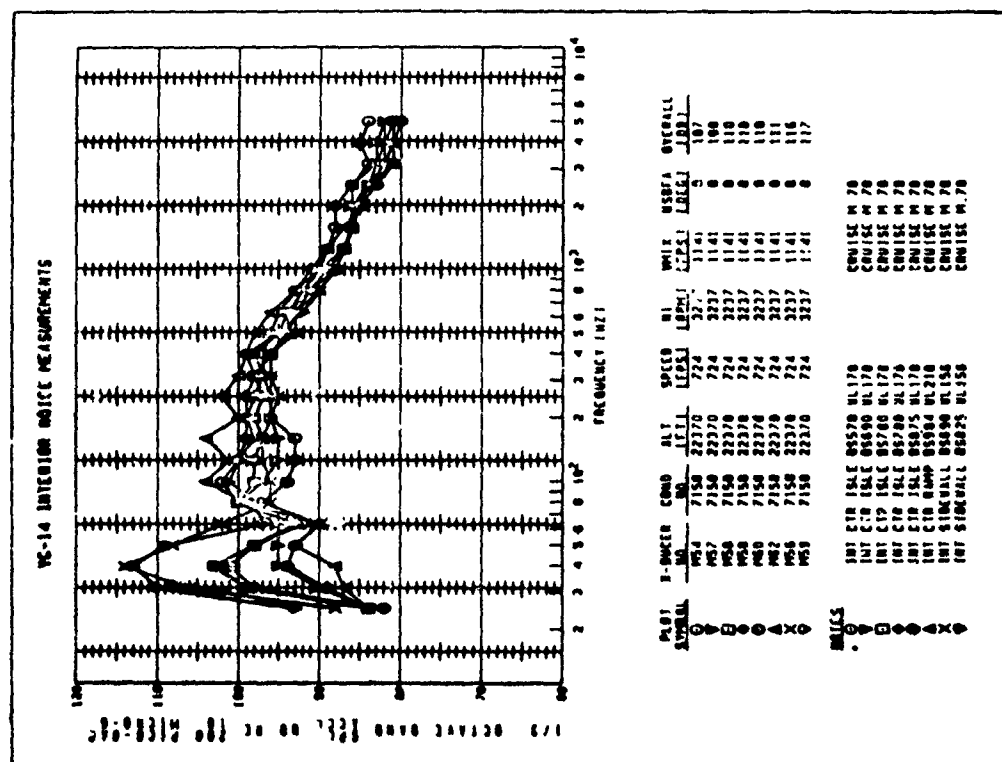


Figure A-78 Interior Noise, Cruise, M70

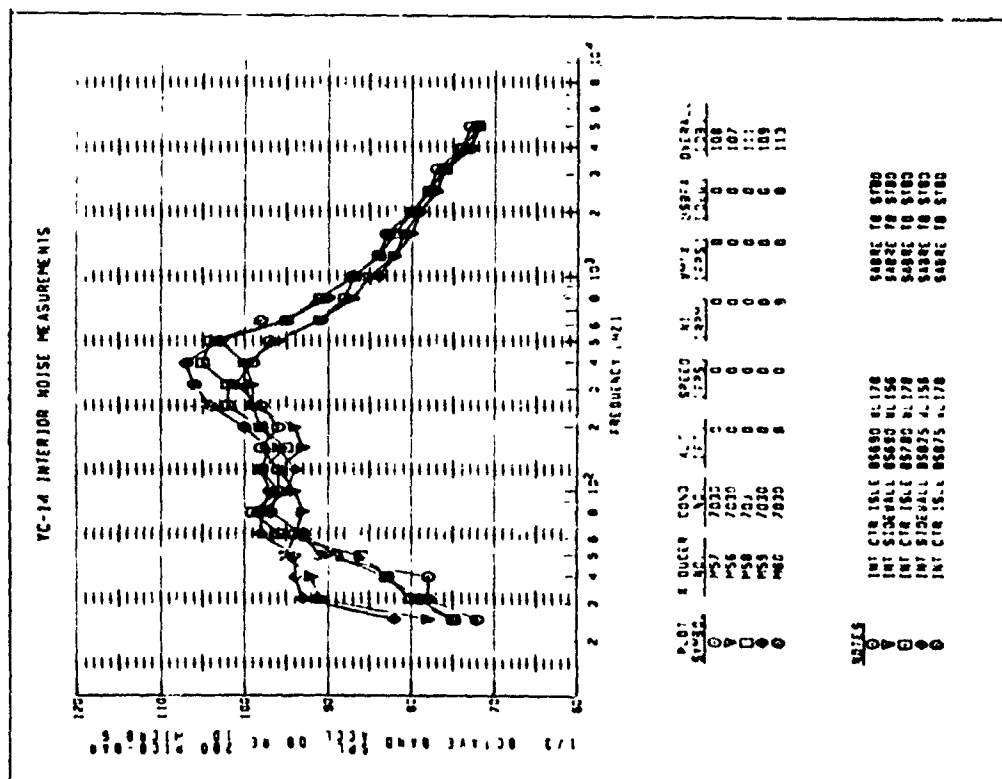


Figure A-79 Interior Noise, Sabre to Starboard

REFERENCES

1. Knittel, M. R.; Reed, J. B.; and Butzel, L. M., "*Estimation of the Exterior and Interior Noise Environments for the YC-14 STOL Transport*," Boeing Commercial Airplane Co. Document D6-42727, December 1975 (COMPETITION SENSITIVE).
2. Bartan, C. K., "*Interior Noise Consideration for Powered-Lift STOL Aircraft*," NASA TMX-72675, April 1975.
3. Shaw, L. L.; Smith, D. L.; and Wafford, J. H., "*AMST Interior Noise Considerations*," AFFDL-TM-75-116FYA, August 1975.
4. Reed, J. B., et al, "*YC-14 Ground and Flight Experiments for NASA-Flight Test Final Report*," (USAF Contract F33657-72-C-0829, change P00023), Boeing Commercial Airplane Co. Document D748-10113-2, July 1977 (COMPETITION SENSITIVE)
5. Lieberg, D. L., and Butzel, L. M., "*YC-14 Interior Noise Measurements Program for NASA/AFFDL*," (USAF Contract F33657-72-C-0829, change P00028), Boeing Commercial Airplane Co. Document D6-44350-1, June 1977 (COMPETITION SENSITIVE).
6. Lieberg, D. L., and Butzel, L. M., "*YC-14 Interior Noise Measurements Program for NASA/AFFDL. Compilation of 1/3 Octave and Narrow Band Microphone and Accelerometer Plots*," Boeing Commercial Airplane Co. Document D6-44350-2, October 1977 (COMPETITION SENSITIVE).